# Investigation of protein adsorption on nanocarriers for intravenous drug targeting

Inaugural-Dissertation

to obtain the academic degree

Doctor rerum naturalium (Dr. rer. nat.)

submitted to the Department of Biology, Chemistry and Pharmacy

of Freie Universität Berlin

by

Yujuan Zhang

from Jiangxi, China

2013

This work was carried out from September 2010 to June 2013 under the supervision of Prof. Dr. Rainer H. Müller at the Institute of Pharmacy of Freie Universität Berlin.

1st Reviewer: Prof. Dr. Rainer H. Müller

2nd Reviewer: Prof. Dr. Cornelia M. Keck

Date of defence: 28.08.2013

# Acknowledgments

I would like to express my gratitude to all those who helped me during the preparation and writing of this thesis.

First of all, I would like to thank my most respected research supervisor, Professor Dr. Rainer H. Müller, for giving me the opportunity to work in this excellent group and guiding me on the research field during the last three years.

Secondly, I deeply appreciate Dr. Inge Volz's and Dr. Mirko Jansch's introducing 2D-PAGE to me, and Mr. Sven Staufenbiel's and Miss Gabriela Karsubke's translation of summary, and Miss Corinna Schmidt's, Mr. Run Chen's and Miss Pricillia Sinambela's helping, and my special thanks also go to all the people in the group who helped me. The completion of this thesis would not have been possible without their helping.

Thirdly, I would like to acknowledge the Erasmus Mundus LOT-14 program for doctoral fellowship that lets me have the chance to study in Germany, and to thank the staff in the international office of Freie Universität Berlin for their kindness during the last three years.

Fourthly, I would like to thank my friends for their helping which is important for making this thesis a reality as well.

The last but not the least, I would also like to thank my parents and younger brother Zhou for their support over these past years.

# Contents

# 1. General introduction

The concept of targeted drugs, for the purpose of reducing side effects and achieving selective effectiveness of drugs *in vivo*, was first proposed by Ehrlich at the beginning of last century (Ehrlich, 1906). One approach to achieve drug targeting *in vivo* is the intravenous (i.v.) injection of particulate drug carriers (e.g., polymeric nanoparticles (Illum et al., 1987), emulsions (Müller, 1991), liposomes (Gregoriadis, 1993), or solid lipid nanoparticles (Müller et al., 2000)). For instance, in Figure 1.1, the *in vivo* behaviors of four particles are shown after i.v. injection: (a) a typical behavior of $^{131}$I-labeled polystyrene particles (60 nm) in rabbit is shown, and this particles are mainly accumulated in the liver due to the uptake of macrophages in the liver; (b) after surface modification with Poloxamine 908, this particles could obviously avoid the uptake in the liver while circulate in the blood; (c) it is shown the *in vivo* behavior of colloidal antimony trisufide (about 20 nm) which is mainly accumulating in the liver, spleen and skeleton; (d) when surface modification with Poloxamer, the polystyrene particles (60 nm) could result in an enrichment in the bone marrow in the rabbit. Therefore, drug targeting could be achieved by injecting different surfactant-modified particles.

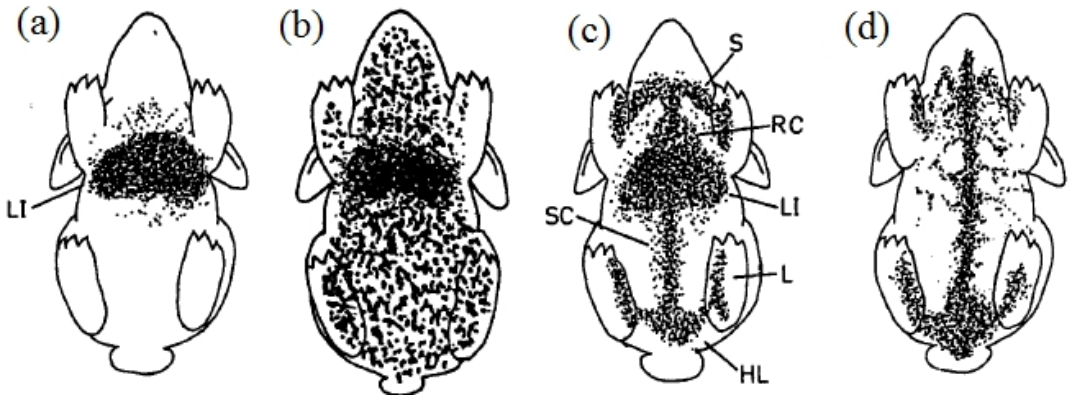


Figure 1.1. Scintigrams attained after injecting particles into rabbits: (a) unmodified $^{131}$I-labeled polystyrene particles (60 nm); (b) the same particles modified with Poloxamine 908 on the surface; (c) colloidal antimony trisufide; (d) polystyrene particles (60 nm) modified with Poloxamer 407 on the surface (Müller et al., 1997).

A major problem for i.v. drug targeting is the removal of drug carriers from the blood circulation by the uptake of macrophages in the body (mainly in liver, spleen, mononuclear phagocytic system (MPS)) (Douglas, 1986; Senior, 1987). The next challenge is to direct the drug carriers to the desired site of action (e.g., brain, bone marrow, tumor tissue).

From the 50s to the 80s of the last century, the physicochemical properties of particles (e.g., size, charge, surface hydrophobicity, major functional groups, etc.) were regarded as the key factors for determining the organ distribution of such i.v. injected drug carriers (Müller, 1991). One tried to develop site-specific drug carriers in a controlled way by varying their properties. However, it has been realized since 1990 and been generally accepted now that the determining factor for the *in vivo* fate and the organ distribution of drug carriers is the adsorbed blood proteins on the their surfaces after i.v. injection, and the blood protein adsorption pattern is affected by physicochemical properties of the drug carriers (Juliano, 1988; Müller and Heinemann, 1989; Price et al., 2001; Thiele et al., 2003), which is shown in Figure 1.2. The two-dimensional polyacrylamide gel electrophoresis (2-DE; 2D-PAGE) has been proven to be a powerful tool to analyze these plasma protein adsorption patterns of

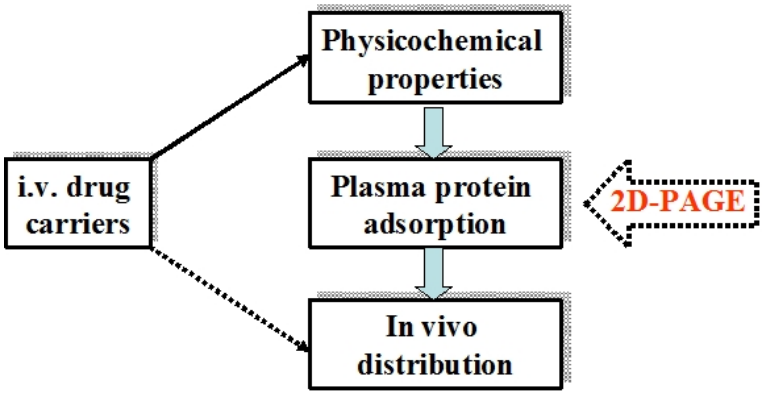


Figure 1.2. The role of plasma protein adsorption for the correlation of physicochemical properties of drug carriers and their organ distribution after i.v. (intravascular) administration.

drug carriers *in vitro* (Blunk et al., 1993; Harnisch and Müller, 1998; Lück et al., 1998; Gessner et al., 2001).

## 1.1 Influence of adsorbed proteins on intravenous drug targeting

In general, binding of opsonins (e.g., immunoglobulin G, complement factors, and fibrinogen) promotes phagocytosis and removal of the drug carriers from the systemic circulation by cells of MPS (Leroux et al., 1995; Camner et al., 2002). On the contrary, binding of dysopsonins (e.g., albumin, apolipoproteins) prolongs circulation time of the drug carriers in the blood (Moghimi et al., 1993; Ogawara et al., 2004). For example, Ogawara et al. (2004) employing pure polystyrene nanoparticle and polystyrene nanoparticle coated with human serum albumin observed that the latter particles had a obviously higher blood concentration and a longer circulation time in the body. Besides, there is tendency to say that the particles will be more easily recognized and faster cleared by the MPS when more proteins adsorb onto them.

Moreover, surface-enriched proteins can mediate uptake of the drug carriers by specific sites (Kreuter et al., 2002; Müller and Schmidt, 2002). For instance, it has been observed by Dehouck et al. (1997) that ApoE played an important role in the transport of lipoproteins into the brain via the low density lipoprotein (LDL) receptor on the blood-brain barrier (BBB), so nanoparticles adsorbing ApoE might mimic the ApoE coated LDL-particles leading to their brain-uptake by endocytic processes (Müller et al., 2001).

In the experiments by Kreuter (Müller and Schmidt, 2002), polymer nanoparticles (polybutylcyanoacrylate nanoparticles) stabilized with Tween 80 and and adsorbing Darlagin on the surface were able to transport the drug to the brain to achieve analgesic effect (Figure 1.3 left), while the negative control group (polymer nanoparticle without Tween 80 but adsorbing Darlagin) showed no brain delivery

effect (Figure 1.3 middle). Analyzed by the 2-DE method, the particles most efficient in brain delivery were found to possess an enrichment of ApoE in their protein adsorption pattern (Lück, 1997), which was proven by the Kreuter's experiments that the polymer nanoparticles without Tween 80 but Darlagin and ApoE adsorbed on the surfaces was able to deliver Darlagin to the brain (Figure 1.3 left). Therefore, ApoE played an important role in the transport of drug carriers to the brain.

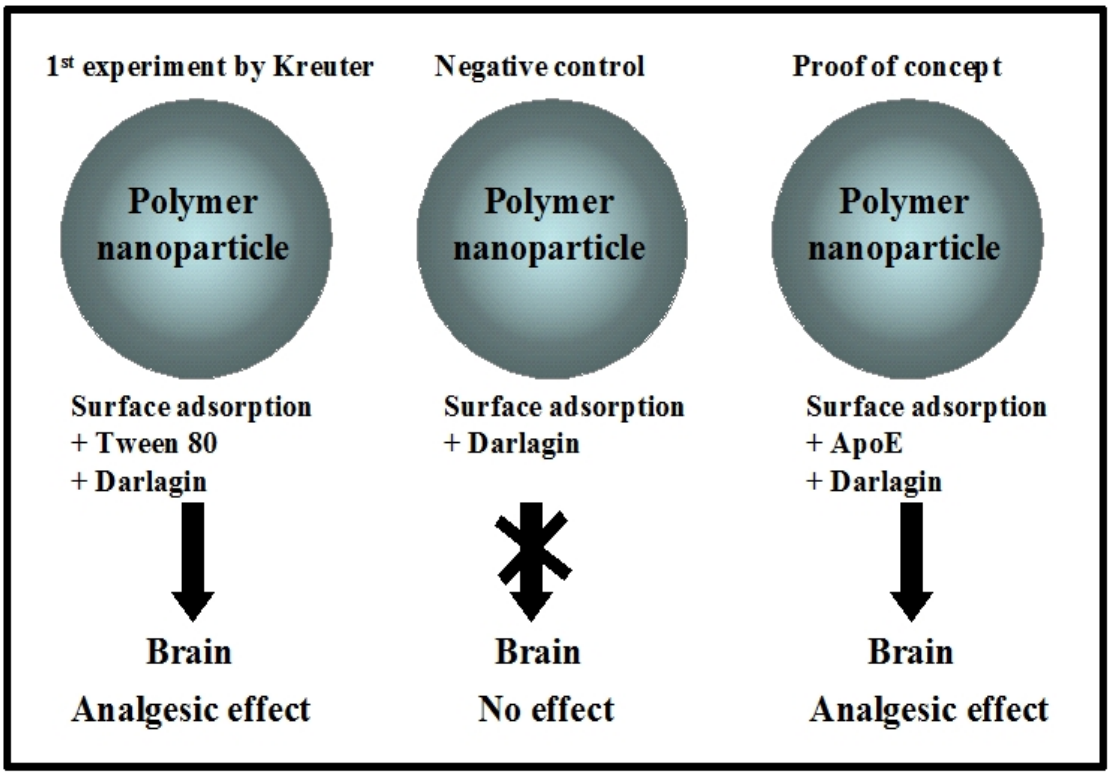


Figure 1.3. Treatment scheme in the experiments by Kreuter (Müller and Schmidt, 2002).

## 1.2 Physicochemical properties of particles that affect protein binding

That proteins adsorb onto particles is a complicated process, which could be affected by many parameters. There are several important properties of particles which influence the amount and identities of bound proteins:

(1) Sizes of particles;

(2) Zeta potential of particles;

(3) Hydrophobicity of particles;

(4) Conformation of the adsorbed polymer on the particle surface.

## 1.2.1 Size of particles

Protein affinities for nanoparticle surfaces basically differ from their affinities to bulk materials because of a variety of effects including small size effect, surface effect and curvature effect of the nanoparticles. Besides, when the size of particles is changed, the surface area and hydrophobicity of particles will be changed as well which will also affect the protein adsorption on particles. For instance, Cedervall et al. (2007)

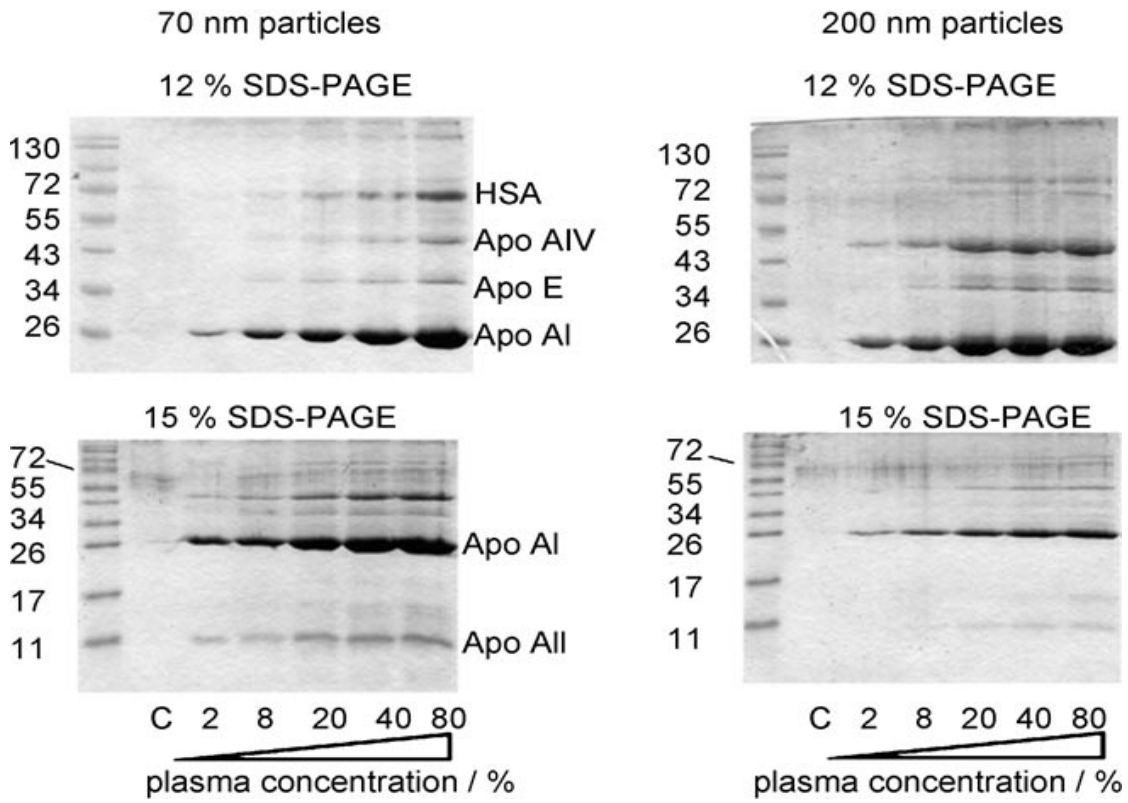


Figure 1.4. SDS-PAGE (12 and 15% gels) of plasma proteins retrieved from 0.5 mg of 70 or 200 nm 50:50 NIPAM/BAM copolymer particles after centrifugation and triple washing (total washing time 20 min). Particles were incubated with the plasma concentrations indicated; total volume 250 mL. Lane C is a control experiment with 80% plasma but without particles (Cedervall et al., 2007).

observed, employing 50:50 NIPAM/BAM copolymer particles with hydrophobic surfaces, that for diameters of particles from 70 nm to 700 nm the amount of adsorbed proteins varied with the changes of particle size and surface curvature, but the adsorbed qualitative protein patterns were the same for all sizes considered (such as the results of 70 and 200 nm particles in Figure 1.4: the protein adsorption patterns of them are the same.). The size and surface area of particles were able to obviously vary the adsorbed amounts of proteins but not qualitative composition of the protein adsorption patterns.

Furthermore, it has been observed that large particles were cleared faster from the blood by the macrophages than small particles (Davis, 1981; Senior et al., 1985; Müller, 1991). In the other words, the size of particles is able to affect their *in vivo* behaviors as well.

## 1.2.2 Zeta potential of particles

Some research has shown that neutrally charged particles have an obviously slower opsonization rate than charged particles, which indicates a direct correlation between particles surface charge and protein binding. Gessner et al. observed that major differences were found when comparing positively charged and negatively charged polymeric particles with similar size and surface hydrophobicity but different zeta potentials in Figure 1.5. Positively charged particles adsorbed preferentially proteins with pI<5.5 (e.g. Albumin) and the negatively ones adsorbed preferentially proteins with pI>5.5 (e.g. Immunoglobulin G, ApoH) in Figure 1.5 (Gessner et al., 2003), whereas with increasing surface charge density in the interval from -3.7 to -8.2 $\mu C/cm^2$, the qualitative protein adsorption pattern did not change as shown in Figure 1.6 (Gessner et al., 2002). Preferential adsorption means that some adsorbed plasma proteins were enriched onto the particle surface compared to the bulk plasma (Blunk, 1994). Besides, Göppert and Müller (2005a) also observed that the identified proteins were similar on negatively charged poloxamer- and poloxamine-stabilized SLN. Thus,

Physicochemical Characterization Data for Latices with Basic (a) and Acidic (b) Functional Groups

| Latex | Functional Group | Particle Size (nm)[b] | Surface Charge Density ($\mu C/cm^2$) (error limit: 0.2 $\mu C/cm^2$) |
|---|---|---|---|
| a) Latices with basic functional groups | | | |
| 1 | $NH_2$ | 97 | +5.3 |
| 2 | $NH_2$ at spacers | 82 | +3.3 |
| 3 | NHR | 89 | +12.0 |
| 4 | $NR_2$ | 89 | +13.2 |
| 5 | $NR_3^+$ | 94 | +10.5 |
| b) Latices with acidic functional groups | | | |
| 6 | $COO^-$ | 96 | −2.2 |
| 7 | $SO_3^-$ | 101 | −8.4 |
| 8 | $SO_4^-$ | 109 | −3.1 |

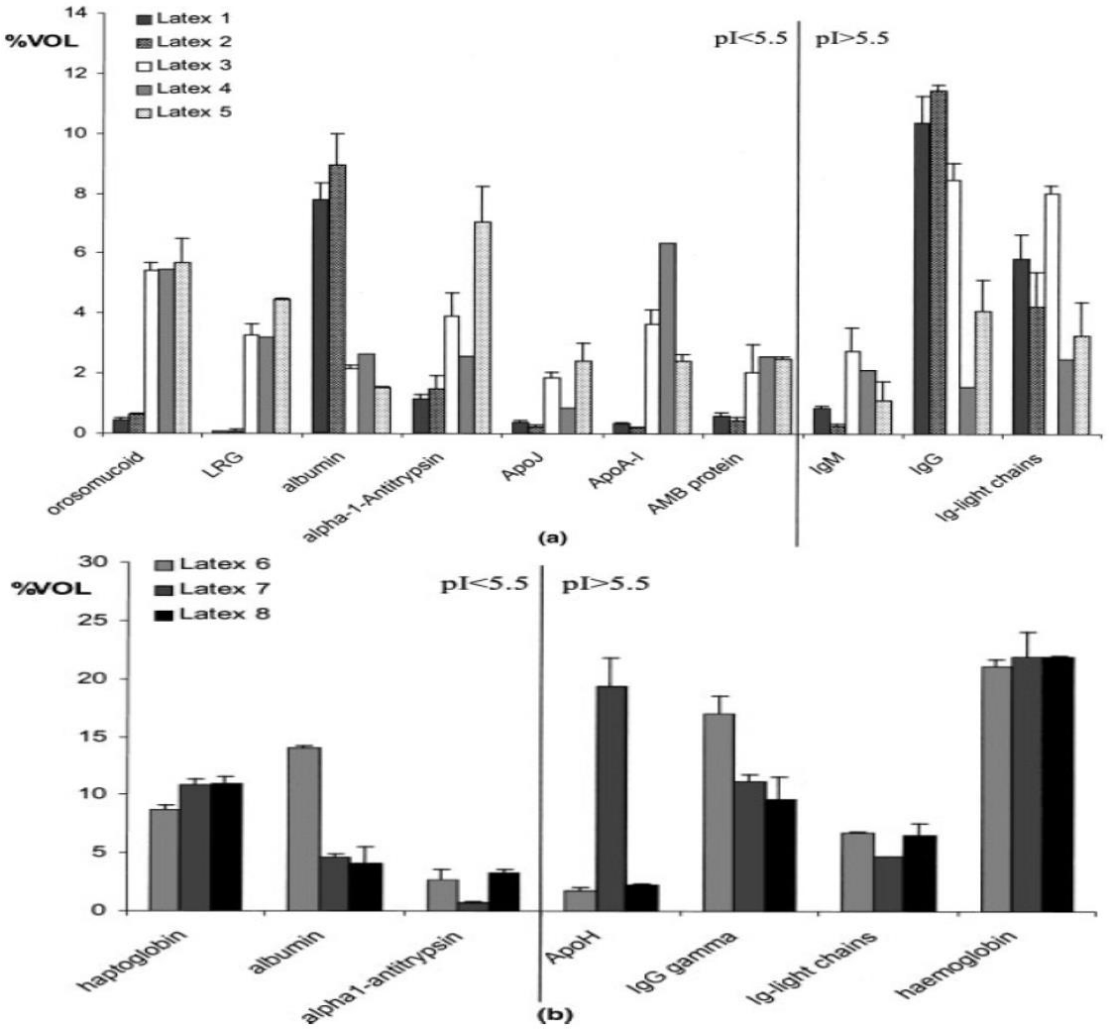


Figure 1.5. Upper table is the physicochemical properties of latex nanoparticles, and lower diagrams show main proteins adsorbed to latex nanoparticles with basic (a) and acidic (b) functional groups. %VOL is an arbitrary unit for the relative protein amount, generated by the evaluation software MELANIE 3. The values are the mean of three experiment; error bars indicate the standard deviation (Gessner et al., 2003).

the protein adsorption pattern on particle could be obviously altered duo to the electrical properties of the particle surface, such as positive or negative. But the protein adsorption patterns of particles were almost the same for different negative surface charge densities.

**(a)** Physicochemical characterization data of model nanoparticles (latex 1–5)

| Latex | 1 | 2 | 3 | 4 | 5 |
|---|---|---|---|---|---|
| Surface charge density ($\mu C/cm^2$) | − 3.7 | − 5.2 | − 6.0 | − 6.7 | − 8.2 |
| Particle size (nm) (SD 0.01) | 54 | 61 | 64 | 57 | 60 |
| Hydrophobicity: slope from Rose Bengal partitioning experiment ($ml/m^2$) | 7 | 7 | 8 | 8 | 10 |

**(b)**

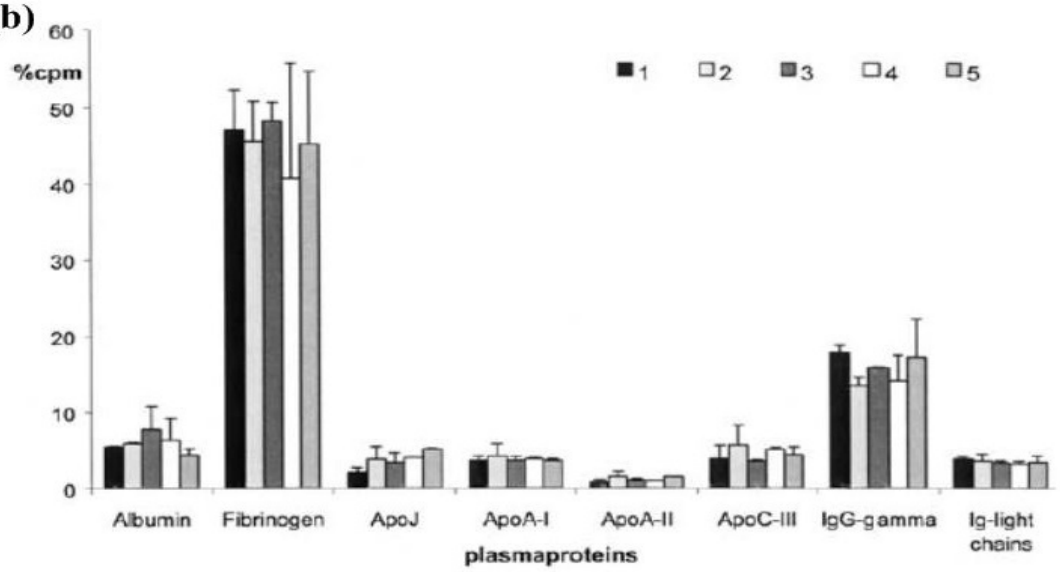


Figure 1.6. (a) Upper table is the physicochemical properties of model nanoparticles, and (b) lower diagram shows major proteins adsorbed on latices 1-5. The protein amounts are expressed in %cpm (percentage of the overall detected protein pattern), error bars represent the standard deviation (n = 3) (Gessner et al., 2002).

## 1.2.3 Hydrophobicity of particles

The previous studies have shown that the hydrophobicity of the particle surface could affect not only the amounts but also the varieties of adsorbed proteins (Göppert and Müller, 2005a, 2005b). Particles with the "right" proteins could escape from the MPS

recognition (Maassen et al., 1993). In general, hydrophilic particles can circulate longer time in the blood stream than hydrophobic particles. For instance, polystyrene model carriers surface-modified with hydrophilic polyethylene oxide chains or poloxamine 908 can circulate in the blood stream (Illum et al., 1987; Moghimi et al., 1993). Figure 1.7 shows that the microspheres coated with poloxamine 908 dramatically reduced hepatic accumulation and have a much higher blood concentration (Moghimi et al., 1993). The 2-DE results indicated that the hydrophilic surface could efficiently avoid the protein adsorption onto it (Ogawara et al., 2004; Gref et al. 2000). Ogawara et al. (2004) observed that the amount of adsorbed protein on HSA (human serum albumin)-coated nanoparticles besides albumin is much less than on unmodified nanoparticles due to possessing the hydrophilic HSA modification layer on them.

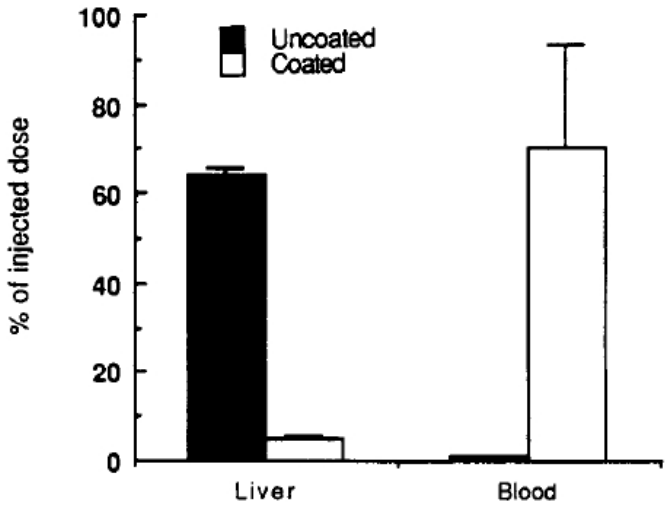


Figure 1.7. Organ distribution of uncoated and poloxamine-coated polystyrene microspheres (60 nm) 1 h following intravenous administration into rats (Moghimi et al., 1993).

## 1.2.4 Conformation of the adsorbed polymer on particles

The conformation of the adsorbed polymer is important for the physical stability of the suspensions. Furthermore, the conformation of the adsorbed polymer on particles

could influence the protein adsorption pattern via the degree of exposure of hydrophilic polyethylene oxide (PEO) chains or hydrophobic polypropylene (PPO) chains (Göppert and Müller, 2005c) and the steric hindrance effect of polymer chains (e.g. PEO) against the adsorption of proteins (Gref et al., 2000; Carignano and Szleifer, 2000; Gessner et al., 2003). The steric hindrance effect always affects the amount of adsorbed proteins with changing length and density of chains on the particle surface. For example, total amounts of adsorbed proteins on PEG-PLA45K nanoparticles decline with increase of the PEG molecular weight in Figure 1.8 (Gref et al., 2000).

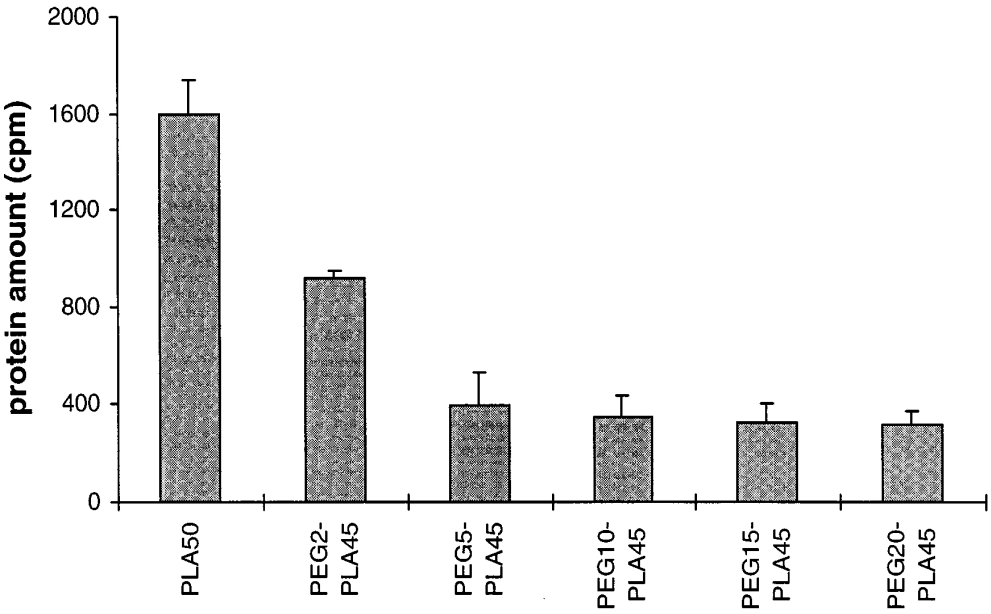


Figure 1.8. Total amounts of adsorbed proteins on PEG-PLA45K nanoparticles with different PEG molecular weight. The protein amount is expressed in arbitrary units. The values are the means of two experiments (Gref et al., 2000).

In brief, controlling the physicochemical properties of a particle (particle engineering) to specifically bind certain proteins of interest for targeting purposes, can greatly enhance the ability to develop drug carriers. For instance, as shown in Figure 1.9, "uncoated" particle adsorbs many proteins in the blood resulting in being quickly removed by the MPS cells; "PEGylated" particle possesses PEG chains spreading on the surface which could avoid the protein adsorption, and is able to circulate in the

bloodstream due to little protein bound on its surface; “polysorbate coated” particles could specially adsorb ApoE that is important for transporting drug carrier to the brain. Therefore the physicochemical properties of particles affect their protein adsorption patterns resulting in various behaviors *in vivo*.

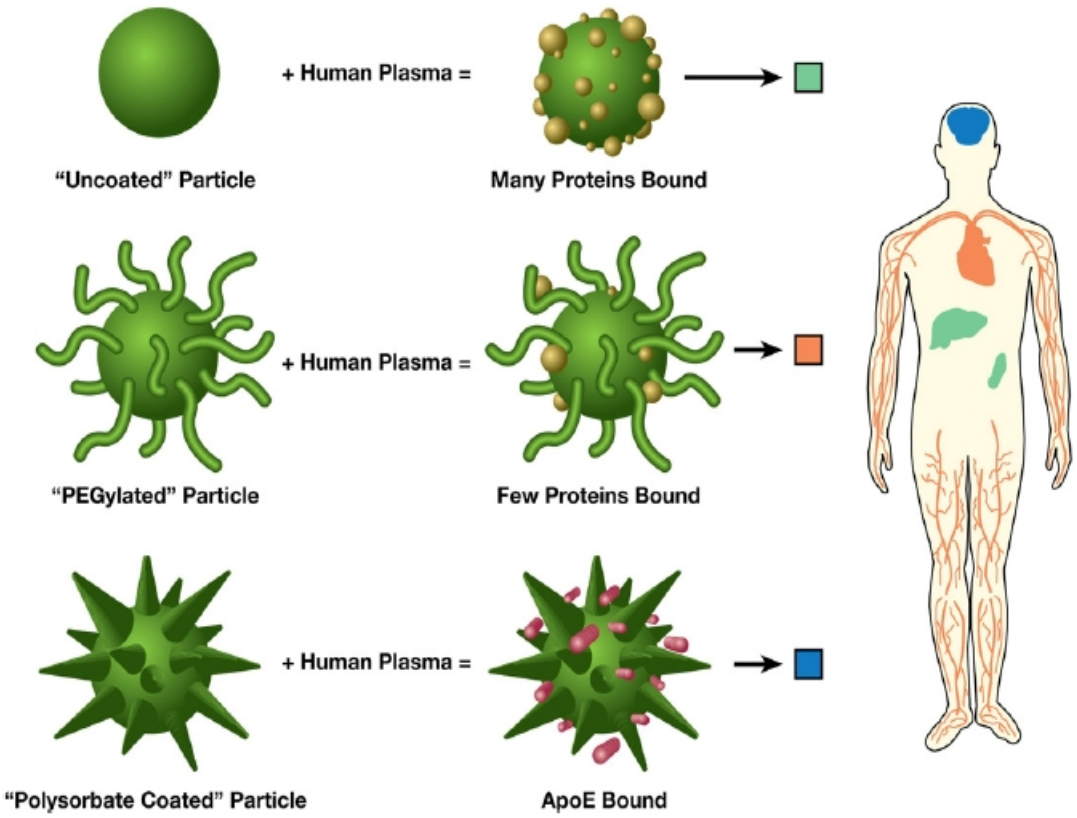


Figure 1.9. Biodistribution of nanoparticles with varying coatings and bound proteins. Uncoated particles bind proteins and are taken up by the reticuloendothelial system (RES) into the liver and spleen. “PEGylated” particles bind very few proteins, avoid uptake by the RES, and are longer circulating in the blood. “Polysorbate-coated” particles can specifically bind ApoE and selectively target to the brain across the blood brain barrier (Aggarwal et al., 2009).

## 1.3 Objective of the thesis

As having been seen in this chapter, protein adsorption patterns as the biological identities of particles control their *in vivo* behaviors, and physicochemical properties of particles could dramatically influence the protein adsorption patterns resulting in

various behaviors *in vivo*. The previous studies proved that 2-DE is a powerful tool for analyzing protein adsorption on particles. In this work, some important instruments are employed for characterizing the properties of drug carriers, and High pressure homogenization (HPH) that is a key technique for preparing drug carriers in pharmacy area has been applied; several particles under research are covered, and their human plasma protein adsorption patterns are analyzed by using the 2-DE method; the interactions between particles and proteins are discussed; their *in vivo* behaviors have been predicted based on the protein adsorption pattern and have to be assessed in the future. The aims of this work are to investigate the protein adsorption onto different nanocarriers then to understand the protein adsorption kinetics on particles and to achieve the desired drug carriers for drug targeting in the body.

Firstly, the 2-DE method in chapter 2 and the photon correlation spectroscopy, laser diffractometry as well as high pressure homogenization instruments in chapter 3 are respectively introduced.

In chapter 4, the protein adsorption patterns on SLN coated with different surfactants are reviewed and compared, and then the interaction between proteins and SLN are discussed. The aim of this chapter is to determine the influence of surfactants on the protein adsorption patterns of SLN to improve the SLN system for drug delivering and targeting.

In chapter 5, firstly, the time-dependent protein adsorption patterns on the i.v. injection of egg lecithin-stabilized oil-in-water emulsions (nanoemulsion) have been analyzed *in vitro* by 2-DE. The experimental results of nanoemulsions are compared to that of SLN although nanoemulsions and SLN both have a hydrophobic core but different surface properties, which is to understand the protein adsorption kinetics on nanoemulsions and to analyze the influence of nanoparticle surface properties on their protein adsorption patterns. Secondly, the two separation methods (gel filtration and centrifugation) are compared, which is to choose the best separation method for

separating nanoemulsions from excess plasma without disturbing the protein adsorption pattern on them.

In chapter 6, three kind of hemoglobin particles (pure hemoglobin particles, hemoglobin particles modified with HSA on the surface, and hemoglobin-hyaluronan-mixture particles) prepared by a novel 3-step-technique (co-precipitation, cross-linking and dissolution) are analyzed. This chapter aims to choose the most promising ones as blood substitutes. Different surface properties of those particles affect their protein adsorption patterns. Their protein adsorption patterns were also obtained by 2-DE.

Antioxidants e.g., rutin are a major player in potential treatment of Alzheimer disease. Chapter 7 aims to achieve the potential formulation of rutin nanocrystals for Alzheimer treatment. In chapter 7, four formulations of rutin nanocrystals (Plantacare 2000 UP-rutin nanoparticles (stabilized with 0.1 % Plantacare 2000 UP), Plantacare 2000 UP-rutin nanoparticles (stabilized with 1.1 % Plantacare 2000 UP), Tween 80-rutin nanoparticles, and Poloxamer 188-rutin nanoparticles) were prepared and their protein adsorption patterns were analyzed with the 2-DE method. Their protein adsorption patterns are affected by the different surfactants on the rutin nanocrystals resulting in different *in vivo* behaviors.

# 2. Two-dimensional polyacrylamide gel electrophoresis (2D-PAGE; 2-DE)

Currently, the plasma protein adsorption pattern on drug carriers is analyzed *in vitro* by the two-dimensional polyacrylamide gel electrophoresis (2-DE; 2D-PAGE). 2-DE has been proven to be a powerful tool to determine these plasma protein adsorption patterns of drug carriers (Blunk et al., 1993; Harnisch and Müller, 1998; Lück et al., 1998; Gessner et al., 2001). The 2-DE method was introduced by O' Farrell (1975) and used for standard plasma samples by Hochstrasser et al. (1988). Later this method was modified and successfully transferred to analyze the adsorption protein patterns of colloidal drug carriers by Blunk et al. (1993). Briefly, in the first dimension (isoelectric focusing, IEF) the proteins were separated according to their isoelectric point (pI) with IPG-strips. After the first dimension, the proteins were separated on the basis of their molecular weight (MW) or sizes in the second dimension of 2-DE (SDS-PAGE) (Görg et al., 1995). After electrophoresis separation, the gels were silver-stained (Bjellqvist et al., 1993) and scanned. The spots on gels were identified by matching the gels with master maps of human plasma (Anderson and Anderson, 1991; Hoogland et al., 2000). The amount of adsorbed protein was assessed in a semi-quantitative manner on the basis of spot size and intensity of silver staining (Blunk et al., 1993; Blunk, 1994).

This 2-DE method is introduced in details in this chapter from several aspects:

(1) Sample preparation method;

(2) Rehydration of IPG strips;

(3) Isoelectric focusing (IEF);

(4) IPG strip equilibration;

(5) SDS-polyacrylamide gel electrophoresis (SDS-PAGE);

(6) Silver stains;

(7) Scan and calculation.

## 2.1 Sample preparation method

To mimic the *in vivo* environments, the sample preparation of protein-particle conjugates is one of the most important steps for accurately analyzing the protein adsorption pattern on particles. In general, the steps of plasma protein-particle sample preparation for 2-DE *in vitro* in our lab are as follows:

(1) Incubating the particle suspension in citrate stabilized human plasma with a volume ratio of 1:3 for 5 min at 37 °C;

(2) Separating the samples from excess plasma by centrifugation at 23000 g for 1h at 20 °C, and then washing them three times with 0.05 M (pH 7.4) phosphate buffer, and subsequent centrifugation; or by gel filtration (chromatography), and the elution performed with 0.05 M (pH 7.4) phosphate buffer at a flow rate of 18 mL/h, then choosing the relevant fraction by employing UV detection at 279 nm (the preparation of 0.05 M (pH 7.4) phosphate buffer is shown in Table 2.1(a));

(3) Desorption of the adsorbed proteins from the particles with 15 µl $H_2O$ and 10 µl solution I (including sodium dodecyl sulfate (SDS) and dithioerythritol (DTE)) at 95 °C for 5 min (the preparation of solution I is shown in Table 2.1(b));

(4) Cooling the samples down to room temperature, and then incubating with a 190 µl solution II (containing DTE, 3-(3-Cholamidopropyl)dimethylammoni-o-1-propansulfat (CHAPS), urea, and Tris(hydroxymethyl)-aminomethan (Tris)), stirring and centrifuging 15 min to obtain the adsorbed protein solutions (the preparation of solution II is shown in Table 2.1(c));

(5) Adding rehydration buffer 125 µl into the adsorbed protein solution to analyze the protein adsorption pattern on particles by the 2-DE, according to relational references, and the 340 µl final sample solution for the next step (rehydration of IPG strips) (the preparation of rehydration buffer is shown in

Table 2.1(d)) (Blunk et al., 1993; Harnisch and Müller, 1998; Lück et al., 1998; Gessner et al., 2001).

Table 2.1. Preparations of 0.05 M (pH 7.4) phosphate buffer (a), solution I (b), solution II (c) and rehydration buffer (d).

(a)

| 0.05 M Phosphate buffer pH 7.4 | |
|---|---|
| $NaH_2PO_4$ | 0.21 g |
| $Na_2HPO_4$ | 1.91 g |
| $H_2O$ (MilliQ water) | Add to 100 ml |

(b)

| Solution I | |
|---|---|
| SDS | 1.000 g (10 % w/v) |
| DTE | 0.232 g (2.32% w/v) |
| $H_2O$ (MilliQ water) | Add to 10.0 ml |

(c)

| Solution II | |
|---|---|
| Urea | 24.00 g (8 M) |
| CHAPS | 2.00 g (4 % w/v) |
| Tris | 0.25 g (40 mM) |
| DTE | 0.5 g (60 mM) |
| $H_2O$ (MilliQ water) | Add to 50.0 ml |

(d)

| Rehydration buffer for IPG Strips | |
|---|---|
| Urea | 4.8 g (8 M) |
| CHAPS | 100 mg (2 %) |
| DTE | 20 mg |
| Servalyt pH 3-10 | 125 µg (0.5 %) |
| $H_2O$ (MilliQ water) | Add to 10 ml |

In the above experiment steps of sample preparation, there are several critical parameters that influence the protein adsorption pattern on particles *in vitro* compared with *in vivo*:

(1) Choice of incubation medium;

(2) Ratio of the particle suspension to incubation medium;

(3) Incubation time;

(4) Separation method;

(5) Washing medium and number of washing steps.

### 2.1.1 Choice of incubation medium

Choice of incubation medium is the first step in the above experiments to analyze the protein adsorption pattern on particles *in vitro*. To mimic the conditions in the bloodstream, there are three kind of incubation media used, including blood, plasma and serum. Ideally blood should be used as incubation medium, but it is very difficult to separate particles from blood cells. In general plasma or serum is used to displace blood. However, the adsorption protein patterns on particles are different for plasma and serum. For instance, serum is depleted from fibrinogen, but in various studies with different types of particles the adsorption of fibrinogen was demonstrated (Göppert and Müller, 2003, 2004, 2005a, 2005b, 2005c; Weyhers et al., 2005). So the use of plasma as incubation medium should be a more reasonable compromise for analysis of the adsorbed proteins on drug carriers *in vitro* to mimic the *in vivo* circumstances (Blunk et al., 1993; Leroux et al., 1996; Lück et al., 1999; Lind et al., 2001). When using plasma, it is necessary to keep in mind that plasma contains additional compounds, e.g. citrate, which may interfere with the adsorption process of proteins on the surfaces of particles. Nevertheless, plasma is still regarded as a better incubation medium for analyzing the protein adsorption patterns of drug carriers *in vitro*.

## 2.1.2 Ratio of the particle suspension to incubation medium

The ratio of the used particle suspension to the incubation medium is important as well. For example, if the ratio is too high (too many particles or too large total surface area of particles compared with the proteins of the incubation medium), some of high affinity proteins for the particle surface in incubation medium may be insufficient (protein depletion) and result in the total amounts of those proteins decreased, which will induce differences of the protein adsorption proteins of drug carriers between *in vitro* and *in vivo*. For most of protein adsorption pattern studies, nanoparticles are incubated with plasma with a proper ratio so that the protein levels of plasma surpass the adsorption amounts needed for the available particle surface area. For instance in our studies, reproducible patterns were obtained at a ratio of 1:3 (Göppert and Müller, 2003, 2004, 2005a, 2005b, 2005c; Weyhers et al., 2005), when the particle concentration was in the range of 10-20 % (w/v). Moreover, to avoid too strong dilution of the incubation medium by the water which reduce artificially the decreases of some protein solubilities, it is recommended that the particle suspension is as highly as concentrated.

## 2.1.3 Incubation time

The protein adsorption pattern on solid surface is time-dependent. The adsorption patterns can be regarded as a product of a series of adsorption and desorption/displacement processes: firstly more plentiful proteins with lower affinity can be adsorbed on the solid surface, then these proteins are displaced by less plentiful proteins with higher affinity to the surface (Vroman et al., 1980; Vroman and Adams, 1986). This displacement is called "Vroman-effect" and occurs in seconds or even less time, which has been proven using the polymeric model particles (polystyrene particles surface-modified with poloxamer 407 and poloxamine 908) incubated with different dilutions of plasma for observing the protein adsorption patterns on the particle surface in seconds or a fraction of a second (Blunk et al.,

1996). The results (Blunk et al., 1996) showed that the most abundant protein in human plasma, albumin (35-50 mg/ml), was first displaced by fibrinogen (2-4.5 mg/ml), and then in turn by IHRP, ApoC-III (0.12-0.14 mg/ml) and Apo J (0.035-0.105 mg/ml). Thus, a proper incubation time should be chosen in the experiments.

To mimic the conditions in the bloodstream, the particles were routinely incubated in plasma for 5 min, because *in vivo* in case recognition by the MPS occurs, in the first 5 min up to 90% of the injected dose are taken up by the liver macrophages (O'Mullane et al., 1987; Müller, 1991; Liliemark et al., 1995). In case particles survive in the first 5 min, prolonged blood circulation of these particles was found (Illum and Davis, 1987; Cattel et al., 2003). For instance in Figure 2.2, HSA-coated NS-50 nanospheres and uncoated NS-50 nanospheres were mainly cleared in the first 5 min while a long blood circulation was observed after 5 min once they escaped from MPS. It can be assumed that in case of particles recognized by the liver macrophages, the responsible proteins have been adsorbed on particles and become detectable after this time of incubation. In many studies the objective is to find drug carriers avoiding recognition by MPS (Camner et al., 2002; Leroux et al., 1994). Therefore, the incubation time is normally 5 min of particles in plasma.

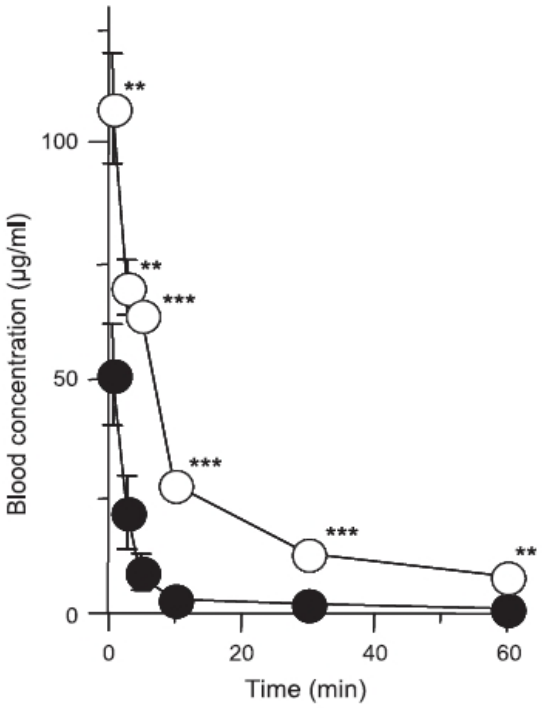


Figure 2.2. Blood concentration-time profile of HSA (human serum plasma)-coated NS (polystyrene nanosphere)-50 (○) and NS-50 (●) after intravenous administration at a dose of 12.5 mg/kg. Results are expressed as the mean ± S.D. Of more than three experiments. ** $p < 0.01$; *** $p < 0.001$, compared with NS-50 (Ogawara et al., 2004).

## 2.1.4 Separation method

There are three main separation methods: centrifugation (Blunk, 1994; Harnisch and Müller, 1998; Gessner et al., 2000; Göppert and Müller, 2003), gel filtration (Diederichs, 1996; Göppert and Müller, 2004; Göppert, 2005) and magnetic separation used for the magnetic materials (Thode, 1996; Thode et al., 1997). The standard separation method of particles from extra plasma is by centrifugation (Lück et al., 1997; Harnisch and Müller, 1998; Gessner et al., 2000; Göppert and Müller, 2003), based on the density difference between particles and plasma. Centrifugation is feasible when the density difference is sufficiently high between the particles and plasma. For example, the density of polymeric particles is about 1.05-1.20 g/cm$^3$, and emulsions around 0.90 g/cm$^3$. Solid lipid nanoparticles (SLN) were always prepared

possessing a sufficiently low density for centrifugation by adding low density compounds, such as cetyl palmitate (0.816-0.819 g/cm$^3$) (Göppert and Müller, 2004).

The other separation methods (e.g. Gel filtration or magnetic separation) always were used when centrifugation was impossible or very long centrifugation time were required. Ideal gel filtration (chromatography) is a mild separation method independent from eluent composition and only according to size differences because of steric effects (Scherphof et al., 1980). Many of experimental results for e.g. P188-SLN, TC450-SLN in Table 2.2 (Göppert and Müller, 2004) showed that gel filtration was comparable to centrifugation used as separation method. Nevertheless, the obtained protein adsorption patterns still had slight differences between use of centrifugation and gel filtration (Göppert and Müller, 2003, 2004), perhaps because after the 5 min of incubation time, the adsorption of proteins onto particles is still going on during the centrifugation separation process. For gel filtration, this is not the case, or the adsorbed proteins on particles may be even desorbed in the separation process. However, the differences between use of centrifugation and gel filtration could be multiplied for the surface properties of nanoparticles. For example, Table 2.2 shows that there is distinctly different protein adsorption patterns on T80-SLN when using centrifugation and gel filtration. A pronounced adsorption of IgG g chain and Ig light chain as well as Ig M chain were observed, and the percentages of the remaining proteins were the similar for centrifugation and gel filtration when IgG g chain, Ig light chain and Ig M chain were ignored and the remaining proteins were set to be 100% (Göppert and Müller, 2003). In brief, the separation of protein-particles from extra proteins without disrupting the adsorbed proteins or inducing additional protein binding is still a challenge.

Table 2.2. Comparison of the influences of centrifugation and gel filtration on the adsorbed proteins of different SLN, including Tween 80-SLN (T80-SLN), Poloxamer 188-SLN (P188-SLN), and Tego Care 450-SLN (TC450-SLN).

| SLN | Identified proteins | Separation method | References |
|---|---|---|---|
| T80-SLN | Apolipoproteins, fibrinogens, IgM | Centrifugation | Göppert and Müller, 2003 |
| T80-SLN | Apolipoproteins, IgG g chain, Ig light chain, IgM | Gel filtration | Göppert and Müller, 2003 |
| P188-SLN | Albumin, apolipoproteins, fibrinogens | Centrifugation | Göppert and Müller, 2003, 2004 |
| P188-SLN | Albumin, apolipoproteins, fibrinogens | Gel filtration | Göppert and Müller, 2003, 2004 |
| TC450-SLN | Albumin, immunoglobulins, fibrinogens, apolipoproteins | Centrifugation | Göppert and Müller, 2003 |
| TC450-SLN | Albumin, immunoglobulins, fibrinogens, apolipoproteins | Gel filtration | Göppert and Müller, 2003 |

## 2.1.5 Washing medium and number of washing steps

During the centrifugation separation method, washing medium and number of washing steps are crucial for properly obtaining the protein adsorption patterns on particles as well. Firstly, the concentration of washing medium can affect the solubilities of proteins. In general, proteins have higher solubilities and are easier to dissolve in 0.02-0.05 M buffer than in distilled water. In most of studies, 0.02-0.05 M

phosphate buffer was chosen as the washing medium (Göppert and Müller, 2003, 2004, 2005a, 2005b, 2005c; Weyhers et al., 2005), which can reduce difficultly dissolved proteins to deposit on the bottom of the centrifugation tubes. Secondly, the pH value also plays an important role for the solubilities of proteins. The isoelectric points (pI) of many plasma proteins is less than 7. Therefore the pH 7.4 phosphate

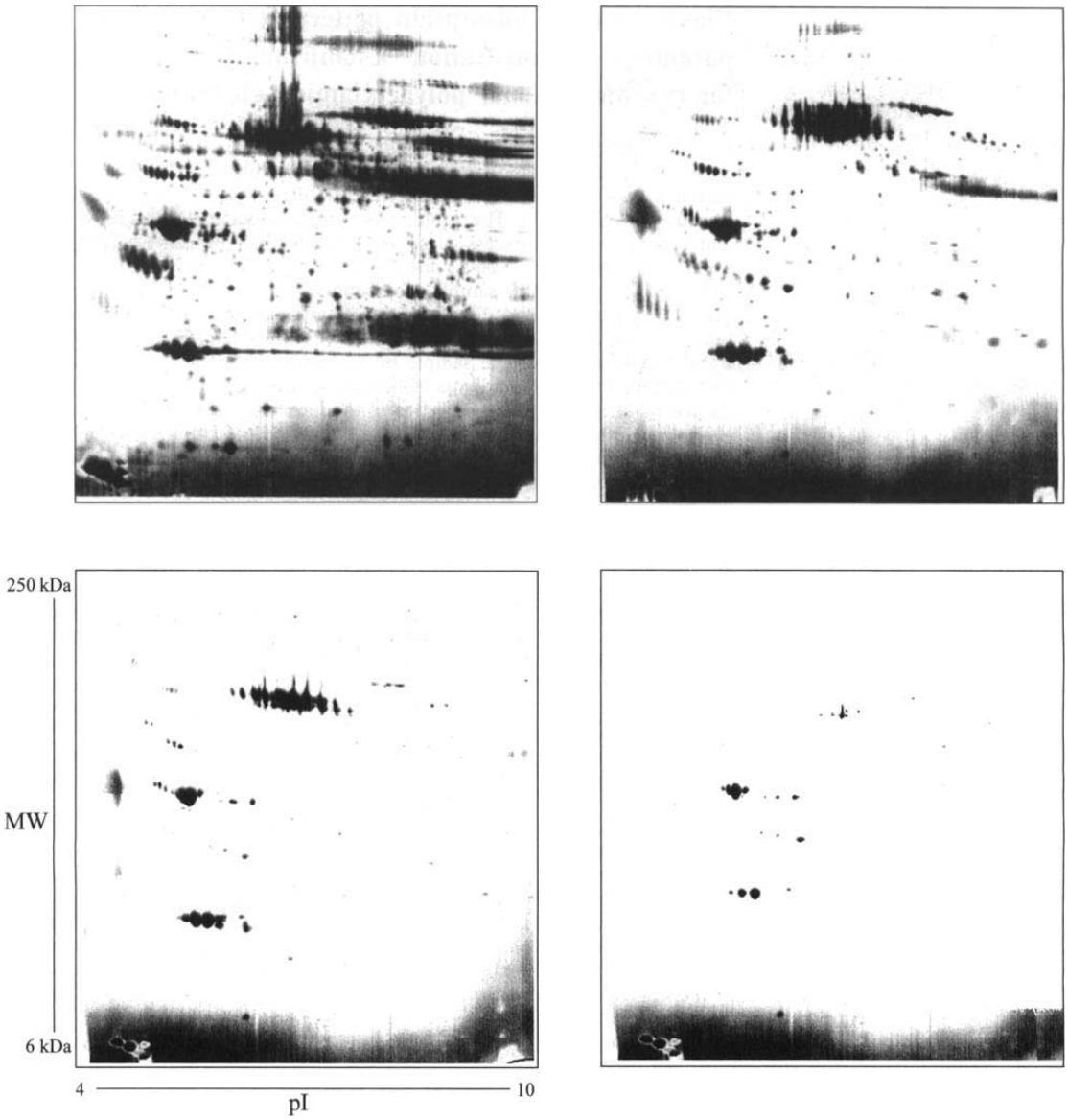


Figure 2.3. Plasma protein adsorption pattern after separation from excess plasma by centrifugation (upper left), the second washing step (upper right), the third washing step (lower left) and the fourth washing step (lower right); washing was performed using phosphate buffer pH 7.4. The first dimension was carried out using IPG strips (Harnisch and Müller, 1998).

buffer was used (Göppert and Müller, 2003, 2004, 2005a, 2005b, 2005c; Weyhers et al., 2005), which could enhance the solubilities of proteins and decrease the artificial protein depositions. Finally, about the number of washing steps, in previous studies, three times were considered as the optimum (Harnisch and Müller, 1998; Blunk, 1994), which is the compromise between possible contamination by residual plasma proteins and loss of large amounts of adsorbed proteins, such as shown by the results in Figure 2.3. Therefore, three times of washing steps are chosen in our experiments.

## 2.2 Rehydration of IPG strips

The steps of IPG strip rehydration:

(1) Removing the obtained sample solution from the centrifugation tube into each slot of rehydration tray;

(2) Putting IPG strip with gel side down into the slot, air bubble-free on the sample, and strip should float on it;

(3) After 5-10 min overlaying each strip with 1-2 ml silicone oil to prevent desiccation of the strips, and covering with rehydration tray lid;

(4) Rehydration overnight at room temperature for the isoelectric focusing.

## 2.3 Isoelectric focusing (IEF)

Isoelectric focusing (IEF) is a technique for separating different molecules due to differences of their isoelectric points (pI) with the supporting matrix of immobilized pH gradient (IPG) gel in a electric current environment.

### 2.3.1 Isoelectric point (pI)

The isoelectric point is the pH at which a particular molecule or a surface of carriers posses no net electrical charge, in other words that the negative and positive charges are equal. Amphoteric molecules contain both positive and negative charges depending on the functional groups presented on the molecule surfaces. The net

charge on the molecule is altered by the pH of its surrounding environment due to the loss or gain of protons ($H^+$). Biological amphoteric molecules such as proteins contain both acidic and basic functional groups in the same molecule. Amino acids which form proteins could be positive, negative, neutral, or polar in nature, and they together give a protein its overall charge in the solution. At a pH below its pI, the protein carries a net positive charge; above its pI it carries a net negative charge. So proteins could be separated according to their isoelectric point (overall charge) using the isoelectric focusing technique which employs an immobilized pH gradient to separate proteins. Isoelectric focusing is the first step in 2-DE.

Proteins consist of one or more chains of amino acids. For an amino acid with only one amine and one carboxyl group, its pI could be calculated by the mean of their acid dissociation constants:

$$pI = \frac{pK_a + pK_c}{2}$$

where pKa and pKc are the acid dissociation constants of the amine and the carboxyl group. For a protein, the accurate pI could be achieved by experiments. For instance, pI of serum albumin is 4.7-4.9.

## 2.3.2 IEF in the immobilized pH gradient (IPG) gels

The IPG gels are polyacrylamide gels with a immobilized pH gradient. The immobilized pH gradient is achieved by the continuous variation in the ratio of Immobilines which contain a set of eight acrylamide derivatives, weak acids and bases, having the following general chemical composition: $CH_2$=CH-CO-NH-R, where R denotes either weak carboxyl group or tertiary amino group. The schematic diagram of IPG gels is shown in Figure 2.4.

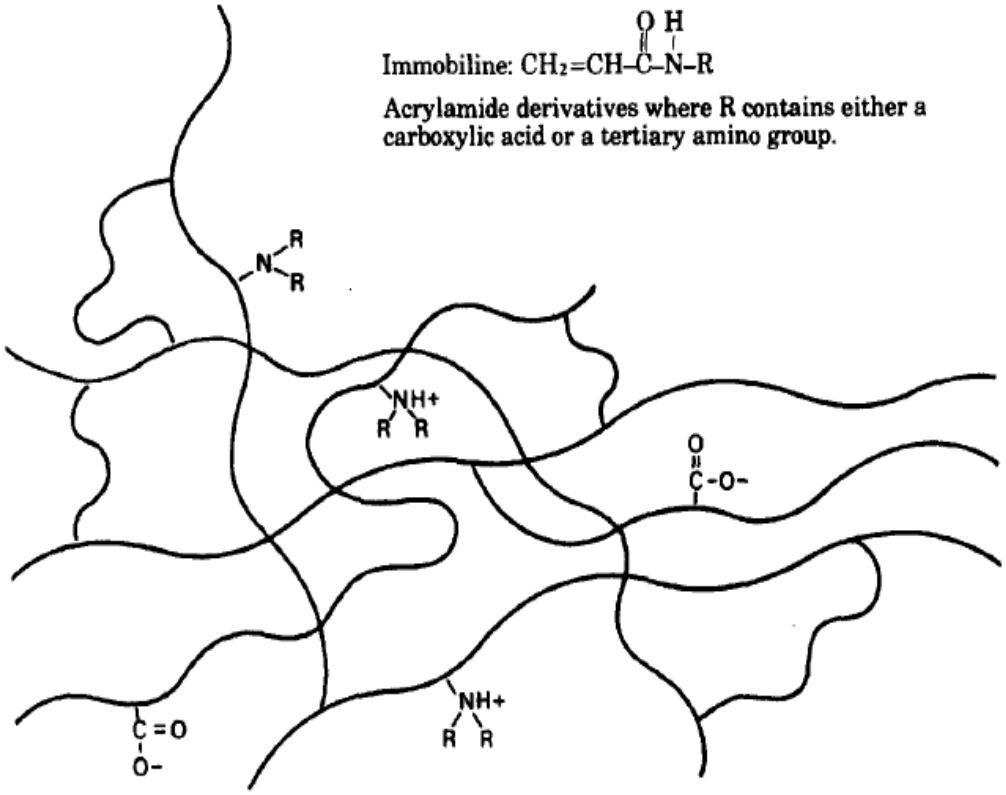


Figure 2.4. Hypothetical gel structure where the lines represent the neutral polyacrylamide, and the positive and negative charges are the immobiline molecules (Hames, 1998).

When an electric current is passed through the medium, it creates a "positive" anode and "negative" cathode end. Negatively charged molecules migrate through the pH gradient in the medium towards the "positive" end while positively charged molecules move towards the "negative" end. As a molecule moves towards the pole opposite of its charge it moves through the changing pH gradient until it reaches a point where the pH corresponds to the isoelectric point of the molecule. At this point the molecule no longer has a net electric charge (due to the protonation or de-protonation of the associated functional groups) and will not proceed any further within the gel. Thus, under an electric current environment, a protein that is in a pH region below its pI will be positively charged and so will migrate towards the cathode (negative). As it migrates through a gradient of increasing pH, however, the protein's overall charge will decrease until the protein reaches the pH region that corresponds to its pI. At this

point it has no net charge and so migration ceases (as there is no electrical attraction towards either electrode). As a result, the proteins become focused into sharp stationary bands with each protein positioned at a point in the pH gradient corresponding to its pI. The experimental operation of IEF in my experiments is:

(1) Setting the IPG strips (17 cm, and pH 3-10) loaded proteins on a Multiphore II from Amersham Pharmacia Biotech with a E 752 power supplied from Consort, and the gel side is up;

(2) Overlaying the IPG strips with paraffin, and covering with the lid;

(3) Adjusting the temperature of cooling water to 20 °C;

(4) Switching the electrical power on (the set of current for IEF is shown in Table 2.3.).

Table 2.3. The set of current for IEF.

| Program step | Voltage (V) | Time (h) |
|---|---|---|
| 1 | 150 | 1 |
| 2 | 300 | 1 |
| 3 | 600 | 1 |
| 4 | 1500 | 1 |
| 5 | 3000 | 12.5 |
| total | | 16.5 |

## 2.4 IPG strip equilibration

After the IEF step, the IPG strip is saturated with the SDS buffer before SDS-PAGE, which calls IPG strip equilibration. The equilibration allows the focused proteins to fully interact with SDS. Firstly, the IPG strips are incubated in the equilibration solution I for 15 min. And then the equilibration solution II is employed to saturate the IPG strips for 20 min. Finally, the running buffer is used to clear residues of the equilibration solution on the surfaces of IPG strips. The preparations of equilibration I and II, 0.5 M Tris-HCL (pH 6.8) and the running buffer for SDS-PAGE are shown in

Table 2.4 2.5 and 2.6, respectively.

Table 2.4. Preparations of equilibration I and II.

| | Equilibration solution I | Equilibration solution II |
|---|---|---|
| DTE | 2.0 g | - |
| Iodoacetamide | - | 4.0 g |
| SDS | 3.0 g | 2.0 g |
| 0.5 M Tris-HCL (pH 6.8) | 10.0 ml | 10.0 ml |
| Glycerol (87 %) | 34.5 g | 34.5 g |
| Urea | 36.0 g | 36.0 g |
| Bromphenol blue | 0.5 ml | 0.5 ml |
| $H_2O$ (Milli Q water) | Add to 100.0 ml | Add to 100.0 ml |
| Time | 15 min | 20 min |

Table 2.5. Preparation of 0.5 M Tris-HCL (pH 6.8).

| 0.5 M Tris-HCL (pH 6.8) | |
|---|---|
| Tris base | 18.15 g |
| $H_2O$ (MilliQ water) | 50 ml |
| 1 N HCL | Adjust to pH 6.8 with 1 N HCL, add $H_2O$ (MilliQ water) to 300 ml, store at 4 °C. |

Table 2.6. Preparation of running buffer for SDS-PAGE.

| Running buffer for SDS-PAGE | |
|---|---|
| SDS | 14.0 g |
| Tris | 42.4 g |
| Glycin | 208.0 g |
| $H_2O$ (MilliQ water) | Add to 14 L |
| After prepared, the running buffer is stored at 4 °C. | |

After equilibration, the IPG strips are applied to SDS-PAGE. Equilibration introduces reagents essential for the SDS-PAGE step. The equilibration solution contains buffer, urea, glycerol, reductant, SDS, and dye:

(1) Equilibration buffer (Tris-HCL (pH 6.8)): maintains IPG strip pH in a range appropriate for SDS-PAGE;

(2) Urea: together with glycerol, reduces the effects of electroendosmosis by increasing the viscosity of the buffer. Electroendosmosis is due to the focused proteins binding strongly to the fixed charged groups of the IPG gel, which interfere protein transfer from the IPG gel to the SDS-PAGE gel;

(3) Glycerol: together with urea, reduces electroendosmosis and improves protein transfer from the IPG gel to the SDS-PAGE gel;

(4) DTE: reduces the disulphide bridges of proteins and preserves them in the reduced state;

(5) Iodoacetamide: alkylates thiol groups on proteins, preventing the thiol groups from re-oxidating during electrophoresis, because that protein reoxidation during electrophoresis can generate streaking and other artifacts; also alkylates residual DTE to prevent point streaking and other artifacts (Görg et al., 1987);

(6) SDS: denatures proteins and form SDS-protein complexes with negative charges. The overall of negative charges is directly proportional to the mass of the protein;

(7) Tracking dye (bromophenol blue): helps to monitor the progress of electrophoresis.

## 2.5 SDS-polyacrylamide gel electrophoresis

Electrophoresis is a relatively simple, rapid and highly sensitive tool to investigate the properties of proteins. The protein separation by electrophoresis is based on the matter that charged molecules will migrate through a matrix upon application of an electric field provided. In general, the proteins are run in a support matrix such as agarose or polyacrylamide gel. Agarose is mainly used to separate larger macromolecules such as

nucleic acids whereas a polyacrylamide gel is widely employed to separate proteins. Within the last several decades, various polyacrylamide gel electrophoretic methods have been developed to resolve different problems. Among different methods, sodium dodecyl sulfate (SDS)-polyacrylamide discontinuous gel electrophoresis is the most commonly used system by which proteins are separated strictly according to their sizes. The analyzed proteins have been denatured in this method.

## 2.5.1 The polyacrylamide gel

Monomeric acrylamide and N,N'-methylene-bisacrylamide (bisacrylamide) are used to form the polyacrylamide gel, the schematic diagram of which has been shown in Figure 2.5.

The co-polymerization reaction of acrylamide and bisacrylamide is triggered by either chemical or photochemical system which is called initiator. Chemical polymerization is initiated by TEMED (tetramethylethylenediamine) and ammonium persulfate. Ammonium persulfate activate the acrylamide monomer to produce a long polymer chain. The elongating polymer chains are randomly cross-linked by bisacrylamide to form a net structure. TEMED is added to serve as a catalyst to accelerate the polymerization reaction because of its ability to carry electrons.

Various factors affect polymerization. Some factors change the rate of polymerization while others alter the properties of the gel such as its pore size, elasticity, and homogeneity.

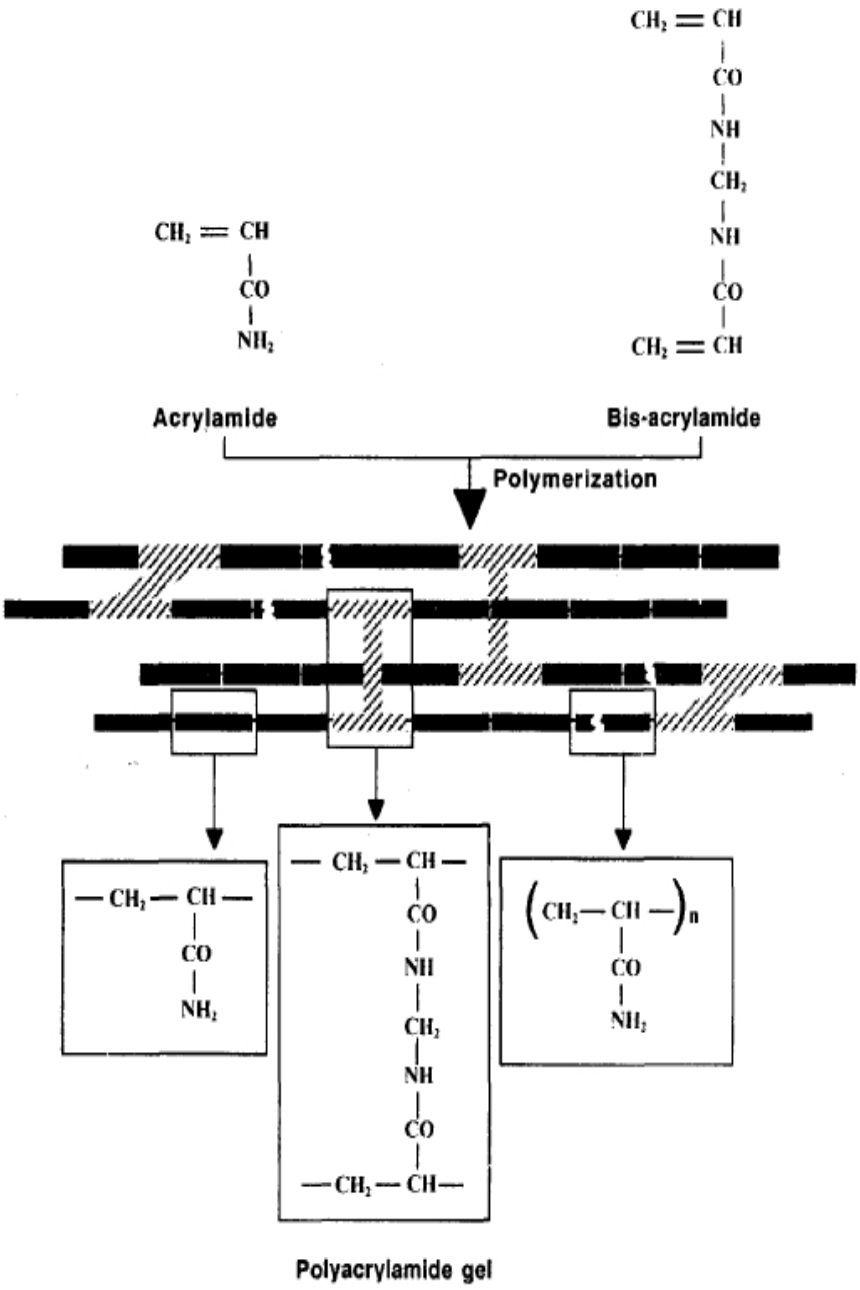


Figure 2.5. Schematic diagram of forming polyacrylamide gel (Hames, 1998).

### 2.5.1.1 The rate of polymerization

The following factors affect the rate of polymerization:

(a) Initiators: a higher concentration of initiator will results in faster polymerization;

(b) Purity of reagents: contaminants may disturb the polymerization with inhibition or acceleration;

(c) Ammonium persulfate: the ammonium persulfate solutions should be prepared fresh daily due to beginning to break down immediately after dissolved in water;

(d) pH: the persulfate system gives optimum efficiency only in the pH 7-10 range (Caglio and Righetti, 1993);

(e) Temperature: higher temperature drives the polymerization faster and vice versa (Gelfi and Righetti, 1981; Righetti and Caglio, 1993), while the optical temperature is from 23 to 25 ℃;

(f) Oxygen: oxygen traps free radicals resulting in inhibiting the polymerization of acrylamide;

(g) Concentration of monomers: a higher concentration of monomer will result in faster polymerization as well.

#### 2.5.1.2 Porosity of the gel

The size of the pores in the gel is mainly controlled by the amount of total acrylamide used per unit volume and the degree of cross-linkage. The latter depends on the relative percentage of bisacrylamide used. When the proportion of cross-linker is increased, the size of pore decreases. It has been observed that the average pore size is a minimum when the amount of bisacrylamide is about 5 % of the total acrylamide (Fawcett and Morris, 1966). But with the proportion of cross-linker increasing above the amount for the minimum pore size, the acrylamide polymer chains become cross-linked to form larger bundles with larger spaces so that the effective pore size increases as well.

The rate of polymerization also affects the pore size. Increasing the rate of polymerization could result in a less porous gel whereas reducing this rate produce a opposite effect. Thus those factors that alter the rate of polymerization will also affect the pore size. For instance, a smaller pore size gel will be achieved by increasing the concentration of acrylamide.

Another factor which could influence the pore size is e.g. the efficiency of monomer to polymer conversion.

#### 2.5.1.3 Homogeneity of the gel

Some factors can affect the homogeneity of polyacrylamide gels:

(a) Lack of thorough mixing of polymerization initiator with the monomer solution causes swirls in the gel. However, too much mixing will add excess oxygen into the solution which will inhibit polymerization step. Thus, a gentle but thorough mixing is required normally;

(b) Gel thickness also influences gel homogeneities. When the thickness of gel is above the critical value of 3 mm, gravity will induce gel inhomogeneities occurred (Righetti et al., 1994). Below this critical thickness, the solution layer before to form gel is devoid of any convective flow;

(c) The persulfate-driven polymerization is very sensitive to oxygen. In case of the top of the gel mixture not entirely sealed during polymerization by 2-butanol (Mixing 20 ml 2-butanol with 20 ml MilliQ water in a tube, and then shaking the mixture a few seconds. After separated from water on the top of the tube, 2-butanol is applied for seal the gel.), a non-homogeneous gel will be produced;

(d) The rate of polymerization also affects the uniformity of the gel since if polymerization is too fast (< 10 min) or too slow (> 60 min), a non-uniform polymerization will occur. But the rate of polymerization could easily be controlled by adjusting the concentration of initiators.

## 2.5.2 Preparation of the gradient polyacrylamide gel

The pore gradient gel with the size of the pores changing from the top to the bottom of the gel could resolve not only large proteins but also smaller polypeptides. The pore range of prepared gradients could be altered based on the size of proteins. A gradient in the concentrations of reagents such as acrylamide/bisacrylamide, glycerol

is achieved too for the gradient gel. Here, glycerol is added in the heavy solution so that the gradient of glycerol is formed during pouring the gel. Glycerol is employed to minimize mixing by convective disturbances for improving the gradient formation of gel. In our experiments, the proportion of reagents for preparing gels is shown in Table 2.7. In Figure 2.6, the gradient gels are cast from bottom to top in which the light solution fill up the glass chamber firstly from the bottom until reaching the same content, then the heavy solution is switched on. The linear gradient gel is prepared

Table 2.7. Proportion of reagents for preparing 6 gels.

| Amounts for 6 full size gels (total volume 380 ml) | | |
|---|---|---|
| light solution [8 %] (195 ml) | reagents | heavy solution [16.5 %] (185 ml) |
| 52.0 ml | 30 % acrylamide/Bis Stock | 101.8 ml |
| 48.8 ml | 1.5M Tris-Cl pH 8.8 Stock (the preparation is shown in Table 2.8.) | 46.3 ml |
| - | 100 % Glycerol | 18.5 ml |
| 0.98 ml | 10 % APS Stock (the preparation is shown in Table 2.9.) | 0.93 ml |
| 48.7 µl | TEMED | 46.3 µl |
| 94.3 ml | $dH_2O$ | 18.5 ml |

Table 2.8. Preparation of 1.5M Tris-HCL (pH 8.8).

| 1.5M Tris-HCL (pH 8.8) | |
|---|---|
| Tris base | 54.45 g |
| H2O (MilliQ water) | 150 ml |
| 1 N HCL | Adjust to pH 8.8 with 1 N HCL, add $H_2O$ (MilliQ water) to 300 ml, store at 4 °C. |

Table 2.9. Preparation of fresh 10 % APS (Ammonium persulfate) stock.

| 10 % APS stock | |
|---|---|
| APS | 0.2 g |
| $H_2O$ (MilliQ water) | Add to 2 ml |

with 8-16 % acrylamide. After prepared, the gels with 1-2 ml 1.5M Tris-HCL (pH 8.8) on the top are stored at 4 ℃ before electrophoresis.

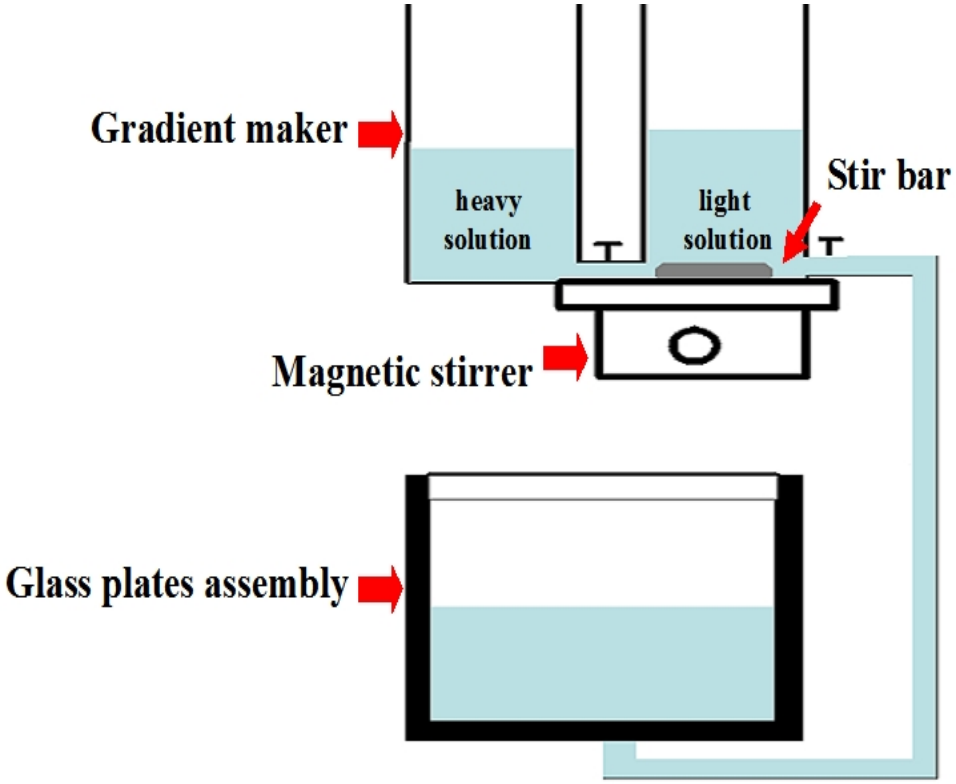


Figure 2.6. Schematic diagram of apparatus for making a gradient gel.

## 2.5.3 Running gel electrophoresis

The gels are fixed and the IPG strips after equilibration are put on the top of the gels. Agarose is used to seal the gel (the preparation of agarose solution is shown in the Table 2.10).

The gel electrophoresis was performed in Protean II Multi-Cells with a 1000 power unit obtained from Bio-Rad. 40 mA current is provided for each gel until bromphenol

Table 2.10. Preparation of 0.5 % agarose solution.

| 0.5 % agarose solution | |
|---|---|
| Agarose | 0.5 g |
| H2O (MilliQ water) | Add to 100.0 ml |

blue appears to the bottom of the gels. The running buffer is attained with the preparation shown in Table 2.6. In the SDS-PAGE system the protein has been denatured by heating at 95 ℃ in the presence of excess SDS and a thiol reagent DTE (dithioerythritol) during the sample preparation step. Under these conditions, all proteins bind SDS in a constant weight ratio to form SDS:polypeptide complexes with identical charge densities. Therefore, based on their sizes, proteins could be separated in polyacrylamide gels with pores. The mobility of protein is relative to its molecular weight, which could be described by the following equation:

$$\log MW = K - bX$$

where MW is molecular weight;

X is mobility;

K, b are constants.

## 2.6 Silver stains

After SDS-PAGE, choosing a most suitable protein visualization procedure is essential. There are several important criteria included, e.g., the ease of use, speed of detection, level of sensitivity, and integrity of the proteins after visualization which is essential for further analysis of proteins. Meanwhile, maintaining a linear and stoichiometric relationship between protein detection intensity and protein concentration on the gel should also be considered for choosing proper methods. In Table 2.11, sensitivities of different staining methods are compared, and the silver stain method is the most sensitive one.

In 1979, Merril et al. (1979) introduced the silver staining technique for protein

Table 2.11. Comparison of staining sensitivities for protein visualization on gel.

| Staining method | Protein (ng) | Reference |
|---|---|---|
| Coomassie blue R-250 | 38 | Switzer et al., 1979 |
| Silver stains | 0.02 | Merril and Goldman, 1984 |
| Negative stains | 5 - 1500 | Lee et al., 1987; Dzandu et al., 1988; Higgins and Dahmus, 1979 |
| Pre-electrophoretic fluorescent stains | 6 - 10 | Ragland et al., 1978 |

detection in polyacrylamide gels, which is greatly enhancing the sensitivity of protein detection compared to other techniques, e.g., coomassie blue staining, negative staining. In our experiments, the protocol of silver staining is shown in Table 2.12.

The typical result of a 2-DE gel by silver staining is shown in Figure 2.7 (human plasma). On the gel (Figure 2.7), the pI is 4.0-8.0 (from left to right, non-liner) and the molecular weight of protein is 6-250 kDa (from bottom to top, non-liner).

Table 2.12. (a) Preparation of reagent for 6 gels; (b) protocol of silver staining.

(a) Reagent Preparation for 6 gels.

| | Reagent [ml] | $dH_2O$ [ml] | Total [ml] |
|---|---|---|---|
| Oxidizer | 120 | 1080 | 1200 |
| Silver Reagent | 120 | 1080 | 1200 |
| Developer | dissolve one bottle in 3.6 litres of $dH_2O$ by stirring for 15 min at room temperature | | |

| | EtOH [ml] | acetic acid [ml] | $dH_2O$ [ml] | Total [ml] |
|---|---|---|---|---|
| FixativeA | 960 | 240 | 1200 | 2400 |
| FixativeB | 480 | 240 | 4080 | 4800 |
| Stop | | 120 | 2280 | 2400 |

(b) Protocol of silver staining.

2. Two-dimensional polyacrylamide gel electrophoresis (2D-PAGE; 2-DE)

| Reagent | Volume [ml] | Duration [min] |
|---|---|---|
| FixativeA 40% ethanol/10% acetic acid (v/v) | 400 | 60 |
| FixativeB 10% ethanol/5% acetic acid (v/v) | 400 | 30 |
| FixativeB 10% ethanol/5% acetic acid (v/v) | 400 | 30 |
| Oxidizer | 200 | 10 |
| Deionized water | 400 | 10 |
| Deionized water | 400 | 10 |
| Deionized water | 400 | 10 |
| | repeat washes until all the yellow color is removed from the gels | |
| Silver reagent | 200 | 30 |
| Deionized water | 400 | 2 |
| Developer | 200 | ~ 30 sec |
| | develop until solution turns yellow or until brown precipitate appears | |
| Developer | 200 | ~5 |
| Developer | 200 | ~5 |
| Stop 5% acetic acid (v/v) | 400 | ~5 |

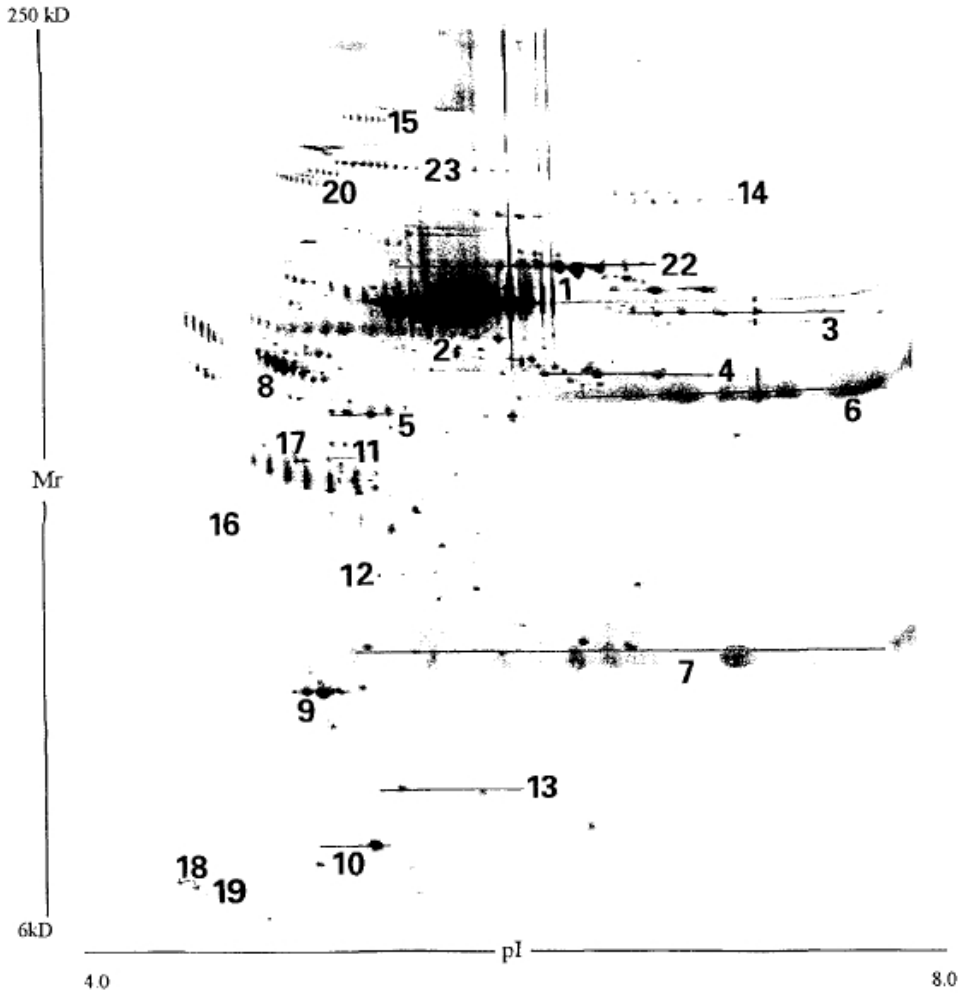


Figure 2.7. 2-DE gel of human plasma. 1, Transferrin; 2, Albumin; 3, Fibrinogen α; 4, fibrinogen β; 5, fibrinogen γ; 6, IgG γ; 7, Ig light chains; 8, α1-antitrypsin; 9, apolipoprotein A-I; 10, transthyretin; 11, actin; 12, apolipoprotein E; 13, haptoglobin α2 chain; 14, plasminogen; 15, α2-macroglobulin; 16, apolipoprotein J; 17, apolipoprotein A-IV; 18, apolipoprotein C-II; 19, apolipoprotein C-III; 20, PLS:6; 22, IgM μ chain; 23, PLS:5 (Anderson and Anderson, 1991).

## 2.7 Scan and calculation

After silver staining, the gels fixed between two sheets are scanned by an ImageScanner (Amershan Pharmacia Biotech). The spots on gels were recognized by matching the master map of human plasma (Anderson and Anderson, 1991; Hoogland et al., 2000). The amount of adsorbed protein was analyzed using a semi-quantitative manner based on the spot size and intensity on the gel (Blunk et al., 1993; Blunk,

1994). The data of spots on gels are calculated by the Melanie III software (Swiss Institute of Bioinformatics, Geneva, Switzerland).

# 3. Introduction of instruments

## 3.1 Photon correlation spectroscopy

### 3.1.1 Size and polydispersity index

#### 3.1.1.1 Mono-particle model

Dynamic light scattering (DLS) is a versatile and useful of technique for measuring the sizes (the range of size from 5 nm to 3-5 μm) and size distribution of nanoparticles in a liquid. Photon correlation spectroscopy (PCS) is one of the DLS techniques. PCS measures and analyses the fluctuation of the intensity of light scattered from particles in suspension. This fluctuation itself is a result of "Brownian motion" of the water molecules in the dispersion medium, which keeps the particles in steady movement. The molecules of a supporting liquid move randomly at a defined speed that is determined by temperature and viscosity. Whenever such molecules collide with a particle suspended in the liquid an elastic impact is produced, which moves the suspended particle. The speed at which the particle moves depends on the size of the particle. Small particles will move quickly whereas coarser particles will move at a much slower rate because of their greater mass. Such bigger particles have a statistically-increased chance of being impacted from different directions by more than one molecule at the same time. This diffusion effect can be described by the well-known "Stokes-Einstein" equation:

$$D = \frac{k_B T}{3\pi\eta x}$$

where:

D is the diffusion constant;

$k_B$ is Boltzmann's constant;

T is the absolute temperature;

Ŋ is dynamic viscosity of the liquid;

x is the particle diameter.

Since the change in the intensity of light scattered by the particle depends on its diffusion velocity, which can be described by the follow equations. The normalized scattered intensity time autocorrelation function of the scattered light intensity could be written as:

$$g_2(\tau) = \frac{\langle I(0)I(\tau)\rangle}{\langle I(0)^2\rangle} = 1 + \gamma|g_1(\tau)|^2$$

where:

$g_1$ is the normalized scattered electric field time autocorrelation function;

$\tau$ is the decay time;

$\gamma$ is a constant determined by the experimental apparatus (In an ideal apparatus, the constant $\gamma$, often called the "coherence factor", is equal to 1, so the normalized intensity autocorrelation function of the scattered light intensity starts at a value of 2 at zero time delay and eventually decays to 1, but in practice $\gamma$ is usually less than 1 (Pecora, 2000). Note that the $g_1(\tau)$ is given in the below equation.).

The scattered electric field time autocorrelation function is described by:

$$g_1(\tau) = \exp(-\Gamma\tau)$$

where:

$\Gamma = Dq^2$;

D is the diffusion coefficient;

q is the scattered light vector.

The $g_1(\tau)$ is determined by the translational self-diffusion coefficient of the particle D and the scattered light vector. The scattered light vector q is related to the scattering angle $\theta$ and wavelength $\lambda$ of the light in the scattering medium. The scattering vector length is described as:

$$q = (4\pi n/\lambda_0)\sin(\theta/2)$$

where:

n is the refractive index of dispersion medium;

$\lambda_0$ is the wavelength of laser;

$\theta$ is the angle of scattered light.

Thus, after the self-diffusion coefficient (D) of the particle is known, the particle size could be obtained by the "Stokes-Einstein" equation.

When the nanoparticles are non-spherical or flexible, the radius derived from the self-diffusion coefficient and the Stokes-Einstein relation is called the "hydrodynamic radius". The hydrodynamic radius for non-spherical nanoparticles is not equal to a the geometrical particle radius. The relation between the hydrodynamic radius and the actual dimensions of non-spherical particles depends on the particle shape.

### 3.1.1.2 nanoparticle dispersions

For nanoparticle dispersions, the particles are always with a distribution of sizes and shapes instead of a single size and shape. In general, the particles have different translational self-diffusion coefficients (D). Thus, the normalized scattered electric field time autocorrelation function of the dilute solution can be rewritten:

$$g_1(\tau) = \sum_i A_i \exp(-\Gamma_i \tau) = \sum_i A_i \exp(-q^2 D_i \tau)$$

where $A_i$ is a weighting factor proportional to the fraction of the scattered intensity contributed by this subset of particles (i).

Nevertheless, in analyzing PCS data, take the continuous limit of the sum in the above normalized scattered electric field time autocorrelation function of the dilute solution:

$$g_1(\tau) = \int_0^\infty A(\Gamma) \exp(-\Gamma \tau) d\Gamma$$

where $\int_0^\infty A(\Gamma) d\Gamma = 1$.

Thus, the mean value of $\Gamma$ and the mean size of nanoparticles ($x_{PCS}$):

$$\langle \Gamma \rangle = \int_0^\infty \Gamma A(\Gamma) d\Gamma$$

$$\frac{1}{x_{PCS}} = \int_0^\infty \frac{1}{x} A[\Gamma(x)] H(\frac{1}{x})$$

and the polydispersity index (PI) are obtained by the following equation:

$$PI = \frac{\mu_2}{\langle \Gamma \rangle^2}$$

where $\mu_2 = \int_0^\infty (\Gamma - \langle \Gamma \rangle) A(\Gamma) d\Gamma$ .

### 3.1.1.3 Schematic diagram of a PCS apparatus

Figure 3.1 shows the schematic diagram of latest PCS setup from the Malvern company (UK). In our experiments, the Zetasizer Nano ZS is employed to characterize the samples. Light from a laser is focused on a sample and the light scattered at a given scattering angle is collected by a detector (a photomultiplier, or an avalanche photodiode). The output is sent to an digital signal processor (correlator).

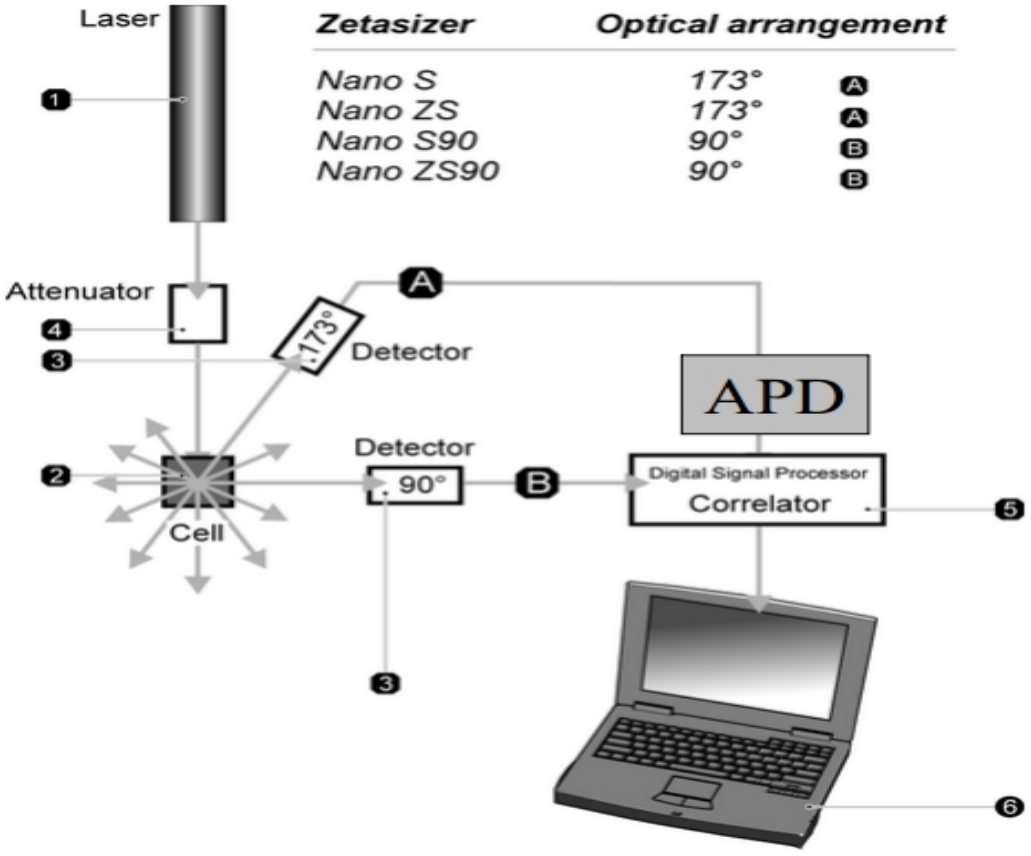


Figure 3.1. Schematic diagram of the PCS apparatus Zetasizer (Malvern company, UK) (APD: Avalanche Photo Diode).

The stability and temperature of the sample are two important factors for repeatability

during the testing. Instability (e.g. aggregation) could affect the light scattering, and the temperature can influence the Brownian motion of the particles. During my experiments, the measurements were performed at 25 ℃ and the dispersion medium is MilliQ water.

## 3.1.2 Zeta potential

Particles are undergoing the Brownian motion in the colloidal system. The scientists Derjaguin, Landau, Verwey and Overbeek developed a theory in the 1940s which estimated the stability of colloidal systems (e.g., suspensions, emulsions). The electrical double layer is assumed in the DLVO theory. The liquid layer surrounding the particle exists of two parts: an inner region (Stern layer) where the ions are strongly bound on the particle surface, and an outer layer (diffusive layer) which

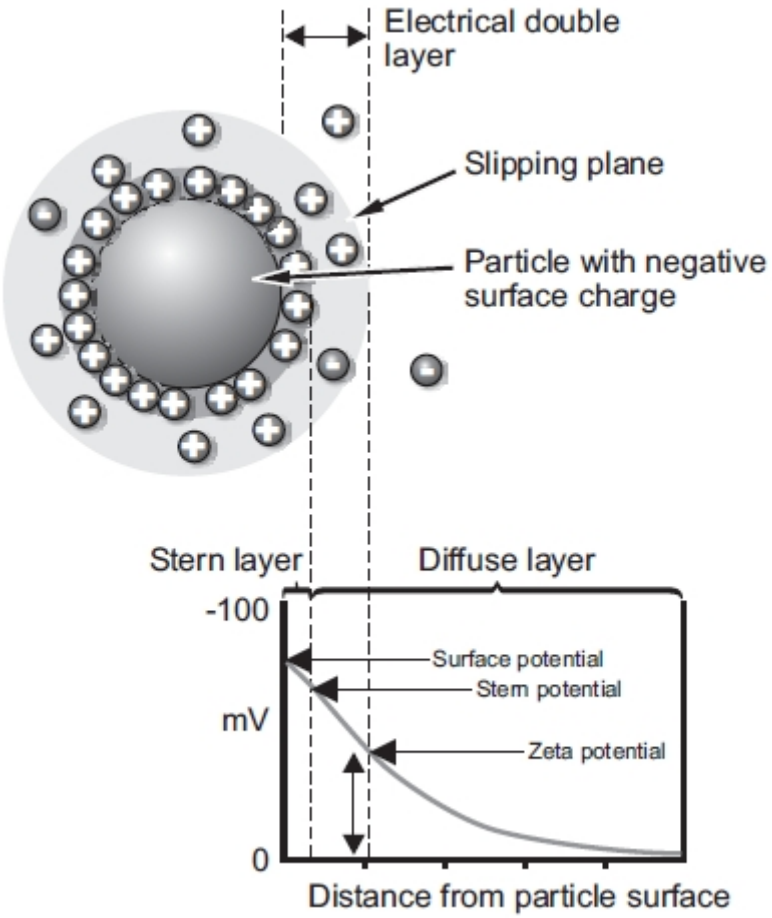


Figure 3.2. The schematic diagram of electrical double layer around the charged particle in liquid (Malvern company, UK).

contains the slipping plane. When the particle moves, the slipping plane is the boundary within which the ions move and beyond which the ions stay. Zeta potential is the potential on the slipping plane, which is an important index of the surface potential of the particle as well as the stability of the colloidal system.

### 3.1.2.1 DLVO theory

DLVO theory suggests that the stability of a particle in the medium depends on its total potential energy function $V_T$ which is the balance of several competing contributions:

$$V_T = V_A + V_R$$

where $V_A$ and $V_R$ are respectively the attractive and repulsive contributions. When $H_0 << a$, the van der Waals attractive force ($V_A$) could be written as:

$$V_A = -\frac{Aa}{12H_0}$$

where A is the Hamaker constant and a is the radius of nanoparticle, and $H_0$ is the shortest distance between nanoparticles; $V_R$ is the electrical double layer repulsive force:

$$V_R = \frac{64\pi a n_0 kT\gamma^2}{\kappa^2}\exp(-\kappa H_0)$$

where $n_0$ is the number density of ion in the bulk solution, and k is the Boltzmann constant, and $\gamma = \tanh\left(\frac{ze\psi_0}{4kT}\right)$ ($\psi_0$ is the potential on the particle surface), and κ is a function of the ionic composition in the solution ( $\kappa = \left(\frac{e^2\sum_i z_i^2\rho_i}{\varepsilon kT}\right)^{1/2}$ , where $\rho_i$ is the number density of ion i in the bulk solution, and $z_i$ is the valency of the ion i and ε is the medium permeability or dielectric constant.) and $\frac{1}{\kappa}$ is the thickness of the double layer. The sum of van der Waals attractive and electrical double layer repulsive

forces is:

$$V_T = \frac{64\pi a n_0 kT\gamma^2}{\kappa^2}\exp(-\kappa H_0) - \frac{Aa}{12H_0}$$

The variation of net energy with particle separation according to the DVLO theory is shown in Figure 3.3. When the particles have a sufficiently high repulsion the colloidal system will be sTable. Thus, the potential on the particle surface ( $\psi_0$ ) is recognized as a very good index for assessing the stability of colloidal systems.

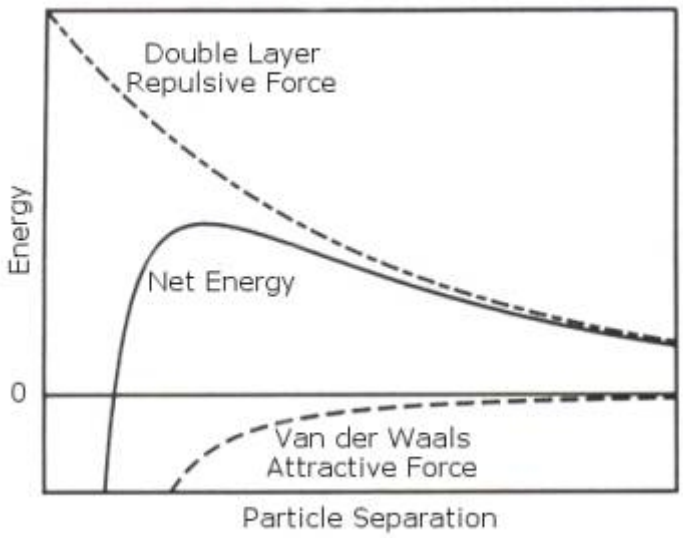


Figure 3.3. Schematic diagram of the variation of net energy with separation distance according to DLVO theory (Malvern company, UK).

### 3.1.2.2 Zeta potential

Zeta potential is the electric potential in the interface between slipping plane of the dispersed particle and the dispersion medium. It is an essential index to characterize the surface potential of nanoparticle. Therefore it is also important for assessing the stability of colloidal system according to the DLVO theory.

The zeta potential is measured with the electrophoretic mobility by the Henry equation:

$$U_E = \frac{2\varepsilon\zeta f(\kappa a)}{3\eta}$$

where

$U_E$ is electrophoretic mobility of the charged particle under employing an electric field;

ε is the medium dielectric constant;

ζ is zeta potential;

η is the medium viscosity;

f(κa) is Henry's function;

$\kappa^{-1}$ is the thickness of the electrical double layer and a is the radius of the particle, so $\kappa a$ is the ratio of the particle radius to electrical double layer thickness. Two values are generally used as approximations for the f(κa) determination: 1.5 or 1.0. As shown in Figure 3.4, for the large particles (larger than 200 nm), when electrophoretic mobility is measured in aqueous medium and moderate electrolyte concentration (more than 0.001 M salt) , f(κa) is 1.5 and thus the calculation of zeta potential fit the Smoluchowski model. However, for the small particle in low dielectric constant medium (e.g., non-aqueous medium), f(κa) is 1.0 and thus the Huckel model is employed in the calculation.

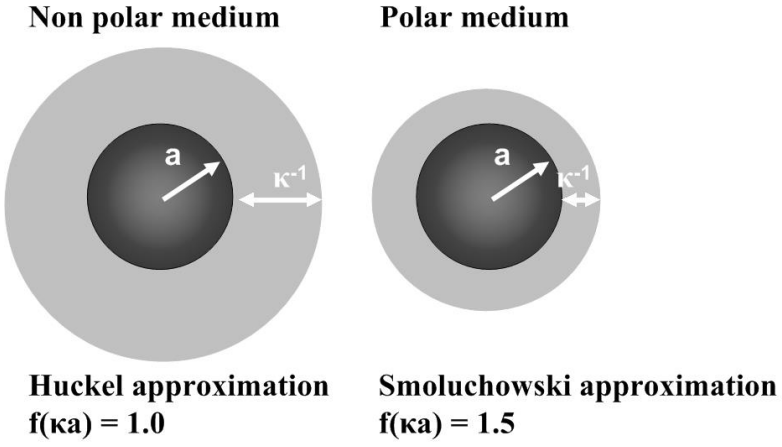


Figure 3.4. Schematic illustrating Huckel and Smoluchowski approximations used for converting the electrophoretic mobility of particle under the electric field into zeta potential (Malvern company, UK).

The relationship of the zeta potential values and the stability of colloidal systems is shown in Table 3.1. Therefore, the general dividing line between sTable and unsTable suspensions is generally taken as either +30 or -30 mV. In other words, when the zeta potential of particles are more positive than +30 mV or more negative than -30 mV the suspension systems are normally considered sTable.

Table 3.1. Relationship of the zeta potential values and the stability of the colloidal systems (Müller, 1996).

| Zeta potential (mV) | Stability behavior of the colloid |
|---|---|
| from 0 to ± 5 | Rapid coagulation or flocculation |
| from ± 10 to ± 30 | Incipient instability |
| from ± 30 to ± 40 | Moderate stability |
| from ± 40 to ± 60 | Good stability |
| more than ± 61 | Excellent stability |

### 3.1.2.3 Measuring electrophoretic mobility

In our experiments, a Malvern's Zetasizer Nano ZS apparatus is used to obtain the zeta potential of samples. This apparatus consists of six main components as shown in Figure 3.5, the light from the laser is split to the incident beam and the reference beam. The incident beam passes through the sample cell and the scattered light is detected at a given angle (θ). The scattering light is combined with the reference beam. The combination light is passed to the digital signal processor and then to the computer.

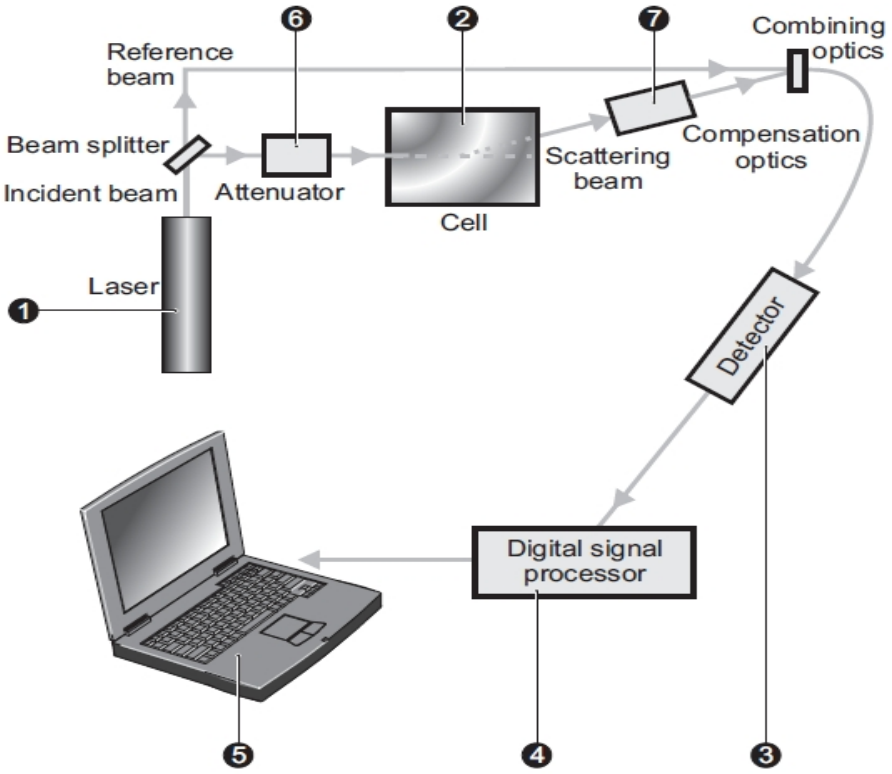


Figure 3.5. Schematic diagram of the setup for zeta potential measurements (Malvern company, UK).

The technique applied to measure the electrophoretic mobility in this apparatus is Laser Doppler Velocimetry (LDV). LDV uses the Doppler shift in the laser beam to measure the electrophoretic velocity of particles. The relationship of frequency deviation of scattered light and the electrophoretic velocity is described by the following equation:

$$\Delta f = \frac{2v\sin(\theta/2)}{\lambda}$$

where v is the electrophoretic velocity of the particle ($U_E$) in the electric field;

$\lambda$ is wavelength of the laser source;

$\theta$ is the scattering angles of light, which is shown in Figure 3.6. The schematic diagram of combination between the reference light and the scattering light is shown in Figure 3.7. Therefore, the $\Delta f$ is obtained and then the electrophoretic velocity of particle is achieved. Finally, according to the Henry equation, zeta potential is gained. In the experiments, a field strength of 20 V/cm was applied. The zeta potential calculation was performed using the Helmholtz–Smoluchowski equation. The zeta

potential has been measured in Milli-Q water adjusted to 50 μS/cm using 0.9 % NaCl solution and in Milli-Q water with 2.5 % glycerol (ω), respectively.

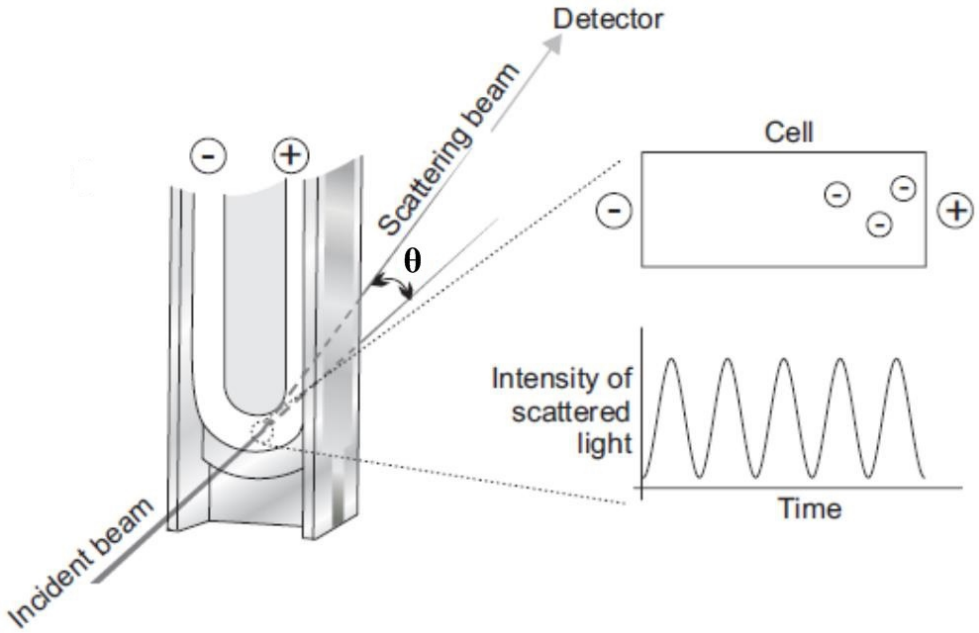


Figure 3.6. The scattering angle (θ) after the incident beam passing through the sample cell (Malvern company, UK).

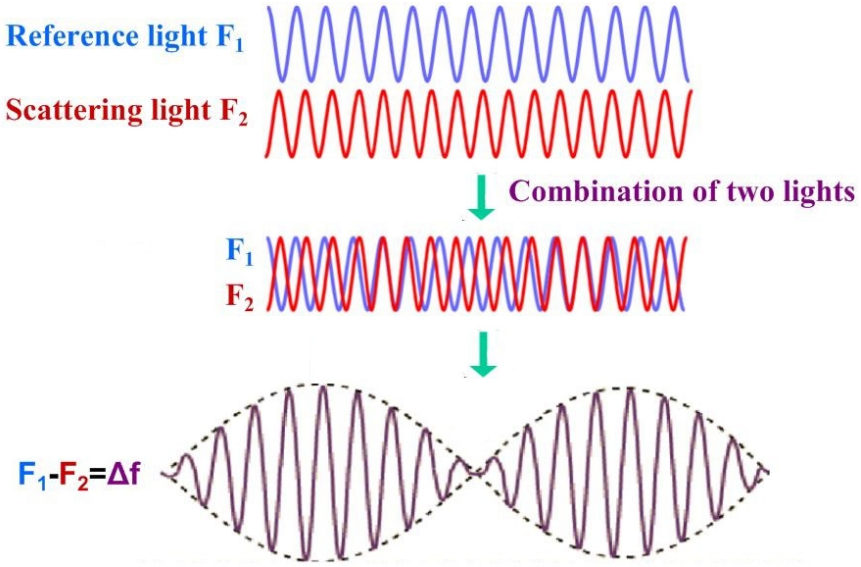


Figure 3.7. Combination of the reference light and the scattering light (F = frequency).

## 3.2 Laser diffractometry

Compared with the dynamic light scattering technique, laser diffraction is another widely used particle sizing technique for materials ranging from hundreds of nanometers up to several millimeters in size. In the experiments, the Mastersizer 2000 (Malvern Instruments, UK) was employed. The Mie theory is used to calculate the sizes of particles, and the optical parameters of particles should be given for the calculation, e.g., egg lecithin-stabilized oil-in-water emulsion nanoparticles 1.497 for the real refractive index and 0.000 for the imaginary refractive index.

## 3.3 High pressure homogenization

High pressure homogenization (HPH) is a very important top-down technology for preparing nanometer drugs. A homogenizer consists of a high-pressure pump and a homogenizing valve (Figure 3.7). The pump forces the coarse product into the valve seat at high pressure and low velocity. High pressure forces the coarse product into the gap between the valve and the valve seat. When arriving at the gap, the coarse product looses pressure and increases speed, which results in cavitation forces, shear forces, and particle collision. Under the action of such composite forces, the hole in the product expands to achieve homogenization and then the size of particle reduces. The homogenized product leaves the gap and hits against the impact ring. Finally, the homogenized product flows out the impact ring and exits from the homogenizer at low velocity and atmospheric pressure for the next process. To preserve the particle size, stabilization with surfactants and stabilizer is required.

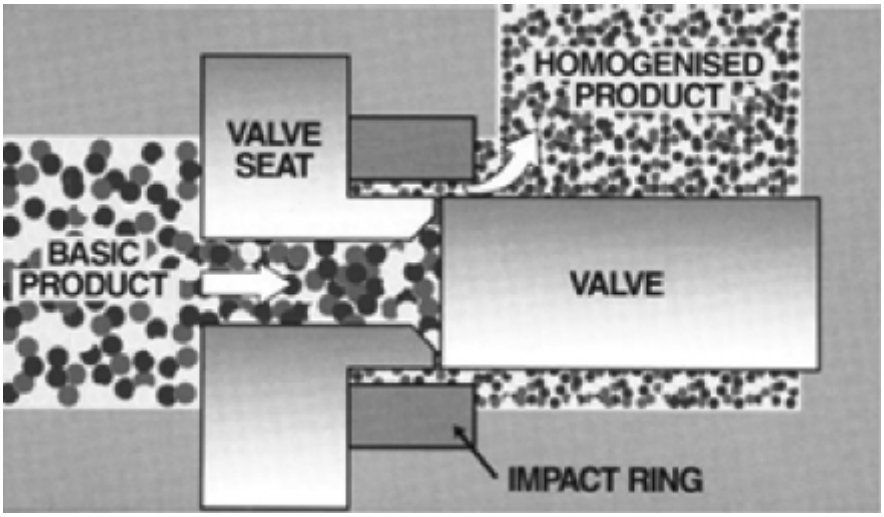


Figure 3.7. The flow path of product through a simple homogenizing valve (Diels and Michiels, 2006).

# 4. Protein adsorption pattern on solid lipid nanoparticles for drug targeting and their interactions

## 4.1 Introduction

In 1991 solid lipid nanoparticles (SLN) were introduced an alternative colloidal drug carrier for oral, parenteral or topical use (Müller and Lücks, 1996; Müller et al., 2000a): similar to polymeric nanoparticles, SLN possess a solid biodegradable matrix, and the solid matrix allows a controlled modification of the release profile of incorporated drugs; similar to emulsions and liposomes, they can be produced on an industrial scale using the high pressure homogenization technology, coating with a layer of surfactant (Müller et al., 2000b; Müller and Souto, 2005); besides, the major disadvantages of polymeric particles (use of organic solvents in production, cytotoxicity of monomers, lack of large scale production technology) and of emulsions (burst release of incorporated drugs) can be eliminated (Müller et al., 1995; Müller et al., 2000c); finally, SLN showed a very good tolerability in *in vitro* cell culture studies (Müller et al., 1996). Based on those, SLN has the potential to be accepted by the regulatory authorities and to be used in patients for i.v. administration (Schwarz et al., 1994).

A relatively large number of research groups are working with this promising drug carrier system SLN. There are several important articles to review SLN as the carrier for drug delivery (Müller et al., 1995; Müller et al., 2000c; Mehnert and Mader, 2001). However, many recent works focus on the studying of proteins adsorption pattern on different SLN *in vitro* (Göppert and Müller, 2003, 2004, 2005a, 2005b; Weyhers et al., 2005) and of adsorption kinetics to understand the interaction between plasma

proteins and SLN (Göppert and Müller, 2005c). Here, the adsorbed protein patterns on different SLN are briefly reviewed and the interactions between them are discussed as well, which is important for further understanding protein adsorption behaviors on nanoparticles and preparation of desired drug carrier systems for targeting specific sites in body.

## 4.2 Protein adsorption patterns on solid lipid nanoparticles

That SLN stabilized with different surfactants (different SLN) could have different properties which results in obtaining different protein adsorption patterns on their surfaces after injected into the human body, and the adsorbed proteins as the biological identities of them will control their behaviors, e.g., circulation time, bio-distribution. The protein adsorption patterns are analyzed *in vitro* by the 2-DE method which is introduced in chapter 2 in details. In general, during the plasma protein-SLN sample preparation for 2-DE *in vitro*, plasma or serum is used to displace blood; to mimic the conditions in the bloodstream, the particles were routinely incubated in plasma for 5 min, because *in vivo* in case recognition by the MPS occurs, in the first 5 min up to 90% of the injected dose are taken up by the liver macrophages (O'Mullane et al., 1987; Müller, 1991; Liliemark et al., 1995), and in case particles survive in the first 5 min, prolonged blood circulation of these particles was found (Illum and Davis, 1987; Cattel et al., 2003); In our studies, reproducible patterns were obtained at 1:3 of the ratio of the particle suspension to the incubation medium (Göppert and Müller, 2003, 2004, 2005a, 2005b, 2005c; Weyhers et al., 2005) when the concentration of suspension was generally in the range of 10-20 % (w/v); the standard separation method of particles from extra plasma is by centrifugation (Blunk, 1994; Harnisch and Müller, 1998; Gessner et al., 2000; Göppert and Müller, 2003).

Table 4.1 shows the adsorbed proteins of various SLN (Göppert and Müller, 2003, 2004, 2005a, 2005b, 2005c; Weyhers et al., 2005). The overall impression about Table

4.1 is that albumin, apolipoproteins (including ApoA-I, ApoA-IV, ApoC-II, ApoC-III, ApoE) and fibrinogens could be identified on all of SLN, but their adsorbed amounts have a correlation with the surfactant on SLN. Compared to other proteins, apolipoproteins were mainly absorbed on SLN.

It has been observed that poloxamine 908-coated 60 nm polystyrene model carrier could circulate longer in blood stream (Illum et al., 1987; Illum et al., 1986). Moreover, Müller et al. (1996) observed that poloxamer 407-SLN and poloxamine 908-SLN were also efficient in avoiding phagocytosis. In Table 4.1, the experimental results show that this two SLN (poloxamer 407-SLN and poloxamine 908-SLN) had a relatively high adsorption amount of albumin on the surface as well which may result in a longer circulation time in the blood circulation. When albumin was adsorbed on the surface of nanoparticles, albumin could create more hydrophilic surfaces which were found to reduce the phagocytic uptake *in vitro* (Ogawara et al., 2004). However, the *in vivo* behaviors of particles are controlled by all of adsorbed proteins. For example, the particles are fast cleared by MPS when they adsorb more opsonins (e.g. immunoglobulin G, fibrinogen), because immunoglobulin G (IgG) was known to be a specific activator of the complement system promoting recognition and phagocytic uptake of particulate carriers by the MPS (Patel, 1992), and fibrinogen as one of opsonins promoted phagocytosis and was removed from systemic circulation by cells of MPS as well (Leroux et al., 1995; Camner et al., 2002). The experimental results in Table 4.1 also show that that two SLN have adsorbed a certain amount of immunoglobulin G and fibrinogen. Therefore, their *in vivo* circulation time will be assessed in the next step.

Tween 80 or polysorbate 80-nanoparticles were observed to target the brain. It has been reported that Tween 80-lipid drug conjugate (LDC) nanoparticles showed adhering to the endothelial cells of the brain vessels *in vivo* (Olbrich et al., 2000) and polysorbate-coated polybutylcyanoacrylate (PBCA) nanoparticles showed transport of various drugs into the brain (Alyautdin et al., 1995, 1998; Gulyaev et al., 1999).

Furthermore, Kreuter et al. (1997) observed that overcoating with polysorbate 80 on nanoparticles was more efficient in mediating brain targeting than overcoating with polysorbate 20, 40 and 60 on those. The Tween 80-particles and the PBCA particles might have a targeting to brain. It has been proven that some plasma proteins (ApoE, ApoC-I, ApoC-II, ApoA-I, Apo-IV) are important for nanoparticles to target to brain:

(1) Dehouck et al. (1997) has observed that ApoE played an important role in the transport of lipoproteins into the brain via the low density lipoprotein (LDL) receptor on the blood-brain barrier (BBB), because drug carriers adsorbing ApoE might mimic LDL-particles coated with ApoE leading to their brain-uptake by endocytic processes (Müller et al., 2001);

(2) ApoC-I and ApoC-II inhibited the binding of ApoE-containing lipoproteins such as β-very low density lipoproteins (β-VLDL) to the LDL receptor (Weisgraber et al., 1990). So to achieve brain targeting, it would be advantageous to have a high ApoE/ApoC-II ratio;

(3) It has been published that high amount of ApoA-IV promoted brain uptake (Gessner et al., 2001), due to ApoA-I and Apo-IV were known to suppress the activity of ApoE receptors in the liver (Bisgaier et al., 1989), thus consequently enhancing the uptake via LDL receptor on the BBB.

Table 4.1. Percentages of the adsorbed proteins on SLN.

| Different SLN | Identified proteins (percentage of the amount of single protein to the overall protein amount on the particle) | Reference |
|---|---|---|
| Tween 80-SLN | Albumin (0); ApoA-I (25.5); ApoA-IV (13.9); ApoC-II (5.3); ApoC-III (10.4); ApoE (3.4); Fibrinogen (5.5); Immunglobulins (7.0) | Göppert and Müller, 2003 |
| Poloxamer 188-SLN | Albumin (4.0-5.8); ApoA-I (19.0-24.5); ApoA-IV (6.8-11.2); ApoC-II (5.8-6.0); ApoC-III (12.9-13.5); ApoE (0-2.3); Fibrinogen (2.9-11.5); Immunglobulins (0-1.0) | Göppert and Müller, 2003, 2004, 2005a |
| Poloxamer 407-SLN | Albumin (3.8-41.7); ApoA-I (10.4-19.0); ApoA-IV (5.9-19.8); ApoC-II (0-6.7); ApoC-III (0-23.8); ApoE (0-0.5); Fibrinogen (0-12.1); Immunglobulines (0-22.6) | Göppert and Müller, 2005a, 2005c; Weyhers et al., 2005 |
| Poloxamine 908-SLN | Albumin (7.7-53.8); ApoA-I (10.3-23.5); ApoA-IV (6.7-12.5); ApoC-II (0-7.4); ApoC-III (6.5-20.2); ApoE (0-0.3); Fibrinogen (0-35.4) | Göppert and Müller, 2005a, 2005c; Weyhers et al., 2005 |
| Poloxamer 184-SLN | Albumin (4.1); ApoA-I (17.7); ApoA-IV (22.3); ApoC-II (6.0); ApoC-III (9.5); ApoE (10.4); Fibrinogen (0.4) | Göppert and Müller, 2005a |
| Poloxamer 235-SLN | Albumin (7.0); ApoA-I (15.1); ApoA-IV (19.4); ApoC-II (2.5); ApoC-III (6.8); ApoE (6.3); Fibrinogen (2.9) | Göppert and Müller, 2005a |
| Poloxamer 237-SLN | Albumin (5.1); ApoA-I (14.5); ApoA-IV (12.4); ApoC-II (7.9); ApoC-III (12.8); ApoE (2.6); Fibrinogen (1.9) | Göppert and Müller, 2005a |
| Poloxamer 238-SLN | Albumin (9.5); ApoA-I (18.7); ApoA-IV (9.6); ApoC-II (6.8); ApoC-III (13.8); ApoE (1.3); Fibrinogen (0.5) | Göppert and Müller, 2005a |
| Poloxamer 338-SLN | Albumin (7.8); ApoA-I (20.0); ApoA-IV (9.5); ApoC-II (6.7); ApoC-III (11.6); ApoE (0.1); Fibrinogen (16.2) | Göppert and Müller, 2005a |
| Polysorbate 60-SLN | Albumin (2.0); ApoA-I (14.0); ApoA-IV (14.1); ApoC-II (6.7); ApoC-III (10.3); ApoE (5.4); Fibrinogen (3.8); Immunglobulins (2.1) | Göppert and Müller, 2005b |
| Polysorbate 80-SLN | Albumin (4.0); ApoA-I (14.1); ApoA-IV (10.9); ApoC-II (4.3); ApoC-III (14.4); ApoE (5.4); Fibrinogen (2.2); Immunglobulins (4.1) | Göppert and Müller, 2005b |
| Polysorbate 40-SLN | Albumin (2.4); ApoA-I (15.9); ApoA-IV (9.8); ApoC-II (4.9); ApoC-III (14.5); ApoE (4.4); Fibrinogen (0.9); Immunglobulins (0.8) | Goppert and Muller, 2005b |
| Polysorbate 20-SLN | Albumin (1.2); ApoA-I (22.8); ApoA-IV (8.3); ApoC-II (7.7); ApoC-III (15.2); ApoE (2.3); Fibrinogen (0.9); Immunglobulins (1.2) | Göppert and Müller, 2005b |

By comparison with other SLN in Table 4.1, we have observed that Tween 80-SLN and polysorbate 80-SLN also had adsorbed a relatively high adsorption amount of ApoE, so those both SLN may be brain targeting when injected into the blood as well. For all of SLN, there was a high adsorbed amount of apolipoproteins on their surface, perhaps due to hydrophobicities of SLN and apolipoproteins as well as the small sizes of apolipoproteins compared to some other proteins, such as albumin and fibrinogen, which will be discussed in details in the following section.

## 4.3 Interaction between protein and solid lipid nanoparticles

After exposed into the protein solution, solid lipid nanoparticle coated with surfactant provides the protein adsorption with a solid interface which has been shown in Figure 4.1 Protein adsorption on the given surface is influenced by many factors, such as size of nanoparticle/protein, hydrophobicity/hydrophilicity of surface/protein, zeta potential of nanoparticle/protein. The adsorbed proteins are first separated according to their sizes due to the steric effects, and then instantly adsorbed onto the nanoparticle for hydrophobic interactions, electrostatic interactions. Be that as it may, we will exclude the electrostatic interactions in the following discussions in that many of proteins like albumin, fibrinogen, apolipoprotein as well as SLN themself show a negative charge on their surfaces when the pH value of the mixture is at above 7.0. Gessner et al. (2002) observed that the qualitative protein adsorption pattern on all the negative nanoparticles with increasing surface charge density were almost the same. Besides, almost all of SLN used in the following examples are on the nanoscale about from 200 nm to 300 nm, so the differences of protein adsorption patterns on SLN resulting from nanocurvature effects could be neglected. Therefore the steric effect of surfactant and hydrophobic effects are two most important factors for influencing the protein adsorption pattern of SLN coated different surfactants.

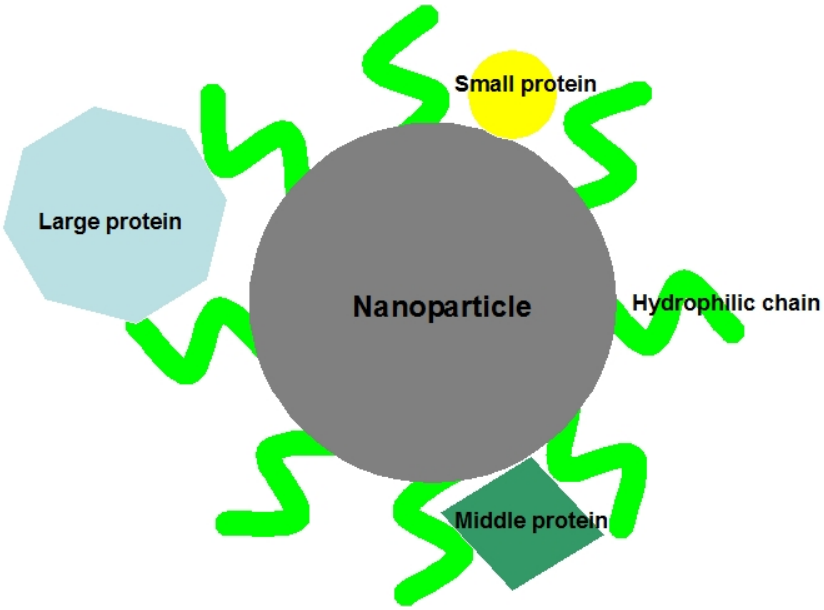


Figure 4.1. Scheme of the protein-surfactant modified SLN conjugation. Compared with the size of nanoparticle and the length of chain, proteins, due to the steric effects, are properly divided into three sorts, including large, middle and small proteins. Hydrophilic chains spread more or less evenly on the particle surface. The particle core is normally hydrophobic. In general, large protein is prevented from contacting the particle core by hydrophilic chains, and to be absorbed on the end of hydrophilic chains; protein on the middle size could be well plugged in among hydrophilic chains so that this interaction is more strong; small protein could easily contact the particle core.

## 4.3.1 Adsorption kinetics

Human plasma protein consists of albumin (55%, pI=5.7), globulins (38%), fibrinogen (7%), and others (1%) such as lipoprotein. SLN coated with surfactants possesses a hydrophobic core. Experimental results (Figure 4.2) for studying protein adsorption kinetics on SLN using TC-SLN in different plasma diluents showed that fibrinogen and apolipoproteins were first adsorbed onto SLN, but by increasing the plasma concentration from 1.2% up to 75% there was a obvious exchange between fibrinogen and apolipoproteins; the adsorbed amount of albumin was slowly increasing with the increasing of plasma concentration.

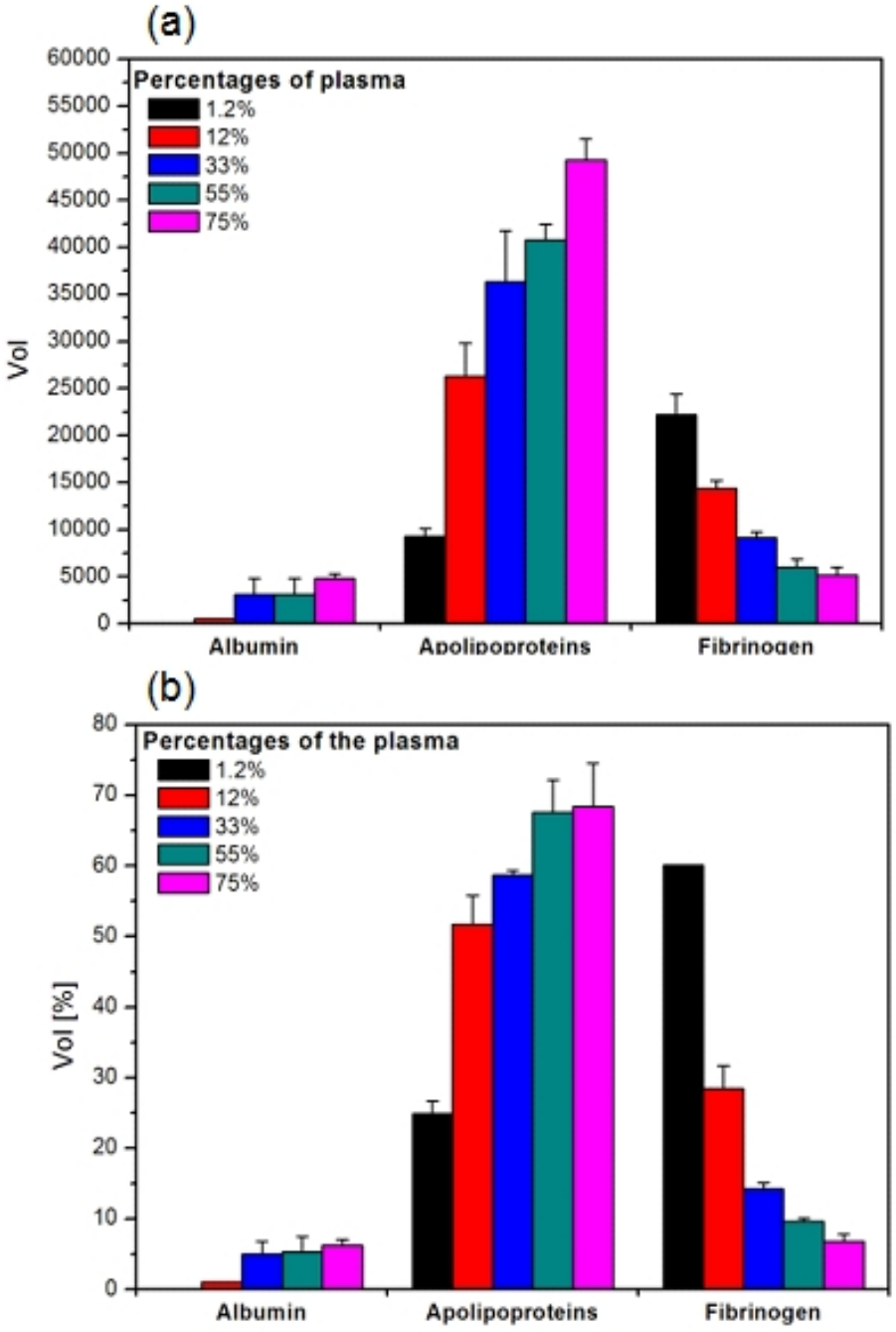


Figure 4.2. (a) Volume and (b) volume percentages of albumin, apolipoproteins, and fibrinogen adsorbed onto TC-SLN incubated with different plasma dilutions (Göppert and Müller, 2005c).

The displacement among different adsorbed proteins also has been observed using the polymeric model particles (polystyrene particles surface-modified with poloxamer 407 and poloxamine 908) incubated with different dilutions of plasma from 0.8 - 80 % (v/v). But this experimental results showed that the most abundant protein in

human plasma albumin (35-50 mg/ml) was first displaced by fibrinogen (2-4.5 mg/ml), and then in turn by IHRP, ApoC-III (0.12-0.14 mg/ml) and Apo J (0.035-0.105 mg/ml) (Blunk et al., 1996), because that the properties of particle surface are very important for protein adsorption, which have been discussed in chapter 1 in details.

This displacement is called "Vroman-effect" and occurs in seconds or even less time: firstly more plentiful proteins with lower affinity can be adsorbed on the solid surface, then these proteins are displaced by less plentiful proteins with higher affinity to the surface (Vroman et al., 1980; Vroman and Adams, 1986). Compared to fibrinogen, apolipoproteins have higher affinities to the SLN surface because of smaller molecules and higher hydrophobicities. Thus, the lower affinity fibrinogen was obviously displaced by the higher affinity apolipoproteins when the concentration of plasma increased. However, albumin is very soluble protein and extreme hydrophilic, exhibiting a lowly adsorbed amount. Here, we could properly infer that fibrinogen and apolipoproteins possess similar interactions with the SLN surface but albumin different. The interactions between fibrinogen/apolipoproteins and SLN mainly is the hydrophobic effects, but the other interaction effects e.g. electrostatic effects probably play a major role on the conjugation between albumin and SLN due to the large molecule weight with good hydrophilicity of albumin.

## 4.3.2 Steric effects and hydrophobic effects

Influences of the steric effects have been proved by varying the hydrophilic chains on the surfaces of particles. Gref et al. (2000) investigating influence of the steric effects on the protein adsorption pattern by varying the hydrophilic chain length and density on the particle observed in Figure 4.3 and 4.4 that the both variations resulted in dramatically decreasing the adsorbed amount of the proteins, such as fibrinogen and some apolipoproteins, when increasing hydrophilic PEG chain either length or density. However, for the hydrophilic albumin adsorption behavior, there were no changes on

the adsorbed amount. Therefore, the steric effect could affect the adsorption of fibrinogen and apolipoproteins but not albumin, which implies that these proteins have different adsorption sites on the nanoparticles. Fibrinogens and apolipoproteins are manly adsorbed onto the hydrophobic cores of particles by hydrophobic interactions, so increasing the chain length or density of PEG hydrophilic chains, their adsorbed amounts declined dramatically. Albumin is a hydrophilic protein, and Gessner et al. (2003) had observed that the adsorbed amount of albumin had been dramatically varied by changing the zeta potential of charged particles, so it could be properly deduced that hydrophilic albumin is majorly adsorbed probably by electrostatic interactions on the tail ends of hydrophilic chains on the particle surface. As the constant surface when changing the chain length or density, the adsorbed amounts of albumin had no obvious changes. Thus, the decreased amounts of fibrinogen and some apolipoproteins do not displace by the albumin adsorption. At the same time, the overall hydrophobicity of particles decreases when the hydrophilic PEG chains increase, resulting in the hydrophobic effects weakened between particles and proteins, which also could causes the adsorbed amounts of fibrinogens and some large apolipoproteins decreased.

For example, comparing Figure 4.3 and 4.4, the most interesting phenomenon is the apoC-III adsorption. ApoC-III is a small molecule. When prolonging the chain length, the adsorbed amount has a very slight change, but when increasing the density, the adsorbed amount presents a obvious decrease. The steric effect will become distinct on the condition that the density of hydrophilic chain increases. Therefore the adsorbed amount for the small molecular weight protein e.g. apoC-III has been obviously decreased when increasing the density of PEG chains.

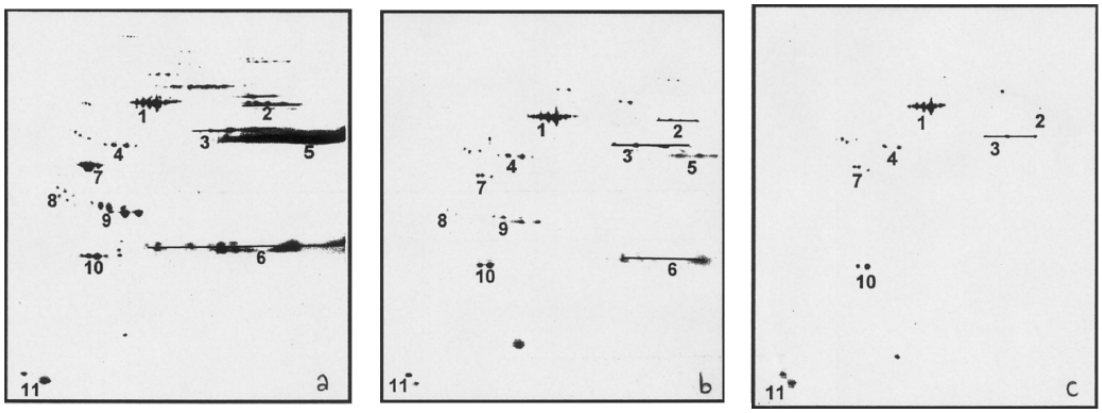


Figure 4.3. Influence of PEG chain length on the plasma protein adsorption. 2D-PAGE gels (pI 4.0-8.0 from left to right with not linear and Mw 6000-250000 g/M from bottom to top with not linear): (a) PEG2K-PLA45K; (B) PEG5K-PLA45K; (C) PEG10K-PLA45K. (1) albumin; (2) fibrinogen α; (3) fibrinogen β; (4) fibrinogen γ; (5) IgG γ; (6) Ig light chains; (7) apoA-IV; (8) apoJ; (9) apo E; (10) apoA-I; (11) apoC-III. (Gref et al., 2000)

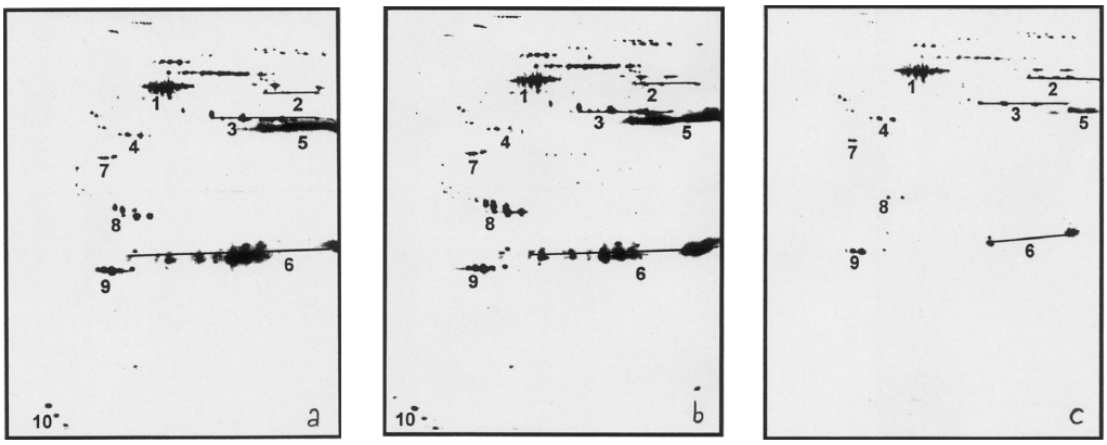


Figure 4.4. Influence of PEG surface density on the plasma protein adsorption. 2D-PAGE gels (pI 4.0-8.0 from left to right with not linear and Mw 6000-250000 g/M from bottom to top with not linear): (a) PEG-PLA (0.5 %); (B) PEG-PLA (2 %); (C) PEG-PLA (5 %). (1) albumin; (2) fibrinogen α; (3) fibrinogen β; (4) fibrinogen γ; (5) IgG γ; (6) Ig light chains; (7) apoA-IV; (8) apo E; (9) apoA-I; (10) apoC-III. (Gref et al., 2000)

The steric effects and hydrophobic effects also have been studied by employing SLN coated with different surfactants that contain different units of PEO (polyethylene

oxide) chain. The PEO chains are hydrophilic surrounding the hydrophobic SLN cores. The same results as the experiments of Gref et al. (2000) has been observed in Figure 4.5. In Figure 4.5, as the steric effects, when increasing the PEO units of surfactants, the adsorbed amounts of such proteins that possess larger size and are combined onto the hydrophobic SLN cores by hydrophobic effects decrease, e.g., ApoE, ApoA-IV, ApoJ, while for smaller size apolipoproteins like ApoC-II, ApoA-I, ApoC-III, there are not obviously declining on the adsorbed amounts. However, those decreased amounts are instantly complemented by fibrinogen for high concentration in the blood and extremely hydrophobic SLN core. Therefore, the experimental results prove that apolipoproteins and fibrinogens have the same adsorption sites on the nanoparticles by the same interaction way (hydrophobic effects). Besides, the adsorbed amount of hydrophilic albumin just has a slight fluctuation as well when increasing the hydrophilic PEO-units of surfactants, due to the constant surface of SLN.

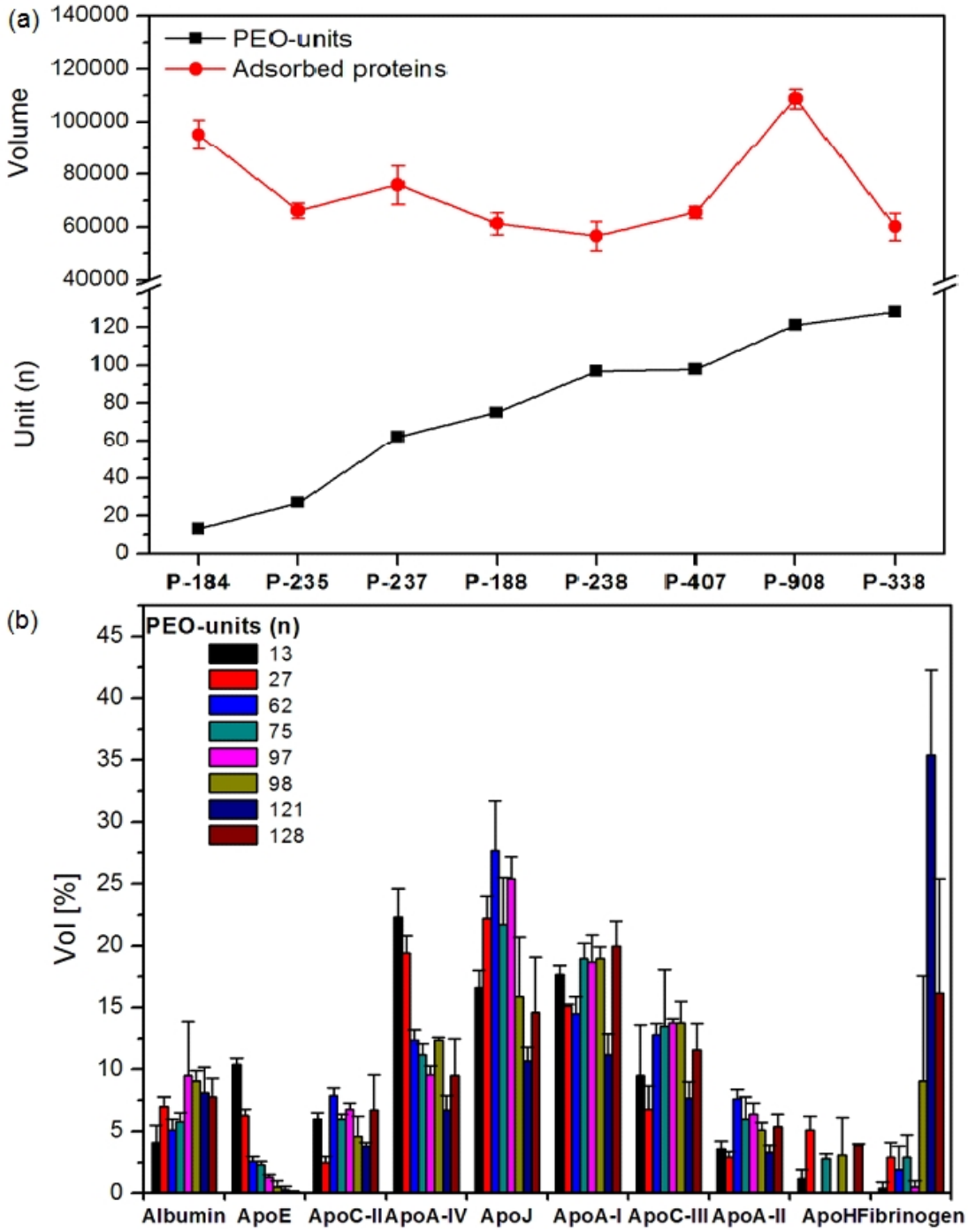


Figure 4.5. (a) PEO-units of surfactants and total volume of adsorbed proteins on different SLN, and (b)volume percentages of adsorbed proteins (Göppert and Müller, 2005a).

## 4.3.3 Incubation time

The incubation time is another important factor for studying the protein adsorption

kinetics onto nanoparticles. In Figure 4.6, SLN were incubated with the same concentration plasma but different incubation time. The experimental results show that the mainly adsorbed proteins were albumin and apolipoproteins, and the adsorbed amounts of them (Figure 4.6(a) and 4.6(c)) were gradually ascending with the incubation time extending from 0.5 min to 240 min. But volume percentage figures (Figure 4.6(b) and 4.6(d)) indicate that the protein adsorption pattern is almost the same for all the incubation periods. With the prolong of incubation time, the protein adsorption layer on SLN is a gradually thickened process while the sorts are the same during all the periods. Thus, the incubation time just influences the adsorbed amounts of proteins rather than the protein adsorption patterns on SLN.

To sum up, the steric effects and hydrophobic effects could drastically influence the adsorption behaviors of apolipoproteins and fibrinogens, while the adsorption behavior of hydrophilic albumin looks like independent from those factors. In the first seconds or even less time, the higher affinity apolipoproteins displace the lower affinity fibrinogen on the SLN surfaces even though having a much lower concentration in the blood than fibrinogen. After the displacement, the protein adsorption patterns on SLN reach a steady stage when prolonging the incubation time up to 240 min, but the adsorbed amounts of proteins have increased.

4. Protein adsorption pattern on solid lipid nanoparticle for drug targeting and their interactions

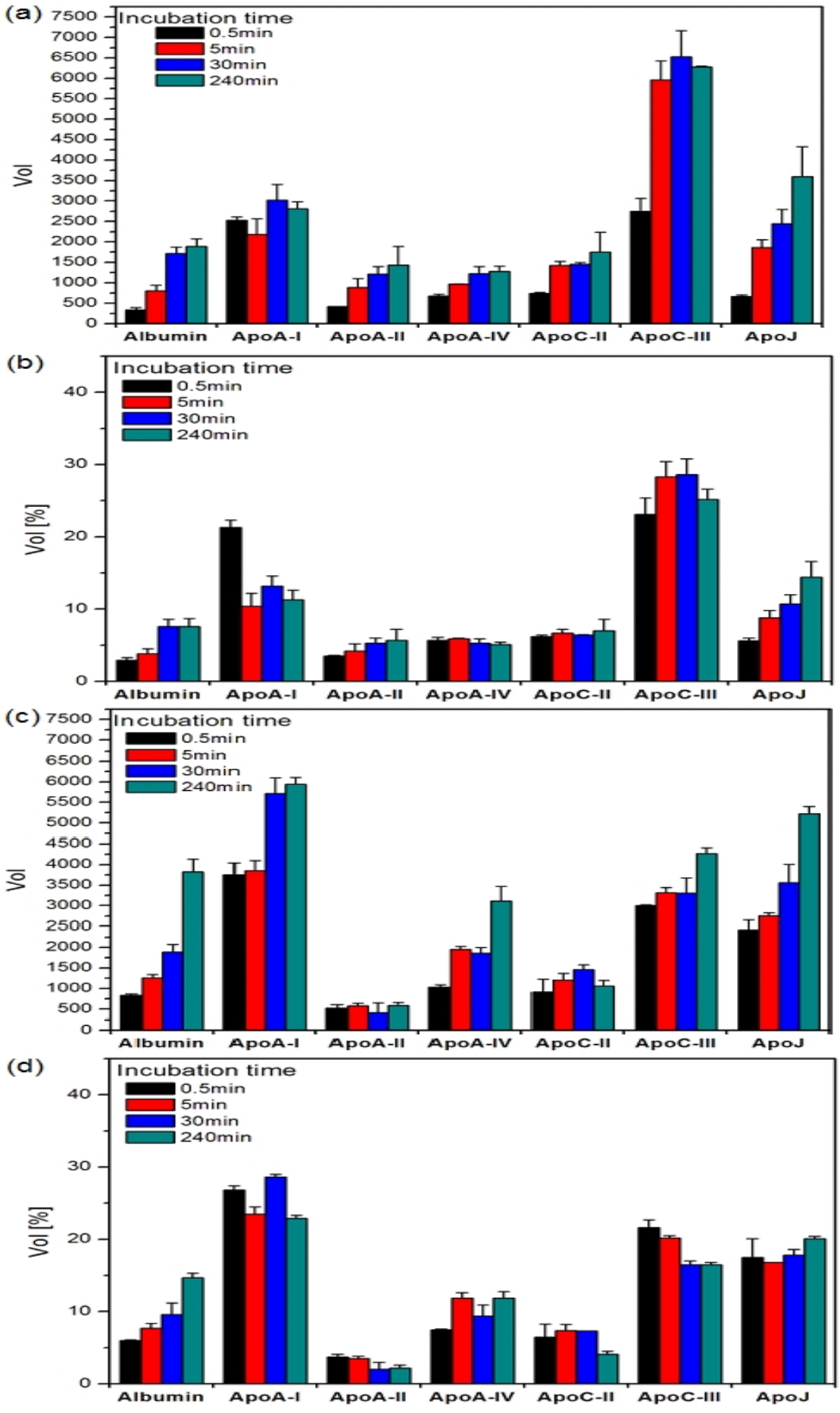

Figure 4.6. (a) Volume and (b) volume percentages of mainly adsorbed proteins on P407-SLN, and (c) volume and (d) volume percentages of major proteins adsorbed onto P908-SLN (Göppert and Müller, 2005c).

## 4.4 Conclusion

The important parts of development SLN as a successful drug carrier are to understand the nature of the SLN-protein complex and realize that the nature of the proteins adsorbed on SLN can influence the uptake of SLN by MPS and the circulation behavior of SLN in the blood stream to the target tissue. 2-DE has been recognized as a powerful tool to analyze the adsorbed protein pattern on SLN.

There are so many important works focusing on this area. Here, we briefly review the adsorbed protein patterns on different SLN and discuss the interactions between them. In general, three kind of proteins could be detected on SLN, including albumin, apolipoproteins and fibrinogens. Under the experimental conditions, the results indicate that fibrinogen and apolipoproteins possess similar interactions with the SLN surface but albumin different. The lower affinity fibrinogen was obviously displaced by the higher affinity apolipoproteins when the concentration of plasma increased, while by increasing of PEO-chain units (hydrophilicity) on the SLN surface, the decreased amounts of apolipoproteins could be complemented by fibrinogen. Compared with apolipoproteins and fibrinogen, the adsorption behaviors of albumin were independent from the hydrophobicity/hydrophilicity of SLN. The incubation time is just observed altering the adsorbed amount of proteins but not protein adsorption pattern on SLN coated with surfactant.

Normally, the steric effects e.g., the conformation of absorbed surfactants, the hydrophobic interactions, and the electrostatic effects are regarded as three important factors of protein adsorption on the particle surface. Experimental results showed that the interactions between fibrinogen/apolipoproteins and SLN mainly is the

hydrophobic effects. But albumin is very different from those two proteins, the electrostatic effects probably play a more important role on the interactions between albumin and SLN. Therefore, the hydrophilic PEO-chains of surfactants could affect the adsorption behaviors of fibrinogens and apolipoproteins by changing the steric effects and hydrophobic effects.

However, many challenges still stay in this area today, such as to understand how plasma proteins adsorb on SLN *in vivo*, better way to control SLN to the target tissue. In-depth study is required in this area in the future. Finally, all the studies aim at developing and improving SLN to better deliver drugs to target tissue and apply in nanomedicine.

# 5. Time-dependent adsorption of plasma proteins on oil-in-water emulsions

## 5.1 Introduction

The i.v. injection of egg lecithin-stabilized oil-in-water emulsions has been used as parenteral nutrition and drug carriers. The adsorbed proteins as their biological identities *in vivo* control the circulation time in the bloodstream and biodistribution (Leroux et al., 1995; Camner et al., 2002; Moghimi et al., 1993; Ogawara et al., 2004). Protein adsorption onto solid surfaces has been reported to be time-dependent (Göppert and Müller, 2005c; Vroman and Adams, 1986; Vroman et al., 1980; Blunk et al., 1996; Baszkin and Lyman, 1980). The plasma protein adsorption patterns on emulsions have been analyzed *in vitro* by two-dimensional polyacrylamide gel electrophoresis (2D-PAGE; 2-DE). For 2-DE, the ideal sample preparation is still a challenge because the separation of protein-particles from extra proteins without disrupting the adsorbed proteins or inducing additional protein binding is a very difficult step.

In this chapter, firstly, the time-dependent adsorption kinetics of plasma proteins onto nanoemulsion has been studied. The results show that the amounts and percentages of adsorbed proteins on nanoemulsion droplets (Lipofundin MCT 20 %) have varied when increasing the incubation time. The variations of adsorbed proteins on nanoemulsion differ from them on solid lipid nanoparticle (SLN), due to nanoemulsion and SLN have different physicochemical properties on the surfaces. There is a obvious desorption of adsorbed proteins from the nanoemulsion surfaces with increasing the incubation time. Secondly, effects from separation methods (gel filtration and centrifugation) on the protein adsorption patterns of emulsions are studied as well. Comparing to centrifugation taking a long time (1-2 hours), the faster

gel filtration separation method (only 15 min) is more suitable for the sample preparation.

## 5.2 Materials and methods

### 5.2.1 Materials

Lipofundin MCT 10 % batch No. 8086A181 and Lipofundin MCT 20 % batch No. 8065A182 were purchased from B. Braun Melsungen AG, Germany. Human plasma was obtained from the German Red Cross (Berlin, Germany) and stored at -70 ℃. Acetic acid, bromophenol blue, liquid paraffin, sodium salt, sodium dihydrogen phosphate ($NaH_2PO_4.2H_2O$) and disodium hydrogen phosphate ($Na_2HPO_4.12H_2O$) were purchased from Merck (Darmstadt, Germany). 1,4-dithioerythritol (DTE), acrylamide-Bis, agarose, ammonium persulfate (APS), cholamidopropyldimethylhydroxypropanesulfonate (CHAPS), glycerol, urea, tris(hydroxymethyl)aminomethan hydrochloride (Tris-HCL), iodoacetamide, N,N,N',N'-tetramethylethylenediamine (TEMED), sodium dodecyl sulphate (SDS) and IPG-strips (pH 3-10) were purchased from Serva Electrophoresis (Heidelberg, Germany). Ethanol was purchased from Berkel AHK (Berlin, Germany). Bio-Rad Silver Stain was purchased from Bio-Rad (Munich, Germany). Milli-Q water (Millipore, Germany) was used in this study.

### 5.2.2 Characterization of emulsions

Photon correlation spectroscopy (PCS) of emulsion samples was performed using a Zetasizer Nano ZS (Malvern Instruments, UK). The emulsion samples were diluted using Milli-Q water and measurements were performed at 25 ◦C temperature. The mean diameter and polydispersity index (PI) of emulsion samples were measured.

Laser diffractometry (LD) of emulsion samples was performed using the Mastersizer 2000 (Malvern Instruments, UK) in deionized water. LD produces diameters D 10%,

D 50%, D 90%, D 95% and D 99% (volume distribution) as characterization parameters. The Mie theory is used with optical parameters 1.497 for the real refractive index and 0.000 for the imaginary refractive index.

The surface charge of emulsion particles was characterized by zeta potential (ZP) using a Malvern Zetasizer Nano ZS (Malvern Instruments, UK) applying a field strength of 20 V/cm at 25 ◦C. The ZP calculation was performed using the Helmholtz–Smoluchowski equation. The surface charge has been measured in Milli-Q water adjusted to 50 μS/cm using 0.9 % NaCl solution and in Milli-Q water with 2.5 % glycerol (ω).

## 5.2.3 Sample preparation and the gel filtration separation method

For analysis of the plasma protein adsorption patterns, the 0.2 ml of the emulsion samples was first incubated with 0.6 ml of the human plasma at 37 ◦C for 5 min, 1 h, 2 h, and 4 h, respectively, and then the gel filtration separation method was performed to separate the emulsion sample from the extra plasma. The gel filtration step used a 1×20 cm column (C 10/20 column; Amersham Pharmacia Biotech) filled with a volume of 10 ml of Sepharose 2B in the bottom. The sample of emulsion with human plasma was eluted in the column with 0.05 M sodium phosphate buffer (pH 7.4) at a flow rate of 18 mL/h. Sample fractions were collected in subvolumes of 1.0 mL each for ten times. Absorption spectra were measured using UV-1700 PharmaSpe 230 VC (Shimadzu, Japan). Detection wavelengths were 279 nm and 350 nm. To evaluate which 1 ml sample fraction was completely free of extra plasma proteins and suitable to be used for 2-DE, a two-equation system was used to calculate the concentrations of emulsions and plasma (Göppert and Müller, 2004; Diederichs, 1996). After the last step by centrifuging at 22,940×g for 1 h at 20 ◦C (Biofuge 22 R, Heraeus, Hanau, Germany) to ensure complete separation of emulsions from extra plasma, the suitable samples were processed to desorb the adsorbed proteins by using SDS and DTE for 5

min at 95 ◦C, and then cooled down to room temperature and incubated with a solution containing DTE, CHAPS, urea, and Tris with stirring and centrifuging 15 min at 22,940 g. Finally, the desorbed protein solutions added rehydration buffer were used to analyze the protein adsorption patterns on emulsions by 2-DE.

### 5.2.4 Two-dimensional polyacrylamide gel electrophoresis

The 2D-PAGE was used to analyze the protein adsorption patterns on particle surface. Proteins were separated on IPG-strips according to their isoelectric focusing (IEF) in the first dimension and on gels based on molecular weights (MW) in the second dimension of 2D-PAGE (SDS-PAGE). The first dimension (IEF) was run using a Multiphore II from Amersham Pharmacia Biotech with a E 752 power supplied from Consort (Turnhount, Belgium). The second dimension (SDS-PAGE) was performed in Protean II Multi-Cells with a 1000 power obtained from Bio-Rad. Between the IEF and SDS-PAGE steps, the IPG strip is saturated with the IPG strip equilibration I for 15 min and then II for 20 min. The equilibration I contains DTE, SDS, Glycerol, Urea, as well as Bromphenol blue, and the equilibration II includes Iodoacetamide, SDS, Glycerol, Urea, and Bromphenol blue.

The gels were silver-stained and scanned after 2D-PAGE. The gels were scanned by ImageScanner (Amershan Pharmacia Biotech). The spots on gels were recognized by matching the master map of human plasma. The amount of adsorbed protein was analyzed using a semi-quantitative manner based on the spot size and intensity on the gel. The data of spots on gels were measured by Melanie III software (Swiss Institute of Bioinformatics, Geneva, Switzerland).

## 5.3 Results and discussion

### 5.3.1 Time-dependent protein adsorption patterns on nanoemulsions

Figure 5.1 shows the whole 2-DE gels of Lipofundin MCT 20 % incubated with human plasma for different time: (a) 5 min, (b) 1 h, (c) 2 h and (d) 4h, and Figure 5.2 is the calculations of volume and volume percentages of adsorbed proteins on it. The experimental results (In Figure 5.1 and 5.2) show that the emulsion mainly adsorb apolipoproteins (ApoA-IV, ApoJ, ApoE, ApoA-I, ApoC-II, and ApoC-III). The apolipoproteins' affinities to emulsion surfaces are obviously much higher than the affinities of other proteins, e.g., albumin, although the concentrations of these apolipoproteins in the human plasma are much lower than the concentration of albumin (35-50 mg/ml). In details in Figure 5.2, the volume and volume percentages of ApoA-IV on emulsion particles start to decrease after 5 min incubation with human plasma; the volume and volume percentages of ApoA-I, ApoC-II and ApoC-III on emulsion particles are increasing in the first one hour and then begin to decline; Apo E, albumin and Apo J have a more complex protein adsorption behavior on emulsion droplets, but at the end of the incubation time of 4 h, the volume and volume percentages of these proteins distinctly decrease. In Figure 5.3, the results show that the total amount of adsorbed proteins decreases with increasing incubation time. The desorptions of adsorbed proteins (e.g., albumin, γ-globulin, fibrinogen) from solid films have been observed in the previous studies (Baszkin and Lyman, 1980). For instance, Baszkin and Lyman observed that the albumin desorption from all the polymer surface on the bulk scale was rapid in the first hour and reached a plateau value after 4 hours (Baszkin and Lyman, 1980). Thus, the experimental results show that there is a obviously desorption for all the adsorbed proteins from the nanoemulsion surface.

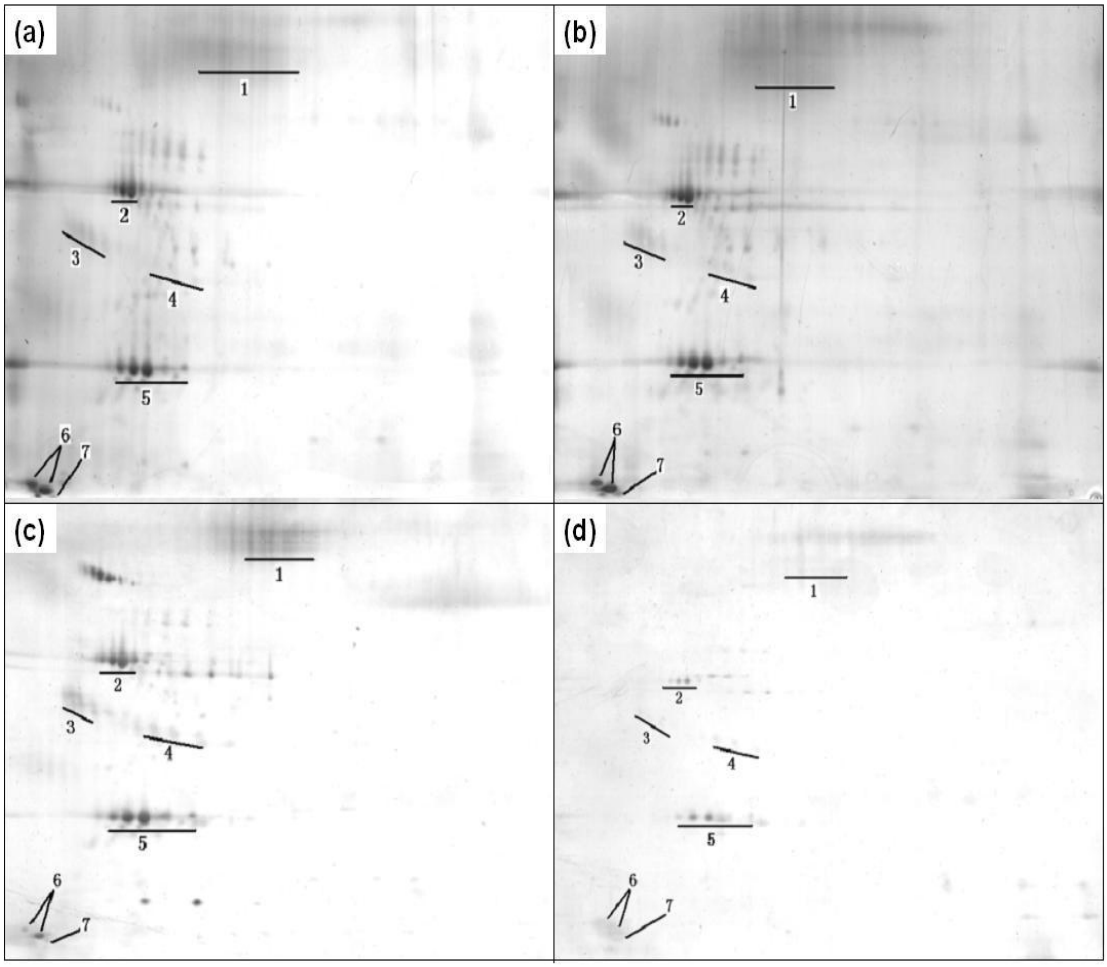


Figure 5.1. Gels of plasma protein adsorption patterns on Lipofundin MCT 20 % with different incubation time: (a) 5 min, (b) 1 h, (c) 2 h and (d) 4h. 1: Albumin, 2: ApoA-IV, 3: ApoJ, 4: ApoE, 5: ApoA-I, 6: ApoC-II, 7: ApoC-III.

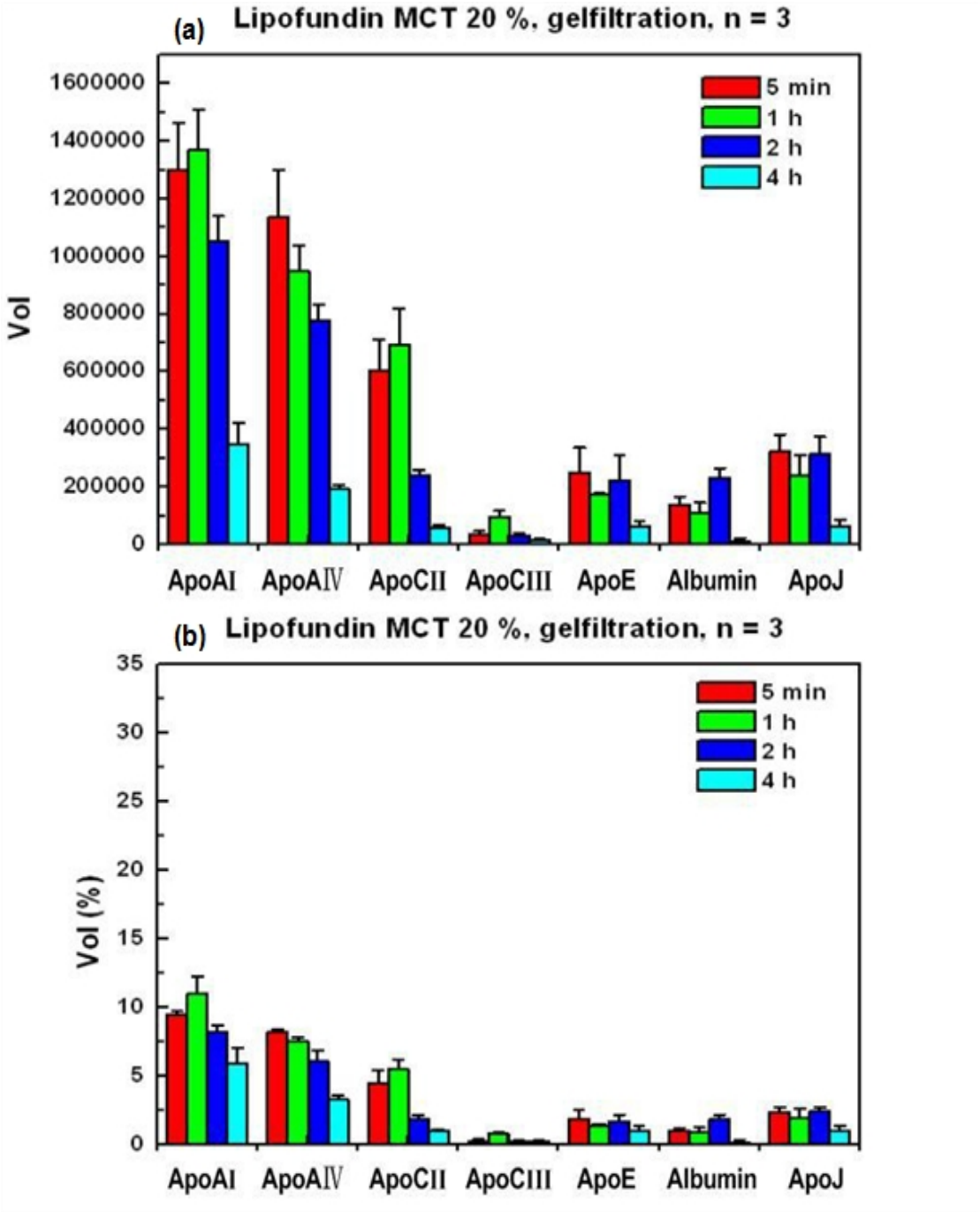


Figure 5.2. Plasma protein composition on Lipofundin MCT 20 % with different incubation time which were analyzed using 2-DE: (a) volume and (b) volume percentages. Error bars represent the standard deviation (n=3).

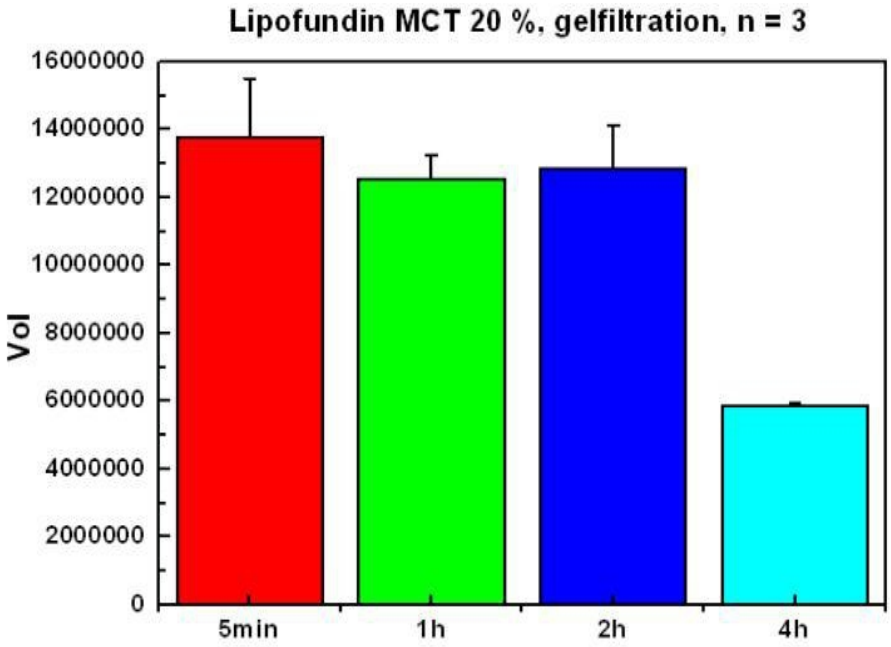


Figure 5.3. Total volume of protein adsorbed onto Lipofundin MCT 20 % with different incubation time which was analyzed using 2-DE. Error bars represent the standard deviation (n=3).

## 5.3.2 Protein adsorption kinetics on nanoparticle surfaces

The behaviors of adsorbed proteins on different nanoparticles are also different. The differences among the adsorbed protein behaviors on various nanoparticles are mainly due to the diversities of nanoparticle properties, such as size of nanoparticle (the curvature effects), the chain length and density of surfactant (the steric effects), hydrophobicity/hydrophilicity of surface (the hydrophobic interactions), zeta potential of nanoparticle (the electrostatic interactions). For instance, compared with SLN, nanoemulsion possesses different protein adsorption behaviors. Harnisch and Müller (2000) employing Lipofundin MCT 20 % incubated for 5 min in different concentration plasma from 11 % to 75 % observed that the amounts of adsorbed proteins e.g. apolipoproteins and fibrinogens increased with increasing the plasma concentration, which is different from the Göppert and Müller's (2005c) results. In the Göppert and Müller's (2005c) experiments using the TC-450 SLN incubated for 5 min in different concentration plasma from 1.2 % to 75 %, the lower affinity

fibrinogens was obviously displaced by the higher affinity apolipoproteins with the increase of the plasma concentration, even though apolipoproteins haves a much lower concentration in the blood than fibrinogen. Therefore, the physicochemical properties of particle surfaces are important for understanding the adsorption kinetics of proteins on the surface.

Here, to better study the time-dependent protein adsorption on nanoemulsion (Lipofundin MCT 20 %), the experimental results are compared with the

Table 5.1. Characterization data of size (by photon correlation spectroscopy (PCS) and laser diffractometry (LD)) and zeta potential (ZP) of Lipofundin MCT 20 % and Lipofundin MCT 10 %.

| System | | Lipofundin MCT 20 % | Lipofundin MCT 10 % |
|---|---|---|---|
| PCS | mean diameter (nm) | 234.2±4.8 | 213.1±2.9 |
| | polydispersity index (PI) | 0.244 | 0.214 |
| LD (μm) | D 10 % | 0.201 | 0.136 |
| | D 50 % | 0.330 | 0.269 |
| | D 90 % | 0.529 | 0.469 |
| | D 95 % | 0.590 | 0.530 |
| | D 99 % | 0.685 | 0.626 |
| ZP (mV) | in 50 μs/cm NaCl solution | -47.6 | -49.5 |
| | in water with 2.5 % glycerol | -25.5 | -24.1 |

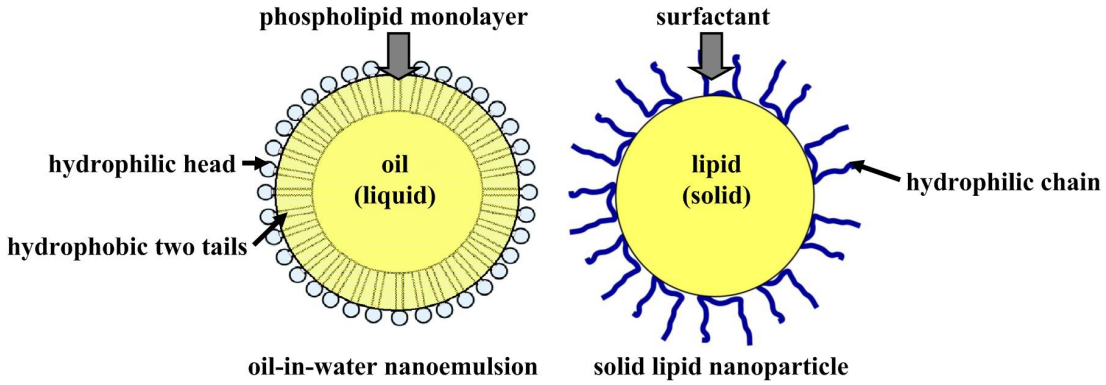


Figure 5.4. The schematic diagrams of oil-in-water nanoemulsion and solid lipid nanoparticle.

time-dependent protein adsorption on SLN which Göppert and Müller (2005c) investigated using the P407-SLN and P908-SLN. The characterization data of nanoemulsions are in Table 5.1. The nanoemulsion and SLN systems possess similar sizes between 200 and 300 nm and negative charges on the surfaces. Figure 5.4 shows the structures of oil-in-water nanoemulsions and solid lipid nanoparticles. Oil-in-water nanoemulsion has a liquid oil core stabilized by a phospholipid monolayer. A phospholipid molecule contains a hydrophilic head to form the hydrophilic surface on nanoemulsion and two hydrophobic tails spread into the oil core. Compared to the nanoemulsion structure, solid lipid nanoparticle has a solid oil core coated with surfactant that consists of hydrophobic and hydrophilic parts. The hydrophilic chains scatter on the SLN surface. The hydrophilic chains are PEO chains for poloxamer 407 and poloxamine 908.

Under the same experimental conditions, Göppert and Müller observed that on the SLN samples (P407-SLN and P908-SLN), the adsorbed amounts of proteins including albumin and apolipoproteins were gradually ascending with the incubation time extending from 0.5 min to 240 min, and the protein adsorption pattern is almost the same for all the incubation periods, which indicates the protein adsorption layer on SLN is a gradually thickened process with the prolong of incubation time. However, for oil-in-water nanoemulsion system, the experimental results show that there is a obviously desorption for all the adsorbed proteins from the nanoemulsion surface with the prolong of incubation time. So the experimental results indicate that the properties of nanoparticle surface play an important role on the protein adsorption. The both nanoemulsion and SLN systems have similar sizes and negative charges, so the curvature effects and electrostatic interactions could be excluded to create their different protein adsorption behaviors. But as shown in Figure 5.4, this two systems possess two different surface structures. SLN like P407-SLN and P908-SLN are stabilized on the surfaces with surfactants that consists of the hydrophilic chains e.g. PEO chains to create the steric effects on SLN. The steric effects disturbs not only adsorption of proteins onto the particles but also desorption of adsorbed proteins from

the surface. Therefore, the experimental results (Göppert and Müller, 2005c.) showed that the lower affinity fibrinogens was gradually displaced by the higher affinity apolipoproteins with the increase of the plasma concentration and the adsorbed amounts of proteins including albumin and apolipoproteins were gradually ascending with the incubation time extending from 0.5 min to 240 min. Compared to the SLN surface, the nanoemulsion surface is like a smooth surface just as the polymer surface in the reference (Baszkin and Lyman, 1980) that the desorption of adsorbed proteins occurred. Thus, without the interference of hydrophobic chains on the surface, Lipofundin MCT 20 % incubated 5 min in different concentration plasma from 11 % to 75 % was observed that the amounts of adsorbed proteins e.g. apolipoproteins and fibrinogens increased with increasing the plasma concentration, and a obviously desorption for all the adsorbed proteins from the nanoemulsion surface happens with the incubation time extending from 0.5 min to 240 min. Nevertheless, the SLN and nanoemulsion both are mainly adsorbing apolipoproteins because of the hydrophobic interactions and the sizes on the nanoscale (Lynch and Dawson, 2008) which result in apolipoproteins possessing a high affinity onto their surfaces.

### 5.3.2 Separation methods of nanoemulsions from extra plasma for 2-DE

Centrifugation and gel filtration (chromatography) are two important methods for separating samples from extra plasma. Centrifugation is based on the density difference between samples and plasma. Ideal gel filtration is a mild separation method just depending on the size difference due to the steric effects. When employing the centrifugation separation method, the adsorption of proteins onto particles is still continuing during the centrifugation separation process after the 5 min of incubation time, because the centrifugation process normally needs a long time compared to the 5 min, e.g., 1 hour for our experiments. By contrast, the gel filtration method merely needs about 15 min for the separation step. Besides, the protein adsorption pattern differences between use of centrifugation and gel filtration could be

multiplied due to the surface properties of nanoparticles. For instance, as discussed in chapter 2, there is distinctly different protein adsorption patterns on T80-SLN when using centrifugation and gel filtration, while the protein adsorption patterns on P188-SLN or TC450-SLN are almost the same for centrifugation and gel filtration. Regarding the nanoemulsions, they have a more smooth surface without the hydrophilic chains than SLN coated with surfactants in Figure 5.4. Here, we study the influence of separation method on the plasma protein adsorption pattern of nanoemulsion.

The gels of plasma protein adsorption patterns in Figure 5.5 were obtained under the same experimental conditions as the reference (Schmidt, 2002) besides the sample separation methods. The samples were incubated with human plasma for 5 min at 37 ℃. Figure 5.6 shows the volume percentages of plasma protein composition on Lipofundin MCT 10 % and Lipofundin MCT 20 % with different sample separation methods of gel filtration and centrifugation. The volume percentages of the major proteins adsorbed on Lipofundin MCT 10 % and Lipofundin MCT 20 % with the centrifugation separation method comes from the Schmidt's thesis (Schmidt, 2002). Lipofundin MCT 10 % and Lipofundin MCT 20 % have similar protein adsorption patterns when applying the identical separation method, either gel filtration in Figure 5.6(a) or centrifugation in Figure 5.6(b), because that they have similarly physical (the similar sizes and zeta potentials as shown in Table 5.1 for gel filtration or in Table 5.2 for centrifugation) and chemical (the same ingredients) properties. As a matter of fact, by comparison of Table 5.1 and Table 5.2, we could observe that all the used nanoemulsions not only for gel filtration but also for centrifugation have similarly physicochemical properties, such as the PCS size about 200-300 nm, the negative zeta potential, and the same ingredients. Figure 5.7 shows the volume percentages of plasma protein composition on Lipofundin MCT 10 % and Lipofundin MCT 20 % with different separation methods of gel filtration and centrifugation, when the total percentages of these adsorbed proteins on one sample with one separation method are equal to 100 % trying to eliminate the influences from the background during the

semi-quantitative calculation. By comparison of Figure 5.7, the percentages of ApoC-II, ApoC-III and ApoA-II in the case of centrifugation are obviously higher than that for gel filtration, but the adsorbed amount of ApoJ is on the other way round. From the gels (Figure 5.5), we knows that ApoC-II, ApoC-III and ApoA-II have smaller size or less molecular weight (MW) than ApoJ. Due to the small density difference and the small size, centrifugation takes a long time (1-2 hours) compared to gel filtration (about 15 min), and during this centrifugation time the protein adsorption processes continue. In Figure 5.7, centrifugation has obviously induced the adsorption of small size proteins (e.g., ApoC-II, ApoC-III and ApoA-II) and the desorption of large size protein (ApoA-I, ApoA-IV, ApoE, albumin, especially ApoJ) by extending the adsorption process of proteins, because that the nanoemulsion has a more smooth surface without the hydrophilic chains. The hydrophilic chains disturb not only adsorption of proteins onto the particles but also desorption of adsorbed proteins from the surface due to the steric effects. Thus, to obtain the proper protein adsorption patterns on nanoemulsions by 2-DE, the faster gel filtration separation method is more suiTable for the nanoemulsion sample separation than centrifugation.

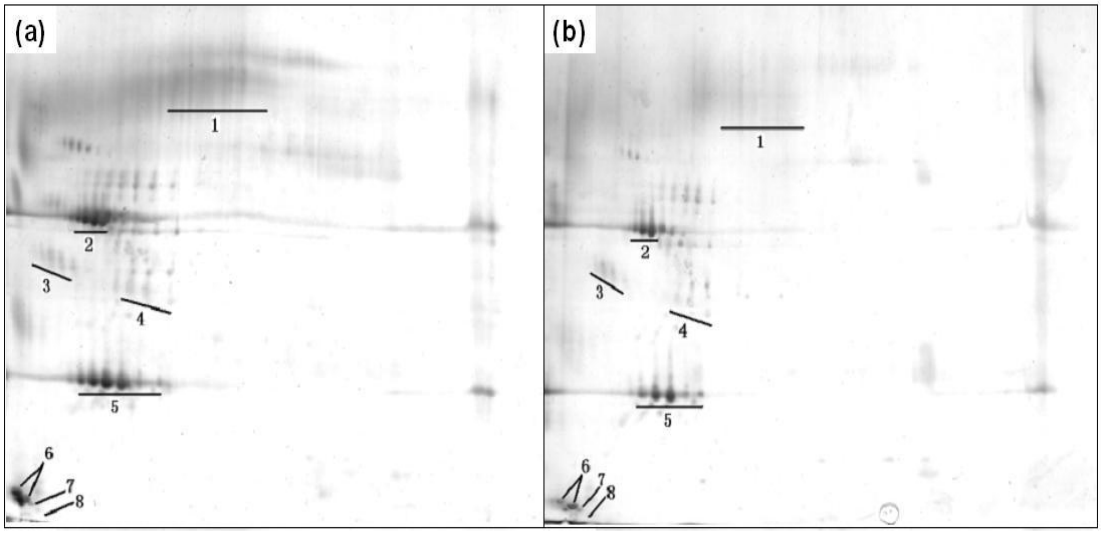


Figure 5.5. Gels of plasma protein adsorption patterns on (a) Lipofundin MCT 10 % and (b) Lipofundin MCT 20 %. 1: Albumin, 2: ApoA-IV, 3: ApoJ, 4: ApoE, 5: ApoA-I, 6: ApoC-II, 7: ApoC-III, 8: ApoA-II.

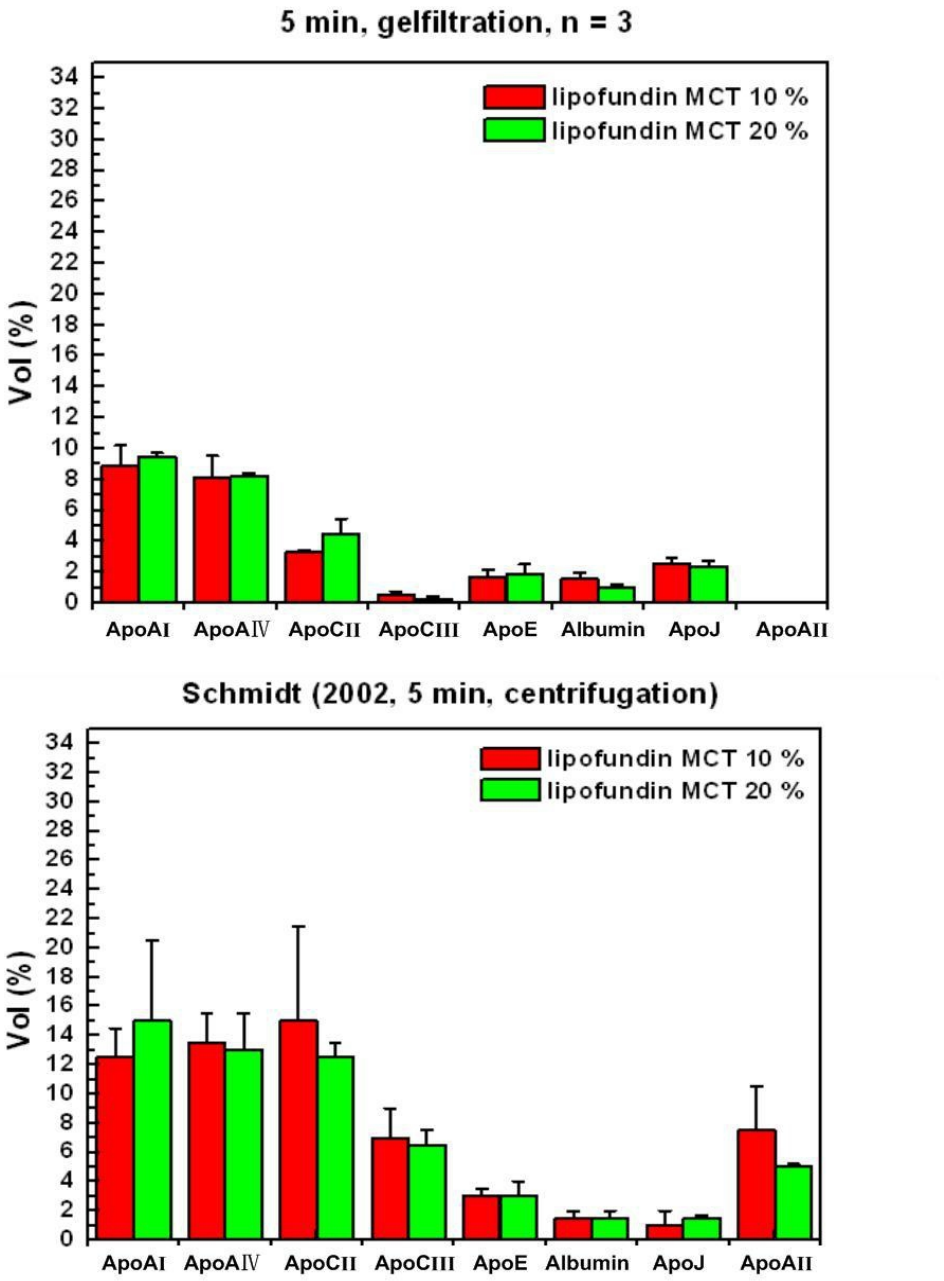


Figure 5.6. Volume percentages of plasma protein composition on Lipofundin MCT 10 % and Lipofundin MCT 20 % were analyzed using 2-DE with different separation methods: (a) gel filtration and (b) centrifugation (Schmidt, 2002). Error bars represent the standard deviation (n=3).

Table 5.2. Characterization data of size (by photo correlation spectroscopy (PCS) and laser diffractometry (LD)) and zeta potential (ZP) of Lipofundin MCT 20 % and Lipofundin MCT 10 % (Schmidt, 2002).

| System | | Lipofundin MCT 20 % | Lipofundin MCT 10 % |
|---|---|---|---|
| PCS | mean diameter (nm) | 265 | 251 |
| | polydispersity index (PI) | 0.101 | 0.086 |
| LD (µm) | D 99 % | 0.534 | 0.493 |
| ZP (mV) | in 50 µs/cm NaCl solution | -37 | -33 |

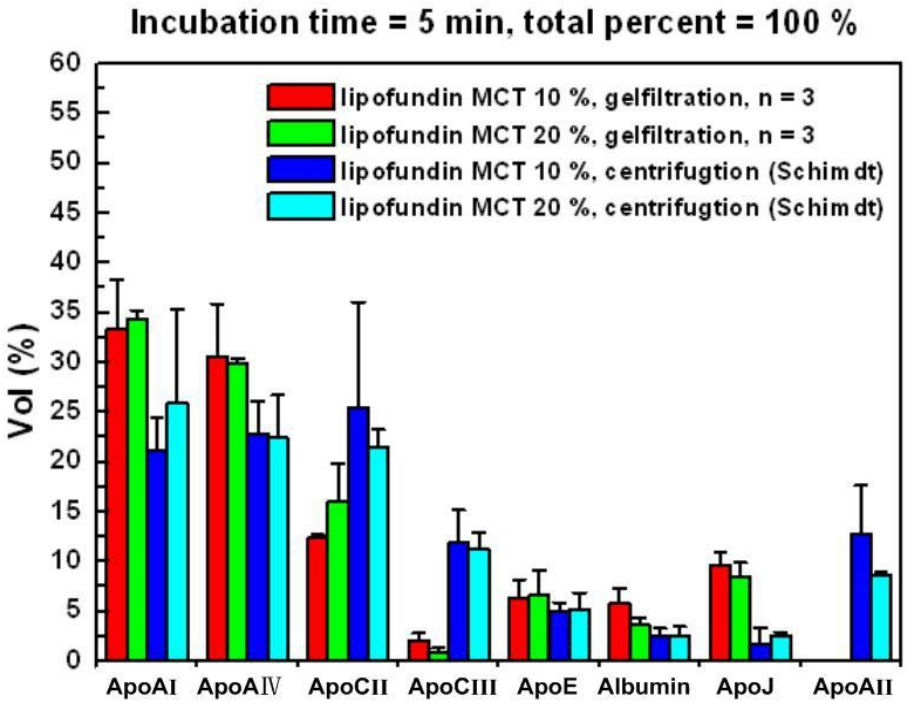


Figure 5.7. Volume percentages of plasma protein composition on Lipofundin MCT 10 % and Lipofundin MCT 20 % were analyzed using 2-DE with different separation methods: gel filtration and centrifugation (Schmidt, 2002), when total percentages of these adsorbed proteins on one sample with one separation method are equal to 100 %. Error bars represent the standard deviation (n=3).

## 5.4 Conclusion

The 2-DE results show that nanoemulsion samples mainly adsorb apolipoproteins as same as SLN. The amounts and percentages of adsorbed proteins on emulsion samples clearly change with incubation time: adsorbed proteins trend to desorb and different adsorbed proteins start to decrease their amounts and percentages at different incubation time. The changes of protein adsorption with incubation time on

nanoemulsion are different from them on SLN because of e.g., steric effects of the hydrophilicity of PEO-chains on the SLN surfaces. The total amount of adsorbed proteins on the nanoemulsions decreases with increasing the incubation time. The knowledge of time-dependent protein adsorption pattern will be helpful for understanding the protein adsorption kinetics on the drug carrier system.

Besides, the experimental results indicate that centrifugation has obviously induced the adsorption of small size proteins (e.g., ApoC-II, ApoC-III and ApoA-II) and the desorption of large size protein (ApoA-I, ApoA-IV, ApoE, albumin, especially ApoJ) due to extending the adsorption processes of proteins about 1-2 hours. Compared to centrifugation, the faster gel filtration method (merely about 15 min) is more suiTable for separating the nanoemulsion system from extra plasma due to the shorter separation time.

# 6. Blood substitutes: Adsorption protein patterns on different i.v. hemoglobin particles

## 6.1 Introduction

Hemoglobin particles were prepared as blood substitutes. A major problem for i.v. particle is the avoidance of particle uptake from the blood circulation by the macrophages of the body (mainly in liver, spleen, mononuclear phagocytic system (MPS)) (Douglas, 1986; Senior, 1987). After intravenous administration, these particles immediately adsorb human plasma proteins. Since 1990, it has been realized and been generally accepted now that the determining factor for the *in vivo* fate and the organ distribution of particles is the blood proteins adsorbing on the particle surface after their injection. For example, binding of opsonins (e.g., immunoglobulin G, complement factors, and fibrinogen) promotes phagocytosis and removal of the particles from the systemic circulation by cells of the mononuclear phagocytic system (MPS) (Leroux et al., 1995; Camner et al., 2002). In contrast, binding of dysopsonins (e.g., albumin, apolipoproteins) promotes prolonged circulation time in the blood (Moghimi et al., 1993; Ogawara et al., 2004). Moreover, surface-enriched proteins can mediate an uptake of the drug carriers by specific site (Kreuter et al., 2002; Müller and Schmidt, 2002).

The protein adsorption pattern is affected by physicochemical particle properties (Juliano, 1988; Müller and Heinemann, 1989; Price et al., 2001; Thiele et al., 2003). In general, hydrophilic particles can circulate longer time in the blood stream than hydrophobic particles. For example, polystyrene model carriers surface-modified with hydrophilic polyethylene oxide chains or poloxamine 908 can circulate in the blood

stream (Illum et al., 1987; Moghimi et al., 1993). Besides, the nanoparticles which adsorbed albumin on the surface had been found to efficiently avoid the phagocytic uptake *in vitro* as well, because that the hydrophilic albumin could create more hydrophilic surface on the nanoparticles (Maassen et al., 1993).

The plasma protein adsorption pattern on particles were analyzed *in vitro* by two-dimensional polyacrylamide gel electrophoresis (2-DE; 2D-PAGE) (Blunk et al., 1993; Harnisch and Müller, 1998; Lück et al., 1998; Gessner et al., 2001). 2-DE has been proven to be a powerful tool to determine these plasma protein adsorption patterns of drug carriers (Blunk et al., 1993). The aim of the study was to determine protein adsorption patterns of different hemoglobin particles to select the most promising ones for blood substitutes.

## 6.2 Material and method

### 6.2.1 Materials

Human plasma was obtained from the German Red Cross (Berlin, Germany) and stored at -70 ℃. Acetic acid, bromophenol blue, liquid paraffin, sodium salt, sodium dihydrogen phosphate ($NaH_2PO_4.2H_2O$) and disodium hydrogen phosphate ($Na_2HPO_4.12H_2O$) were purchased from Merck (Darmstadt, Germany). 1,4-dithioerythritol (DTE), acrylamide-Bis, agarose, ammonium persulfate (APS), cholamidopropyldimethylhydroxypropanesulfonate (CHAPS), glycerol, urea, tris(hydroxymethyl)aminomethan hydrochloride (Tris-HCL), iodoacetamide, N,N,N',N'-tetramethylethylenediamine (TEMED), sodium dodecyl sulphate (SDS) and IPG-strips (pH 3-10) were purchased from Serva Electrophoresis (Heidelberg, Germany). Ethanol was purchased from Berkel AHK (Berlin, Germany). Bio-Rad Silver Stain was purchased from Bio-Rad (Munich, Germany). Milli-Q water (Millipore, Germany) was used in this study.

## 6.2.2 Methods

### 6.2.2.1 Preparations of hemoglobin particles

Three types of particles were prepared by Xiong (2012): Pure hemoglobin particles, hemoglobin particles modified with human serum albumin (HSA) on the surface, and hemoglobin-hyaluronan-mixture particles. All particles were prepared with a novel 3-step-technique (co-precipitation, cross-linking and dissolution) (Bäumler and Georgieva, 2010). The characterization data of pure hemoglobin particles, hemoglobin particles modified with human serum albumin (HSA) on the surface, and hemoglobin-hyaluronan-mixture particles are shown in Table 6.1.

Table 6.1. The mean sizes, concentration and medium used of A (pure hemoglobin particles), B (hemoglobin particles modified with human serum albumin (HSA) on the surface), and C (hemoglobin-hyaluronan-mixture particles) suspensions. (2%HSA-0.9%NaCl: 2 % HSA dissolved in 0.9 % NaCl solution)

| Sample | A | B | C |
|---|---|---|---|
| Mean diameter (µm) | 3.0 | 1.7 | 5.0 |
| Concentration (v/v) (%) | 17 | 10 | 24 |
| Medium | $H_2O$ | $H_2O$ | 0.9%NaCl |
| | 2%HSA-0.9%NaCl | 2%HSA-0.9%NaCl | - |

### 6.2.2.2 Sample preparation

Each sample containing constant surface area (0.2 $m^2$ surface area of sample per ml plasma) were mixed with 0.6 ml citrate stabilized human plasma in a centrifugation tube and incubated at 37 ℃ for 5 min. To mimic the conditions in the bloodstream, the particles were incubated routinely for 5 min in citrated plasma, because *in vivo* in case recognition by the MPS occurs, in the first 5 min up to 90 % of the injected dose are taken up by the liver macrophages (O'Mullane et al., 1987; Müller, 1991; Liniemark et al., 1995). In case particles survive in the first 5 min, prolonged blood circulation of these particles was found (Illum and Davis, 1987; Cattel et al., 2003).

Separation of the particles from the plasma was performed by centrifugation at 22,940 g for 1 h at 20 ℃, and then washing three times with 0.05 M phosphate buffer, pH 7.4 and subsequent centrifugation respectively at 22,940 g for 1 h at 20 ℃. The adsorption proteins on particles were desorbed using sodium dodecyl sulfate (SDS) and dithioerythritol (DTE) for 5 min at 95 ℃, then cooled down to room temperature and incubated with a solution containing DTE (Dithioerythritol), CHAPS (3-(3-Cholamidopropyl)dimethylammonio-1-propansulfat), urea, and Tris (Tris(hydroxymethyl)-aminomethan), stirring and centrifuging 10-15 min at 22,940 g. Finally, the mixture solution added rehydration buffer for 2-DE was used to analyse the protein adsorption pattern on particles.

#### 6.2.2.2 Two-dimensional polyacrylamide gel electrophoresis

The 2D-PAGE was used to analyze the protein adsorption patterns on particle surface. Proteins were separated on IPG-strips according to their isoelectric focusing (IEF) in the first dimension and on gels based on molecular weights (MW) in the second dimension of 2D-PAGE (SDS-PAGE). The first dimension (IEF) was run using a Multiphore II from Amersham Pharmacia Biotech with a E 752 power supplied from Consort (Turnhount, Belgium). The second dimension (SDS-PAGE) was performed in Protean II Multi-Cells with a 1000 power obtained from Bio-Rad. Between the IEF and SDS-PAGE steps, the IPG strip is saturated with the IPG strip equilibration I for 15 min and then II for 20 min. The equilibration I contains DTE, SDS, Glycerol, Urea, as well as Bromphenol blue, and the equilibration II includes Iodoacetamide, SDS, Glycerol, Urea, and Bromphenol blue.

The gels were silver-stained and scanned after 2D-PAGE. The gels were scanned by ImageScanner (Amershan Pharmacia Biotech). The spots on gels were recognized by matching the master map of human plasma. The amount of adsorbed protein was analyzed using a semi-quantitative manner based on the spot size and intensity on the gel. The data of spots on gels were measured by Melanie III software (Swiss Institute of Bioinformatics, Geneva, Switzerland).

## 6.3 Result and discussion

### 6.3.1 Protein adsorption patterns on different hemoglobin nanoparticles

The whole 2D-PAGE gels of protein adsorption patterns on different hemoglobin particles were shown in Figure 6.1. Figure 6.2 is the total amount of proteins adsorbed on the particle surface and Figure 6.3 provides the volume and volume percentages of main proteins identified on the gels. As shown in Figure 6.2, pure hemoglobin particles and hemoglobin-hyaluronan-mixture particles exhibited almost identical total amounts of adsorbed proteins, but hemoglobin particles modified with HSA just have about one fourth of the total amount of adsorbed proteins on pure hemoglobin particles and hemoglobin-hyaluronan-mixture particles. In Figure 6.3, compared to hemoglobin particles modified with HSA, pure hemoglobin particles and hemoglobin-hyaluronan-mixture particles adsorb obviously high amounts of proteins (e.g., IGHA, Albumin, Alpha-1-antitrypsin, Haptoglobin, ApoJ, Alpha-2-HS-glycoprotein, ApoA-I, Transthyretin, ApoC-II, ApoC-III) that have been identified on the gels.

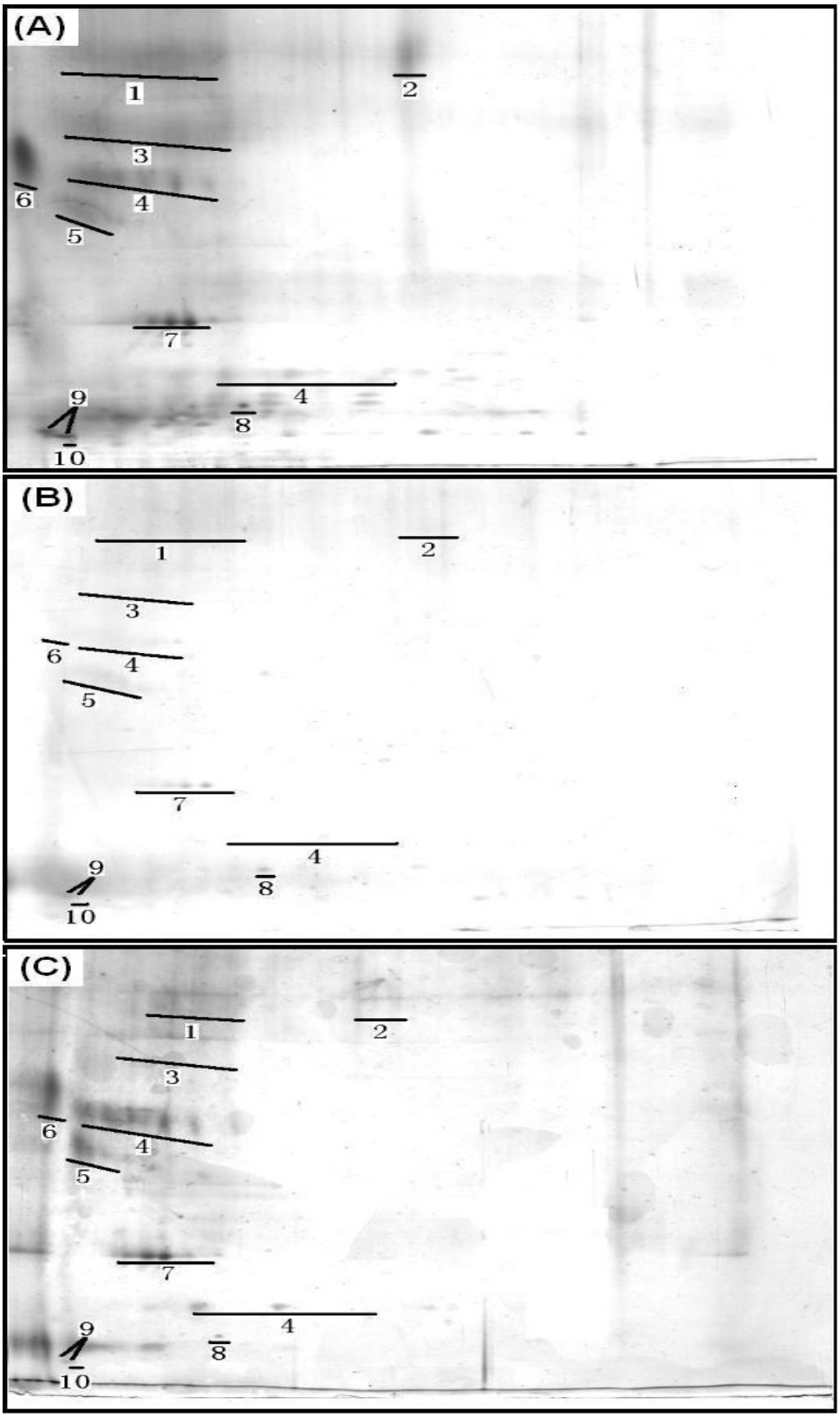


Figure 6.1. Adsorption protein patterns on different particles: (A) Pure hemoglobin particle in water; (B) hemoglobin particles modified with HSA on the surface in water and (C) hemoglobin-hyaluronan-mixture particles in 0.9 % NaCl. 1. Immunoglobulin

heavy chain alpha (IGHA), 2. Albumin (ALBU), 3. Alpha-1-antitrypsin (AIAT), 4. Haptoglobin (HPT), 5. ApoJ, 6. Alpha-2-HS-glycoprotein (FETUA), 7. Apo AI, 8. Transthyretin (TTHY), 9. ApoC-II, 10. ApoC-III.

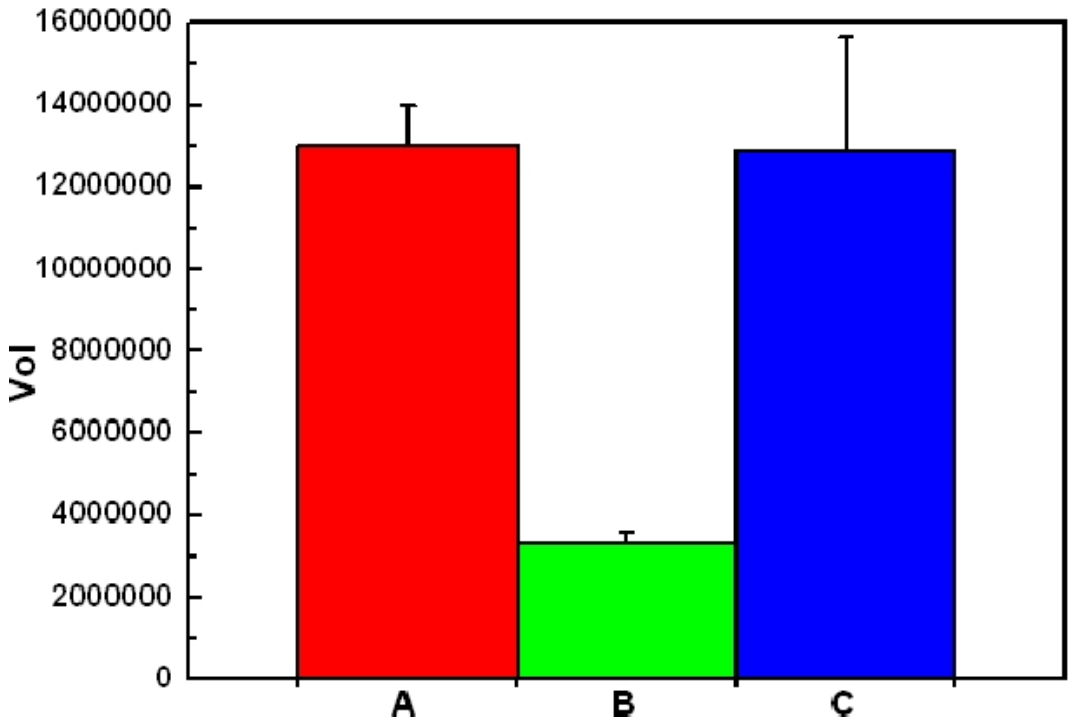


Figure 6.2. Total volume of protein adsorbed on Pure hemoglobin particle (A); hemoglobin particles modified with HSA (B) on the surface and hemoglobin-hyaluronan-mixture particles (C), which were analysed using 2D-PAGE. Error bars represent the standard deviation (n=3).

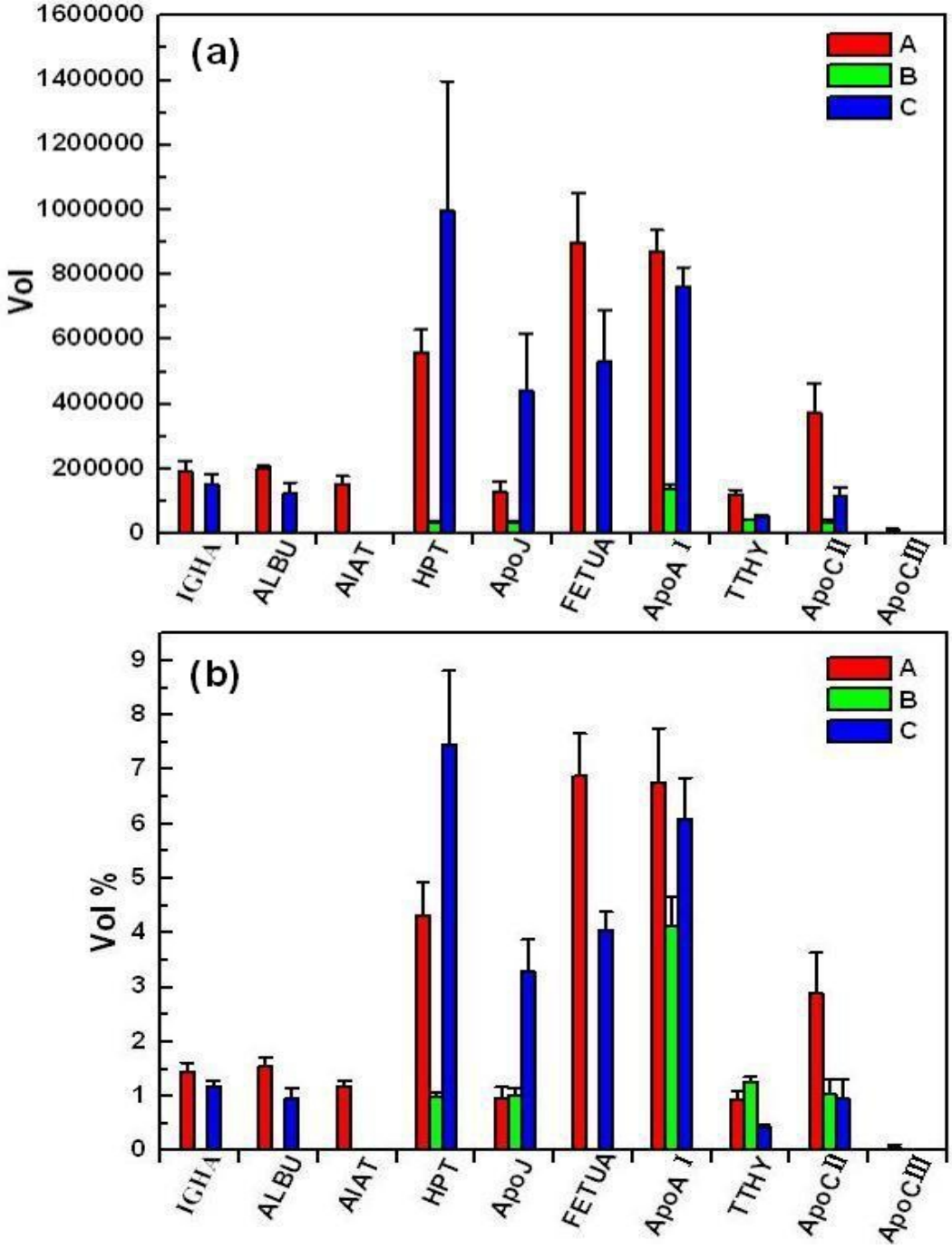


Figure 6.3: Plasma protein composition on Pure hemoglobin particle (A); hemoglobin particles modified with HSA (B) on the surface and hemoglobin-hyaluronan-mixture particles (C), which were analyzed using 2D-PAGE: (a) volume and (b) volume percentage. Error bars represent the standard deviation (n=3).

## 6.3.2 Influence of medium on protein adsorption pattern of particles

Figure 6.4 is the 2-DE gels of pure hemoglobin particle (A) in water (a) and in 2%HSA-0.9%NaCl (b), respectively, and Figure 6.5 is their adsorbed proteins compositions. Comparing their adsorbed protein compositions in Figure 6.5, it is found that the medium has very slight impact on the protein adsorption on pure hemoglobin particle (A). Actually, the protein adsorption on hemoglobin particles modified with HSA (B) has been just slightly affected by the medium as well, which is shown in Figure 6.6 and 6.7. Figure 6.6 is the 2-DE gels of hemoglobin particles modified with HSA (B) in water (a) and in 2%HSA-0.9%NaCl (b), and Figure 6.7 is their adsorbed proteins compositions. Therefore, the protein adsorption pattern is determined by the particles not by the medium.

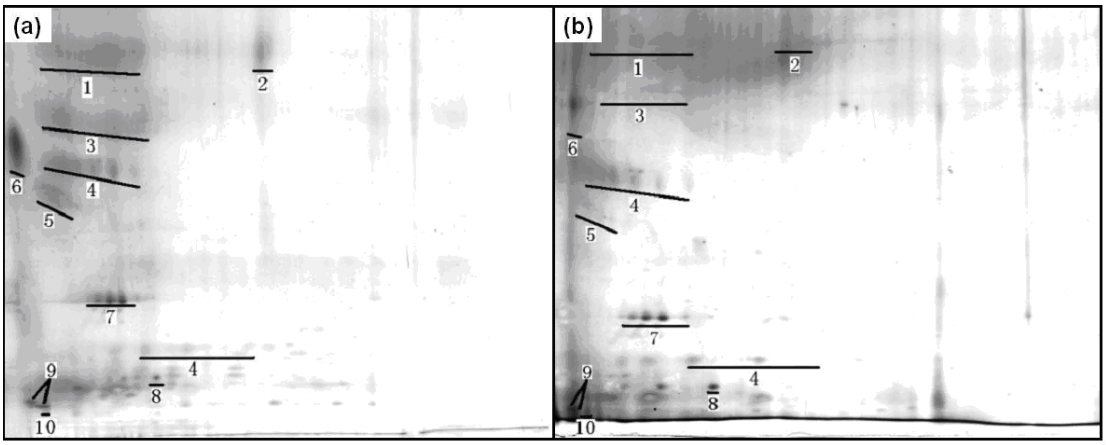


Figure 6.4. Adsorption protein patterns (A) Pure hemoglobin particle in water (a) and in 2%HSA-0.9%NaCl (b). 1. Immunoglobulin heavy chain alpha (IGHA), 2. Albumin (ALBU), 3. Alpha-1-antitrypsin (AIAT), 4. Haptoglobin (HPT), 5. ApoJ, 6. Alpha-2-HS-glycoprotein (FETUA), 7. Apo AI, 8. Transthyretin (TTHY), 9. ApoC-II, 10. ApoC-III.

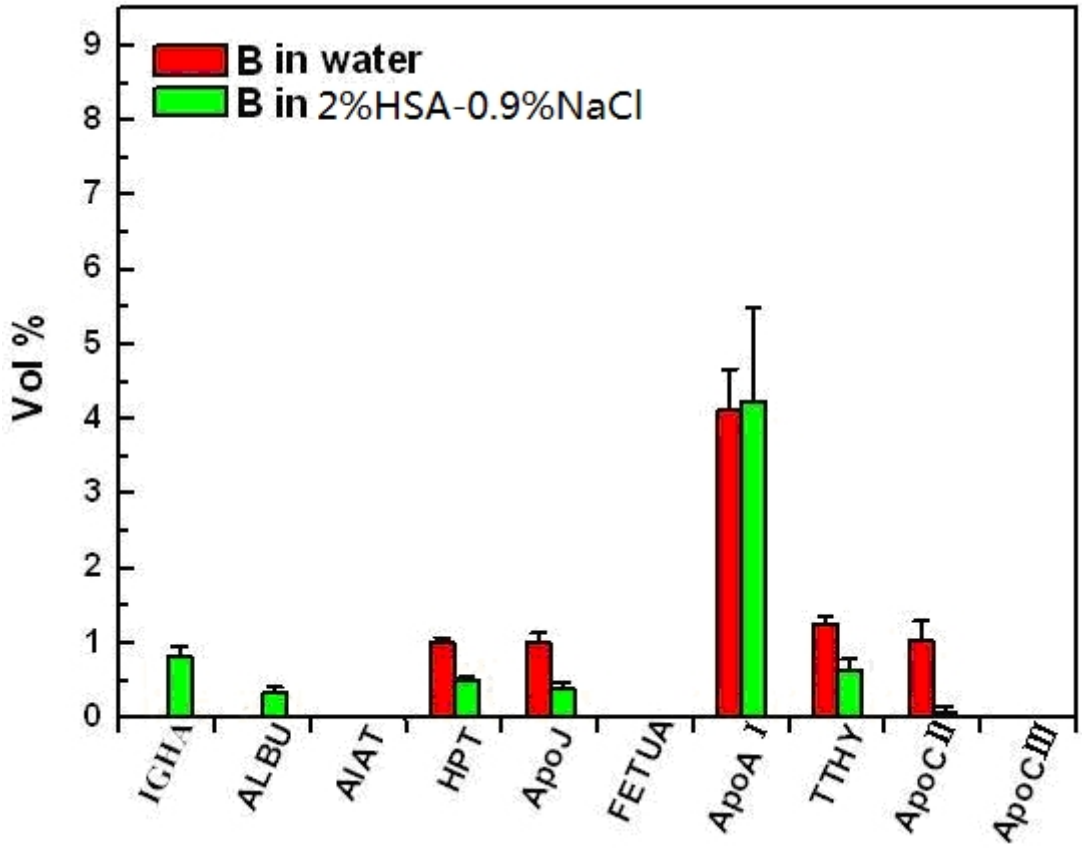


Figure 6.5. Plasma protein composition (A) pure hemoglobin particle in water and in 2%HSA-0.9%NaCl (n=3).

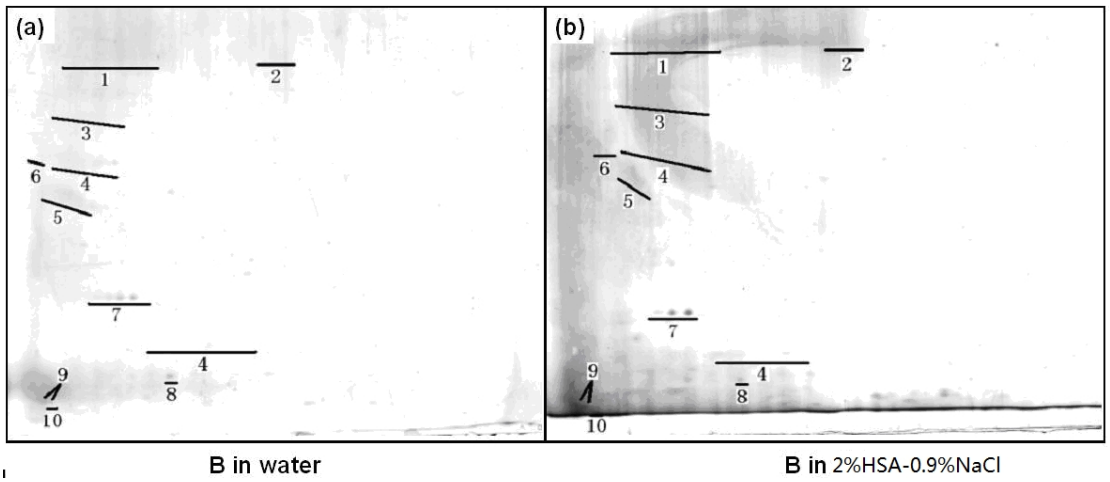


Figure 6.6. Adsorption protein patterns (B) hemoglobin particles modified with HSA in water (a) and in 2%HSA-0.9%NaCl (b). 1. Immunoglobulin heavy chain alpha (IGHA), 2. Albumin (ALBU), 3. Alpha-1-antitrypsin (AIAT), 4. Haptoglobin (HPT), 5. ApoJ, 6. Alpha-2-HS-glycoprotein (FETUA), 7. Apo AI, 8. Transthyretin (TTHY), 9. ApoC-II, 10. ApoC-III.

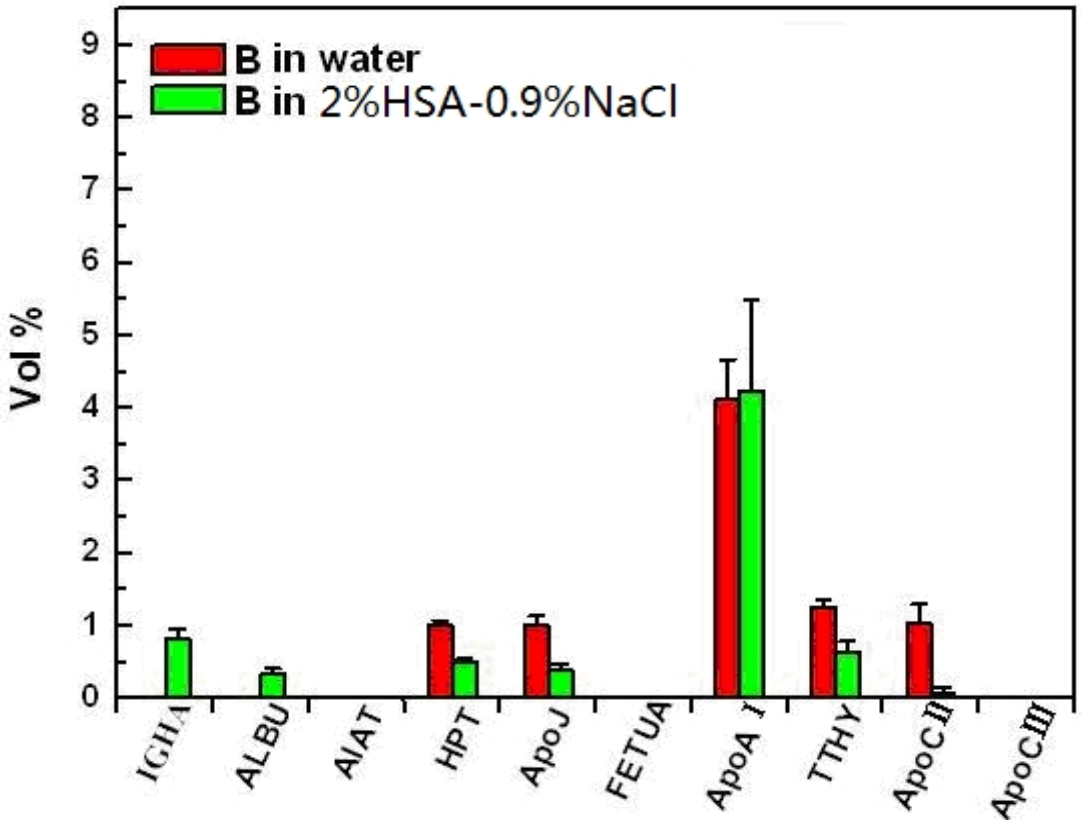


Figure 6.7. Plasma protein composition (B) hemoglobin particles modified with HSA in water and in 2%HSA-0.9%NaCl (n=3).

## 6.3.3 Protein adsorption kinetics on particle surfaces

The experimental results in Figure 6.2 and 6.3 show that hemoglobin particles modified with HSA adsorb much less proteins than pure hemoglobin particles as well as hemoglobin-hyaluronan-mixture particles. Human serum albumin is a hydrophilic protein in the blood. HSA on the particle surfaces decreases the surface hydrophobicity of particles leading to decrease the protein adsorption on the surface. For instance, Ogawara et al. (2004) observed that the HSA-coated polystyrene nanoparticles adsorbed much less proteins besides albumin than the polystyrene nanoparticles. Here, the reason is that HSA on the surface of hemoglobin particles modified with HSA protects this kind of particles from plasma protein adsorption by creating more hydrophilicity on their surface.

Furthermore, the experiments from the reference (Ogawara et al., 2004) also showed

that the HSA-coated polystyrene nanoparticles have a long circulation time in the bloodstream. Less particles will be recognized by the mononuclear phagocytic system, if the particles adsorb less proteins (Ogawara et al., 2004) excluding albumin. Therefore, the hemoglobin particles modified with HSA may have the longest circulation time in the blood.

## 6.4 Conclusion

The 2-DE results show that hemoglobin particles modified with HSA adsorb much less proteins than the other two kind of particles including pure hemoglobin particles and hemoglobin-hyaluronan-mixture particles, because that human serum albumin, a hydrophilic protein, could create more hydrophilic surface on the particles to restrain the protein adsorption onto them in the blood. Besides, the medium is observed to have very slight impact on the protein adsorption of the pure hemoglobin particle as well as the hemoglobin particles modified with HSA, so the protein adsorption pattern on the particles is determined by the particles not by the medium. The particles are less recognized by the MPS to achieve longer circulation time in the bloodstream, if they absorb less proteins excluding albumin. Therefore, hemoglobin particles modified with HSA on the surface may have a longer circulation time in the blood than the other two kind of hemoglobin particles because of the much less adsorbed protein amounts, and will be the most promising ones for blood substitutes. Their *in vivo* behaviors will be assessed in the next step in animals.

# 7. Intravenous rutin nanocrystals with potential use for Alzheimer treatment

## 7.1 Introduction

Nanocrystals are a smart formulation to create i.v. injectable formulations of poorly soluble drugs (e.g. NANOEDGE by Baxter, US). In most cases, accumulation in the liver is undesired, the crystals should either circulate in the blood and dissolve, or ideally accumulate in a target region, e.g. the brain. The blood proteins adsorbing on the particles after i.v. injection determine their organ distribution. For example, binding of opsonins (e.g., immunoglobulin G, complement factors, and fibrinogen) promotes phagocytosis and removal of the particles from the systemic circulation by cells of the mononuclear phagocytic system (MPS) (Leroux et al., 1995; Camner et al., 2002). In contrast, binding of dysopsonins (e.g., albumin, apolipoproteins) promotes prolonged circulation time in the blood (Moghimi et al., 1993; Ogawara et al., 2004). Moreover, surface-enriched proteins can mediate an uptake of the drug carriers by specific site (Kreuter et al., 2002; Müller and Schmidt, 2002). For instance, ApoE adsorbed on drug carriers might mimic LDL-particles adsorbing ApoE leading to their brain-uptake by endocytic processes (Müller et al., 2001). Analysis of the adsorption patterns allows to estimate the *in vivo* behavior.

The protein adsorption pattern is affected by the physicochemical particle properties, so by modification of the particle surface properties the protein pattern can be optimized to reach specifity to a certain target (e.g. preferential adsorption of Apo E for brain targeting). For instance, it has been observed that Tween 80-SLN had adsorbed a relatively high adsorption amount of ApoE (Göppert and Müller, 2003 and 2005b). Besides, the conformation of the adsorbed polymer on particles influences the protein adsorption pattern via the degree of exposure of hydrophilic polyethylene

oxide (PEO) chains or hydrophobic polypropylene (PPO) chains (Göppert and Müller, 2005c) and the steric hindrance effect of polymer chains (e.g. PEO) against the adsorption of proteins (Gref et al., 2000; Carignano and Szleifer, 2000; Gessner et al., 2003).

The plasma protein adsorption pattern on particles were analyzed *in vitro* by two-dimensional polyacrylamide gel electrophoresis (2-DE; 2D-PAGE) (Blunk et al., 1993; Harnisch and Müller, 1998; Lück et al., 1998; Gessner et al., 2001). Antioxidants e.g. rutin are a major player in potential treatment of Alzheimer disease. Therefore nanocrystals of the poorly soluble anti-oxidant rutin were produced. As the surfactants could affect the protein adsorption patterns on the particles, those rutin nanocrystals were stabilized with three different surfactants to form four kind of nanocrystals including Plantacare 2000 UP (0.1 %)-rutin nanoparticles, Plantacare 2000 UP (1.1 %)-rutin nanoparticles, Tween 80-rutin nanoparticles, and Poloxamer 188-rutin nanoparticles. Their protein adsorption patterns were analyzed to assess their potential for brain targeting in Alzheimer treatment after i.v. Injection in this chapter. The experimental results show that Tween 80-rutin particles adsorb the highest amount of ApoE, which indicates that this particles may have the potential of brain targeting.

## 7.2 Materials and methods

### 7.2.1 Preparations of rutin nanocrystals

Rutin nanocrystals were prepared by Chen (2013) via high pressure homogenization (Homogenizer Micron LAB 40, APV Deutschland GmbH, Germany) and then stabilized with different surfactants in Milli-Q water (Millipore, Germany). Briefly, rutin was firstly dispersed in Plantacare 2000 UP solution, and then Glycerol was added. In turn, 2 cycles 250 bar, 2 cycles 500 bar, 2 cycles 750 bar, 2 cycles 1000 bar and 10 cycles 1500 bar high pressure homogenization were performed to achieve the

stock rutin nanosuspension. The formulation of stock rutin nanosuspension is shown in Table 7.1.

Table 7.1. Formulations of stock rutin nanosuspension.

| | rutin | Plantacare 2000 UP | Glycerol |
|---|---|---|---|
| Original rutin nanosuspension | 2.0 % | 0.2 % | 2.5 % |

To investigate the influence of the stabilizer on the absorption of specific protein, the stock rutin nanosuspension was diluted with gentle stirring into four various formulations in Table 7.2.

Table 7.2. Formulations of rutin nanoparticles coated with different surfactants.

| Formulation | Rutin (%) | Plantacare 2000 UP (%) | Tween 80 (%) | Poloxamer 188 (%) | Glycerol (%) |
|---|---|---|---|---|---|
| A | 1.0 | 0.1 | 0 | 0 | 2.5 |
| B | 1.0 | 1.1 | 0 | 0 | 2.5 |
| C | 1.0 | 0.1 | 1.0 | 0 | 2.5 |
| D | 1.0 | 0.1 | 0 | 1.0 | 2.5 |

## 7.2.2 Characterization of rutin nanocrystals

Photon correlation spectroscopy (PCS) was performed using a Zetasizer Nano ZS (Malvern Instruments, UK). The samples were diluted using Milli-Q water and measurements were performed at 25 ◦C temperature. The mean diameter and polydispersity index (PI) of samples were measured.

Laser diffractometry (LD) of samples was performed using the Mastersizer 2000 (Malvern Instruments, UK) in deionized water. LD produces diameters D 10%, D 50%, D 90%, D 95% and D 99% (volume distribution) as characterization parameters. The Mie theory is used with optical parameters 1.593 for the real refractive index and

0.000 for the imaginary refractive index.

The surface charge of particles was characterized by zeta potential (ZP) using a Malvern Zetasizer Nano ZS (Malvern Instruments, UK) applying a field strength of 20 V/cm at 25 ◦C. The ZP calculation was performed using the Helmholtz–Smoluchowski equation. The surface charge has been measured in Milli-Q water adjusted to 50 µS/cm using 0.9 % NaCl solution and in original medium.

The characterization data of different rutin nanocrystals are shown in Table 7.3. Compared with the LD results, the increased PCS size of Tween 80-rutin particles may result from a loose bridging effect among the Tween 80 molecules. All the rutin nanoparticle systems possess similar sizes around 300 nm and negative charges on the surfaces.

Table 7.3. Different rutin particle formulations and their characterization data on size (by photo correlation spectroscopy (PCS) and laser diffractometry (LD)) and zeta potential (ZP).

| System | | stock | A | B | C | D |
|---|---|---|---|---|---|---|
| PCS | mean diameter (nm) | 313 | 308 | 260 | 1394 | 319 |
| | polydispersity index | 0.206 | 0.187 | 0.180 | 0.231 | 0.211 |
| LD (µm) | D 10 % | 0.158 | 0.161 | 0.160 | 0.171 | 0.164 |
| | D 50 % | 0.291 | 0.292 | 0.290 | 0.305 | 0.295 |
| | D 90 % | 0.529 | 0.532 | 0.524 | 0.568 | 0.540 |
| | D 95 % | 0.637 | 0.640 | 0.627 | 0.715 | 0.653 |
| | D 99 % | 1.560 | 1.520 | 1.481 | 1.591 | 1.519 |
| ZP (mV) | in 50 µs/cm NaCl solution | -28.4 | -26.0 | -26.4 | -20.0 | -24.2 |
| | in original medium | -33.2 | -32.2 | -17.9 | -8.14 | -25.1 |

## 7.2.3 Sample preparation for 2D-PAGE

The two-dimensional polyacrylamide gel electrophoresis (2D-PAGE; 2-DE) was used to analyze the protein adsorption patterns on particle surface. The particle samples (system A, B, C, and D) were incubated with human plasma at 37 ◦C for 5 min (1 ml sample per ml plasma). To mimic the conditions in the bloodstream, the particles were incubated routinely for 5 min in citrated plasma, because *in vivo* in case recognition by the MPS occurs, in the first 5 min up to 90 % of the injected dose are taken up by the liver marcophages (O'Mullane et al., 1987; Müller, 1991; Liniemark et al., 1995). In case particles survive in the first 5 min, prolonged blood circulation of these particles was found (Illum and Davis, 1987; Cattel et al., 2003). Separation of the particles from the excess plasma was performed by centrifugation at 22,940 g for 1 h at 20 ℃, and then washing three times with 0.05 M phosphate buffer, pH 7.4 and subsequent centrifugation respectively at 22,940 g for 1 h at 20 ℃. The adsorption proteins on particles were desorbed using sodium dodecyl sulfate (SDS) and dithioerythritol (DTE) for 5 min at 95 ℃, then cooled down to room temperature and incubated with a solution containing DTE (Dithioerythritol), CHAPS (3-(3-Cholamidopropyl)dimethylammonio-1-propansulfat), urea, and Tris (Tris(hydroxymethyl)-aminomethan), stirring and centrifuging 10-15 min at 22,940 g. Finally, the mixture solution added rehydration buffer for 2-DE was used to analyse the protein adsorption pattern on particles.

## 7.2.4 Two-dimensional polyacrylamide gel electrophoresis

The 2D-PAGE was used to analyze the protein adsorption patterns on particle surface. Proteins were separated on IPG-strips according to their isoelectric focusing (IEF) in the first dimension and on gels based on molecular weights (MW) in the second dimension of 2D-PAGE (SDS-PAGE). The first dimension (IEF) was run using a Multiphore II from Amersham Pharmacia Biotech with a E 752 power supplied from Consort (Turnhount, Belgium). The second dimension (SDS-PAGE) was performed in

Protean II Multi-Cells with a 1000 power obtained from Bio-Rad. Between the IEF and SDS-PAGE steps, the IPG strip is saturated with the IPG strip equilibration I for 15 min and then II for 20 min. The equilibration I contains DTE, SDS, Glycerol, Urea, as well as Bromphenol blue, and the equilibration II includes Iodoacetamide, SDS, Glycerol, Urea, and Bromphenol blue.

The gels were silver-stained and scanned after 2D-PAGE. The gels were scanned by ImageScanner (Amershan Pharmacia Biotech). The spots on gels were recognized by matching the master map of human plasma. The amount of adsorbed protein was analyzed using a semi-quantitative manner based on the spot size and intensity on the gel. The data of spots on gels were measured by Melanie III software (Swiss Institute of Bioinformatics, Geneva, Switzerland).

## 7.3 Result and discussion

### 7.3.1 Protein adsorption patterns on rutin nanoparticles

The whole 2D-PAGE gels of protein adsorption patterns on different rutin particles were shown in Figure 7.1. The adsorbed proteins as the biological identities of injected particles control their behaviors *in vivo*. The experimental results in Figure 7.1 show that all the rutin particles adsorbed mainly ApoA-IV, ApoA-I, ApoE, and ApoJ.

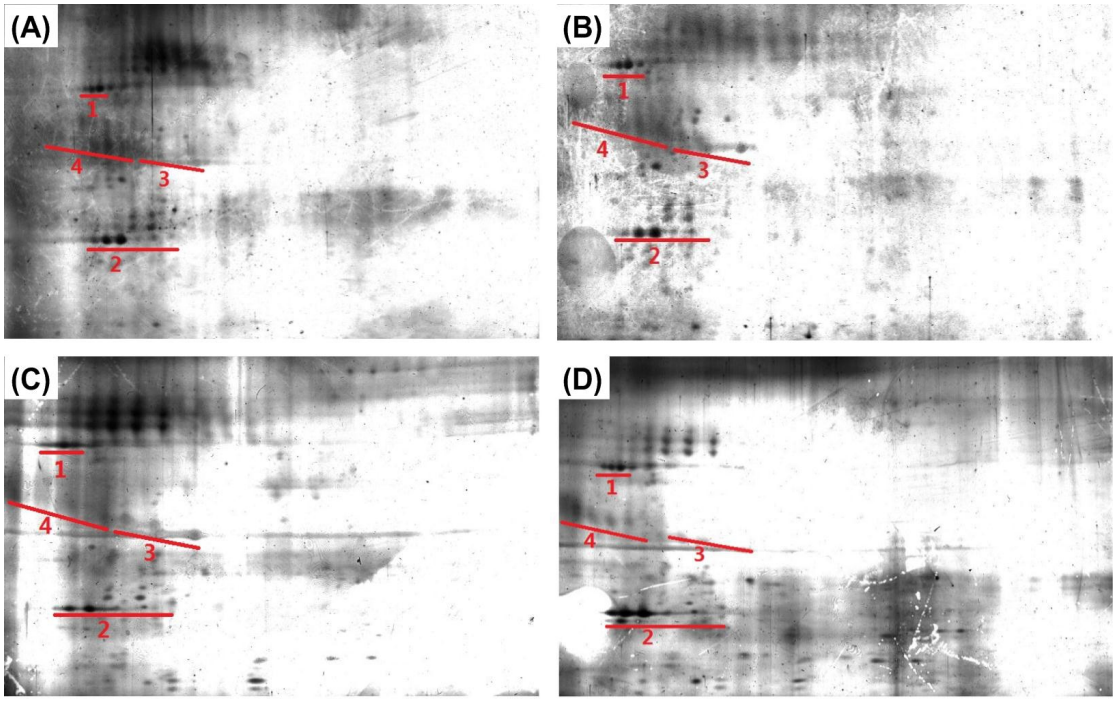


Figure 7.1. Gels of plasma protein adsorption patterns on different rutin particles (system A: Plantacare 2000 UP (0.1 %)-rutin nanoparticles, B: Plantacare 2000 UP (1.1 %)-rutin nanoparticles, C: Tween 80-rutin nanoparticles, and D: Poloxamer 188-rutin nanoparticles). 1: ApoA-IV, 2: ApoA-I, 3: ApoE, 4: ApoJ.

Figure 7.2 is the total amount of adsorbed proteins on those four kind of rutin nanoparticles. The experimental results in Figure 7.2 show that all the rutin particles adsorbed almost identical total amounts of proteins. For instance, all of rutin particles exhibited almost identically adsorbed amounts on ApoA-IV, ApoJ and ApoA-I, excluding ApoE which is generally regarded as an important protein for targeting to brain (Dehouck et al., 1997).

Figure 7.3 shows in detail the adsorption pattern compositions: the Tween-80 rutin particles (formulation C) possess the adsorbed amount of Apo E at the highest; the rutin particles of A (Plantacare 2000 UP (0.1 %)-rutin nanoparticle) and B (Plantacare 2000 UP (1.1 %)-rutin nanoparticle) have similar adsorbed amounts; the Poloxamer 188-rutin particles (D) did not adsorb ApoE. ApoE adsorbed on nanoparticles might mimic LDL-particles coated with ApoE leading to their brain-uptake by endocytic

processes (Müller et al., 2001). Therefore, the formulation of Tween 80-rutin nanoparticles (C) probably has the potential for drug targeting.

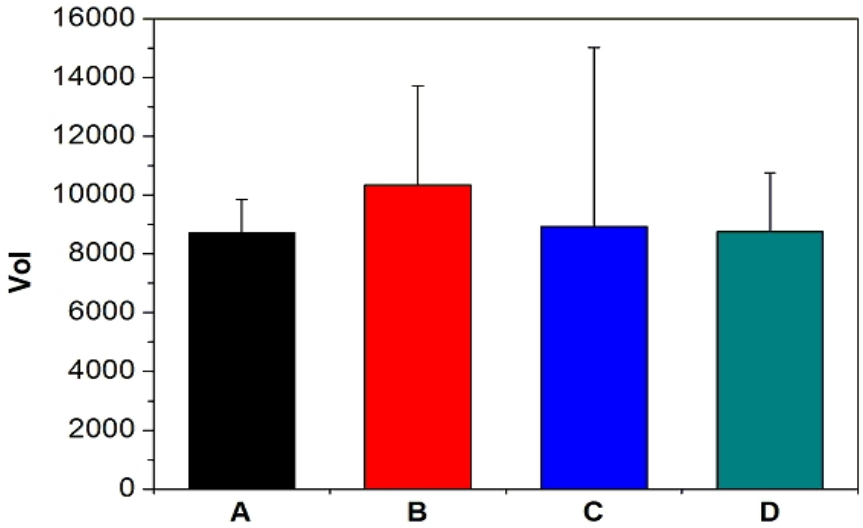


Figure 7.2. Total volume of protein adsorbed onto different rutin particles (system A: Plantacare 2000 UP (0.1 %)-rutin nanoparticles, B: Plantacare 2000 uUP (1.1 %)-rutin nanoparticles, C: Tween 80-rutin nanoparticles, and D: Poloxamer 188-rutin nanoparticles) which was analyzed using 2D-PAGE. Error bars represent the standard deviation (n=3).

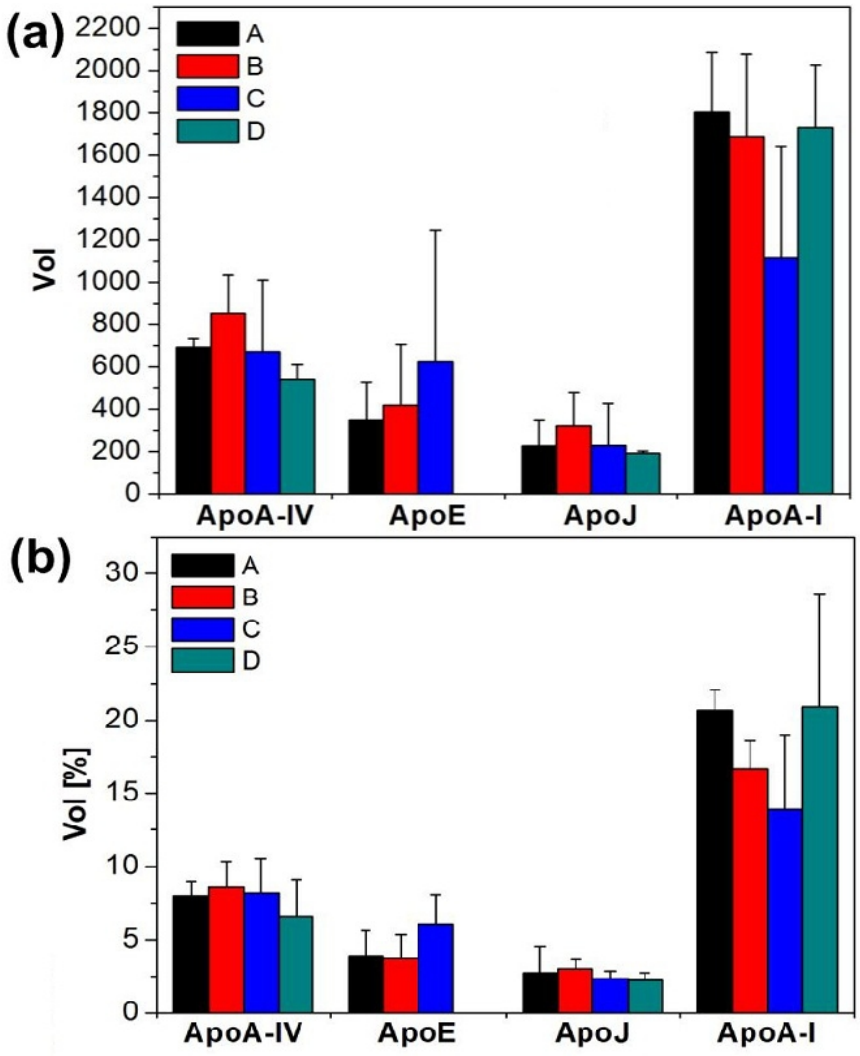


Figure 7.3. Plasma protein composition different rutin particles (system A: Plantacare 2000 UP (0.1 %)-rutin nanoparticles, B: Plantacare 2000 UP (1.1 %)-rutin nanoparticles, C: Tween 80-rutin nanoparticles, and D: Poloxamer 188-rutin nanoparticles) which were analyzed using 2D-PAGE: (a) volume and (b) volume percentages. Error bars represent the standard deviation (n=3).

## 7.3.2 Interaction of proteins and different rutin nanoparticle surfaces

The behaviors of adsorbed proteins on different nanoparticles are influenced by the physicochemical properties of the nanoparticle surface. For instance, Göppert and Müller (2003) observed that the adsorbed amount of ApoE on Tween 80-SLN was

high while Poloxamer 188-SLN did not adsorb any ApoE on the surface in Figure 7.4. The differences among the adsorbed protein behaviors on various nanoparticles are mainly due to the diversities of nanoparticle properties, such as size of nanoparticle (the curvature effects), the chain length and density of surfactant (the steric effects), hydrophobicity/hydrophilicity of surface (the hydrophobic interactions), zeta potential of nanoparticle (the electrostatic interactions).

Here, the surfactant plays a very important role on the adsorption behavior of ApoE on different rutin nanoparticle surfaces. The rutin particles of A (Plantacare 2000 UP (0.1 %)-rutin nanoparticle) and B (Plantacare 2000 UP (1.1 %)-rutin nanoparticle) have similar adsorbed amounts due to their identical composition on their surfaces.

The experimental results in Figure 7.3 also show that Tween 80-rutin nanoparticle possesses the highest adsorbed amount of ApoE of all the samples and Poloxamer 188-rutin nanoparticle does not adsorb any ApoE at all, which is the same as the adsorption of ApoE on Tween 80-SLN and Poloxamer 188-SLN in the reference (Göppert and Müller, 2003).

Tween 80 coating on nanoparticles has specifical adsorption for ApoE (Göppert and Müller, 2003) to be able to deliver drugs to the brain (Kreuter et al., 1997; Kreuter 2001), because that ApoE transports lipoproteins into the brain via the low density lipoprotein (LDL) receptor on the blood-brain barrier (BBB) (Dehouck et al., 1997), and nanoparticles adsorbing ApoE might mimic LDL-particles adsorbing with ApoE leading to their brain-uptake by endocytic processes (Müller et al., 2001).

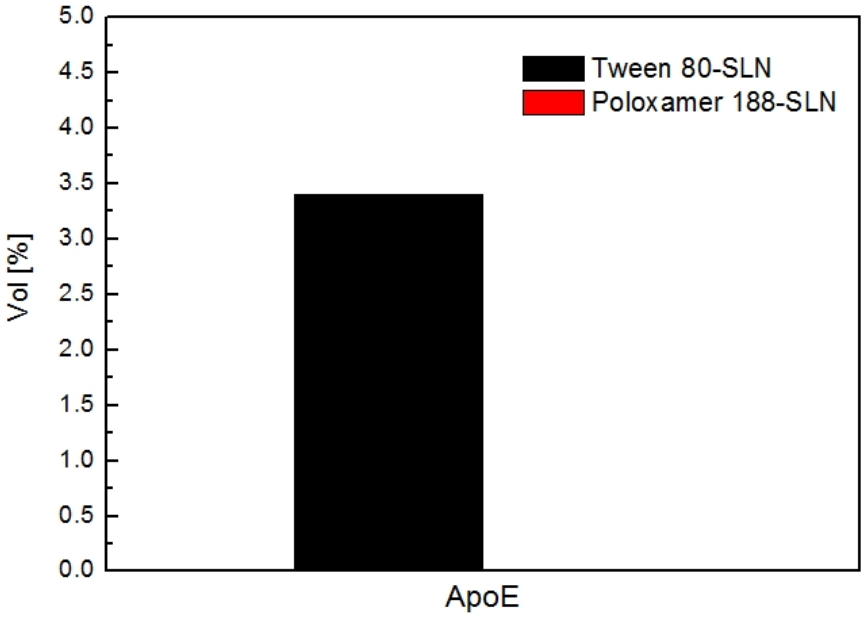


Figure 7.4. Volume percentages of adsorbed ApoE on Tween 80-SLN and Poloxamer 188-SLN (The adsorbed amount of ApoE on Poloxamer 188-SLN is zero.) (Göppert and Müller, 2003).

Besides, Göppert and Müller (Göppert and Müller, 2005a) studying the influence of hydrophilic PEO-units of surfactants on the protein adsorption patterns found that the adsorbed amounts of apolipoproteins declined by increasing the PEO-units on the surfaces due to the steric effects and hydrophilicity increased. The detailed adsorption behavior of ApoE with the increase of hydrophilic PEO-units on particles is shown in Figure 7.5. In Figure 7.5, the adsorbed amount of ApoE was dramatically decreased with the increase of PEO-units. When PEO-units of the surfactant is 128, the volume percentage of ApoE adsorbed on the surface is very low about 0.1 %. PEO-units dramatically affects the adsorbed amount of ApoE on the nanoparticle surface. Therefore, the experimetnal results showed that neither Poloxamer 188-SLN nor Poloxamer 188-rutin nanoparticle adsorbed ApoE on their surface due to the steric effects and hydrophilicity of the PEO chains provided by the surfactant of Poloxamer 188.

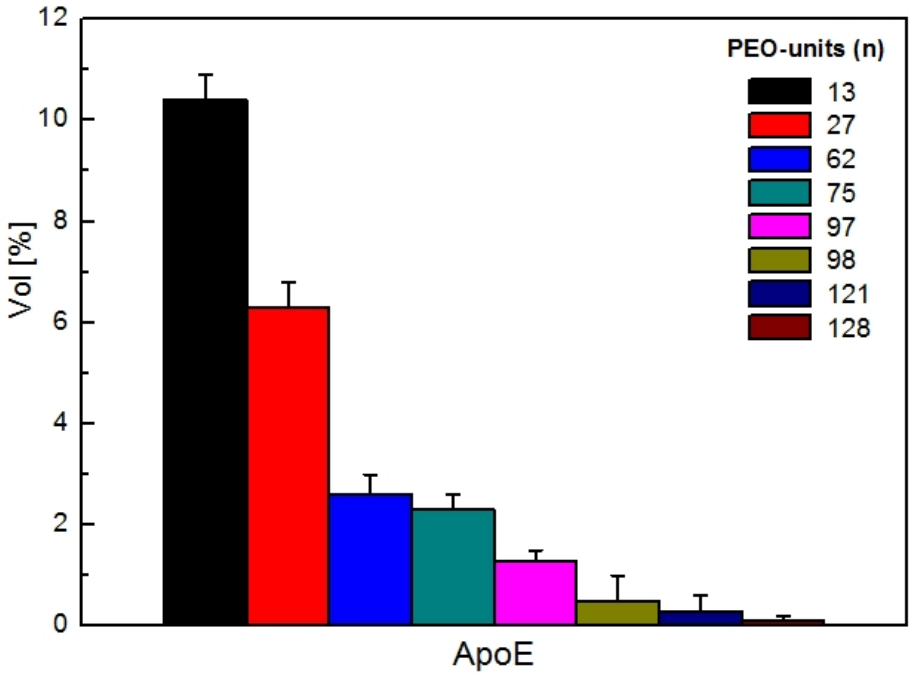


Figure 7.5. Influence of the PEO-units of surfactants on the volume percentages of adsorbed ApoE (Göppert and Müller, 2005a) .

## 7.4 Conclusion

The 2-DE results shows that the four formulations of rutin nanocrystals have similar total amount of adsorbed proteins. Nevertheless, the adsorbed amount of ApoE is altered on different particles. Plantacare 2000 UP (0.1 %)-rutin nanoparticles and Plantacare 2000 UP (1.1 %)-rutin nanoparticles have similar adsorbed amounts of ApoE due to their identical composition on their surfaces. Tween 80-Rutin nanoparticles have the highest amount of ApoE since Tween 80 coating on nanoparticles has specifical adsorption for ApoE. Finally, Poloxamer 188-rutin nanoparticles does not absorb ApoE because of the steric effects and hydrophilicity of the PEO chains on the nanoparticle surface.

ApoE is able to deliver drugs to the brain. Therefore, Tween 80-rutin nanoparticle has the potential for brain targeting, but their *in vivo* behaviors have to be verified in the next step in animals. It opens the perspective of using rutin nanocrystals in Alzheimer treatment.

# 8. Summary

The study of drug targeting is for the purpose of reducing side effects and achieving selective effectiveness of drugs *in vivo.* The determining factor for the *in vivo* fate and organ targeting of drug carriers is the adsorbed blood proteins on the their surfaces after i.v. injection, and their blood protein adsorption patterns as their biological identities in the body are affected by the physicochemical properties of drug carriers. 2-DE has been proved to be a useful tool for analyzing the protein adsorption pattern of particles *in vitro*.

In this work, several particle systems are covered. Their protein adsorption patterns are achieved by the 2-DE method. The interaction between proteins and particles are discussed as well.

Firstly, some important instruments for this work have been introduced including two dimensional polyacrylamide gel electrophoresis (2-DE; 2D-PAGE) in chapter 2, photon correlation spectroscopy (PCS), zeta potential (ZP), laser diffractometry (LD) and high pressure homogenization (HPH) in chapter 3.

Then, the adsorbed protein patterns on different SLN are briefly reviewed and the interactions between them are discussed in chapter 4. In general, three kind of proteins are adsorbed on SLN, including albumin, apolipoproteins and fibrinogen. Under the experimental conditions, the results indicate that fibrinogen and apolipoproteins possess similar interactions with the SLN surface but albumin different. The lower affinity fibrinogen was obviously displaced by the higher affinity apolipoproteins when the concentration of plasma increased, while by increasing of PEO-chain units (hydrophilicity) on the SLN surface, the decreased amounts of apolipoproteins could be complemented by fibrinogen. Compared with

apolipoproteins and fibrinogen, the adsorption behaviors of albumin were independent from the hydrophobicity/hydrophilicity of SLN. The incubation time is just observed altering the adsorbed amount of proteins but not protein adsorption pattern on SLN coated with surfactant. Normally, the steric effects e.g., the conformation of absorbed surfactants, the hydrophobic interactions, and the electrostatic effects are regarded as three important factors of protein adsorption on the particle surface. Experimental results showed that the interactions between fibrinogen/apolipoproteins and SLN mainly is the hydrophobic effects. But albumin is very different from those two proteins, the electrostatic effects probably play a more important role on the interactions between albumin and SLN. Therefore, the hydrophilic PEO-chains of surfactants could affect the adsorption behaviors of fibrinogens and apolipoproteins by changing the steric effects and hydrophobic effects.

In chapter 5, the protein adsorption patterns on the i.v. injection of egg lecithin-stabilized oil-in-water emulsions have been analyzed *in vitro* by 2-DE. The 2-DE results show that nanoemulsion samples mainly adsorb apolipoproteins as same as SLN. The amounts and percentages of adsorbed proteins on emulsion samples clearly change with incubation time: adsorbed proteins trend to desorb and different adsorbed proteins start to decrease their amounts and percentages at different incubation time. The changes of protein adsorption with incubation time on nanoemulsion are different from them on SLN because of e.g., steric effects of the hydrophilic PEO-chains on the SLN surfaces. The total amount of adsorbed proteins on the nanoemulsions decreases with increasing the incubation time. The knowledge of time-dependent protein adsorption pattern will be helpful for understanding the protein adsorption kinetics on the drug carrier system. Besides, the experimental results indicate that centrifugation has obviously induced the adsorption of small size proteins (e.g., ApoC-II, ApoC-III and ApoA-II) and the desorption of large size protein (ApoA-I, ApoA-IV, ApoE, albumin, especially ApoJ) due to extending the adsorption processes of proteins about 1-2 hours. Compared to centrifugation, the faster gel filtration method (merely about 15 min) is more suitable for separating the

nanoemulsion system from extra plasma due to the shorter separation time.

In chapter 6, Hemoglobin particles including pure hemoglobin particle, hemoglobin particles modified with HSA on the surface, and hemoglobin-hyaluronan-mixture particles were prepared as blood substitutes with a novel 3-step-technique (co-precipitation, cross-linking and dissolution). The 2-DE results show that hemoglobin particles modified with HSA adsorb much less proteins than the other two kind of particles including pure hemoglobin particles and hemoglobin-hyaluronan-mixture particles, because that human serum albumin, a hydrophilic protein, could create more hydrophilic surface on the particles to restrain the protein adsorption onto them in the blood. Besides, the medium is observed to have very slight impact on the protein adsorption of the pure hemoglobin particle as well as the hemoglobin particles modified with HSA, so the protein adsorption pattern on the particles is determined by the particles not by the medium. The particles are less recognized by the MPS to achieve longer circulation time in the bloodstream, if they absorb less proteins excluding albumin. Therefore, hemoglobin particles modified with HSA on the surface may have a longer circulation time in the blood than the other two kind of hemoglobin particles because of the much less adsorbed protein amounts, and will be the most promising ones for blood substitutes. Their *in vivo* behaviors will be assessed in the next step in animals.

In chapter 7, four formulations of rutin nanocrystals (Plantacare 2000 UP (0.1 %)-rutin nanoparticles, Plantacare 2000 UP (1.1 %)-rutin nanoparticles, Tween 80-rutin nanoparticles, and Poloxamer 188-rutin nanoparticles) were prepared and their protein adsorption patterns were analyzed with the 2-DE method. The 2-DE results shows that the four formulations of rutin nanocrystals have similar total amount of adsorbed proteins. Nevertheless, the adsorbed amount of ApoE is altered on different particles. Plantacare 2000 UP (0.1 %)-rutin nanoparticles and Plantacare 2000 UP (1.1 %)-rutin nanoparticles have similar adsorbed amounts of ApoE due to their identical composition on their surfaces. Tween 80-Rutin nanoparticles have the

highest amount of ApoE since Tween 80 coating on nanoparticles has specifical adsorption for ApoE. Finally, Poloxamer 188-rutin nanoparticles does not absorb ApoE because of the steric effects and hydrophilicity of the PEO chains on the nanoparticle surface. ApoE is able to deliver drugs to the brain. Therefore, Tween 80-rutin nanoparticle has the potential for brain targeting, but their *in vivo* behaviors have to be verified in the next step in animals. It opens the perspective of using rutin nanocrystals in Alzheimer treatment.

All in all, this work has investigated the protein adsorption patterns on different nanocarriers including SLN coated with different surfactant, nanoemulsion, different hemoglobin particles and different rutin nanocrystals and discussed protein adsorption kinetics on them. The results shows that the properties of particle surfaces could dramatically affect protein adsorption on them due to the steric effects, hydrophobic effects, electrostatic effects and so on. Finally, the most potential of particles for drug carrier are chosen based on their protein adsorption pattern. But their *in vivo* behaviors have to be verified in the next step in animals. Nevertheless, this work has a guide to prepare the desired drugs.

Many challenges still stay in this drug targeting area today, such as to understand how plasma proteins adsorb on particles *in vivo*, better way to control particles to the target tissue. In-depth study is required in this area in the future. All the studies aim at developing and improving drug carriers to better deliver drugs to target tissue and apply in nanomedicine.

# 9. Zusammenfassung

Diese „Drug Targetings“ Studie hatte zum Ziel, die Nebenwirkungen von Arzneimitteln *in vivo* zu reduzieren und deren Selektivität zu erhöhen. Der bestimmende Faktor bei der i. v. Injektion für das *in vivo* Verhalten und dem Organ Targeting der Arzneistofftransporter ist das adsorbierte Blutprotein auf deren Oberfläche. Das Blutproteinadsorptionsmuster der Arzneistofftransporter bestimmt ihre biologische Identität im Körper und wird bestimmt durch deren physikochemische Eigenschaften. 2-DE hat sich als eine wertvolle Methode für die Analyse der Partikelproteinadsorptionsmuster *in vitro* herausgestellt.

In dieser Arbeit wurden mehrere Partikelarten untersucht. Ihre Proteinadsorptionsmuster wurden mit 2-DE untersucht. Weiterhin wurden die Wechselwirkungen zwischen Proteinen und Partikeln diskutiert.

Zuerst wurden einige wichtige Methoden dieser Arbeit vorgestellt. Die zweidimensionale Polyacrylamid Gel Elektrophorese (2D-PAGE; 2-DE) in Kapitel 2 und Photonenkorrelationsspektroskopie (PCS), Zetapotential (ZP), Laserdiffraktometrie (LD) und Hochdruckhomogenisation (HPH) in Kapitel 3.

Dann wurden in Kapitel 4 die Proteinadsorptionsmuster von verschieden SLN kurz beschrieben und die Wechselwirkungen zwischen den Partikeln und Proteinen diskutiert. Im Allgemeinem adsorbierten drei Arten von Proteinen auf den SLN: Albumin, Apolipoproteine und Fibrinogen. Die Ergebnisse der Experimente zeigen, dass Fibrinogen und Apolipoproteine ähnliche Wechselwirkungen zur SLN-Oberfläche haben und diese sich von denen von Albumin unterscheiden. Die geringe Fibrinogenaffinität wurde deutlich, als man die Plasmakonzentration erhöht hat, und anschließend mehr und stärker affine Apolipoproteine als Fibrinogen gefunden hat. Im Gegensatz dazu wurden bei ansteigender PEO-Kettenlänge (Hydrophilie) auf der SLN-Oberfläche die absinkenden Apolipoproteinmengen durch

Fibrinogen ersetzt. Verglichen mit Apolipoproteinen und Fibrinogen, war das Adsorptionsverhalten von Albumin unabhängig von der Hydrophobie/Hydrophilie der SLN. Bei verschiedenen Inkubationszeiten von SLN, welche mit Surfactants beschichtet wurden, wurde nur eine sich ändernde Menge an adsorbierten Proteinen beobachtet, aber keine Unterschiede in den Proteinadsorptionsmustern. Normalerweise werden sterische Effekte (z. B. Konformation der absorbierten Surfactants), hydrophobe Wechselwirkungen und elektrostatische Effekte als drei wichtige Faktoren der Partikelproteinadsorption betrachtet. Die experimentellen Ergebnisse zeigen, dass die Wechselwirkungen zwischen Fibrinogen/Apolipoproteinen und SLN hauptsächlich hydrophober Natur waren. Im Gegensatz dazu dominieren bei Albumin die elektrostatischen Wechselwirkungen. Deswegen konnten die hydrophilen PEO-Ketten der Surfactants das Adsorbtionsverhalten von Fibrinogen und Apolipoproteinen durch sich verändernde sterische und hydrophobe Wechselwirkungen beeinflussen.

In Kapitel 5 wurden die Proteinadsorptionmuster von i. v. injizierbaren, mit Ei-Lecithin stabilisierten Öl-in-Wasser-Emulsionen *in vitro* mit 2-DE analysiert. Die 2-DE Ergebnisse zeigen, dass Nanoemulsionsproben ähnlich SLN hauptsächlich Apolipoproteine adsorbieren. Die Mengen und prozentualen Anteile adsorbierter Proteine auf den Emulsionsproben ändern sich deutlich mit der Inkubationszeit: Verschiedene adsorbierte Proteine neigen dazu zu desorbieren, wodurch sich ihr Anteil reduziert. Die Veränderungen der Proteinadsorption mit sich ändernder Inkubationszeit unterscheiden sich bei Nanoemulsionen und SLN, z. B. wegen sterischer Effekte der hydrophilen PEO-Ketten auf den SLN-Oberflächen. Die Gesamtmenge der adsorbierten Proteine auf den Nanoemulsionen nimmt mit Erhöhung der Inkubationszeit ab. Die Kenntnis von zeitabhängigen Proteinadsorptionsmustern wird hilfreich für das Verständnis der Proteinadsorptionskinetik auf Arzneistoffträgern sein. Außerdem zeigen die Versuchsergebnisse, dass Zentrifugation offensichtlich die Adsorption von kleinen Proteinen (z.B. ApoC-II, ApoC-III und ApoA-II) und die Desorption von großen

Proteinen (ApoA-I, ApoA-IV, ApoE, Albumin und insbesondere ApoJ), durch die Verlängerung des Adsorptionprozesses auf etwa 1-2 Stunden, induziert. Im Vergleich zur Zentrifugation, ist die schnellere Gelfiltrationsmethode (nur ca. 15 min) besser geeignet, um die Nanoemulsion vom überschüssigen Plasma abzutrennen.

In Kapitel 6 wurden verschiedene Hämoglobinpartikel untersucht: Reine Hämoglobinpartikel, Hämoglobinpartikel modifiziert mit HSA auf der Oberfläche und Hämoglobin-Hyaluronsäure-Partikel. Diese wurden als Blutersatz entwickelt und mit einer neuartigen 3-Schritt-Technik (Co-Fällung, Vernetzung und Auflösung) hergestellt. Die 2-DE Ergebnisse zeigen, dass Hämoglobinpartikel mit HSA weniger Proteine als die anderen beiden adsorbieren, weil das hydrophile HSA mehr hydrophile Oberflächen auf den Partikeln erzeugt und so die Proteinadsorption im Blut gehemmt hat. Außerdem wurde der Lösungsmitteleinfluss analysiert, welcher sehr geringe Auswirkungen auf die Proteinadsorption der reinen Hämoglobinpartikel sowie der HSA modifizierten Hämoglobinpartikel hatte. Somit wird also das Proteinadsorptionsmuster durch die Partikel selbst und nicht durch das verwendete Lösungsmittel bestimmt. Partikel werden weniger vom MPS erkannt, was zu einer längeren Zirkulationszeit im Blutkreislauf führt, wenn sie weniger Proteine, ausgenommen Albumin, absorbieren. Daher könnten die HSA Hämoglobinpartikel eine längere Zirkulationszeit im Blut als die beiden anderen Partikeltypen haben, weil sie viel weniger Protein adsorbiert haben. Somit sind diese das vielversprechendste Blutersatzmittel. In zukünftigen Untersuchungen wird ihr *in vivo* Verhalten in Tieren analysiert werden.

In Kapitel 7 wurden vier Formulierungen von Rutin-Nanokristallen (Plantacare UP 2000 (0,1%) Rutin-Nanopartikel, Plantacare 2000 UP (1,1%) Rutin-Nanopartikel, Tween 80 Rutin-Nanopartikel und Poloxamer 188 Rutin-Nanopartikel) hergestellt und ihre Proteinadsorptionmuster wurden mit der 2-DE analysiert. Die 2-DE-Ergebnisse zeigen, dass die vier Formulierungen der Rutin-Nanokristalle eine ähnliche Gesamtmenge von adsorbierten Proteinen haben. Dennoch unterscheidet sich die

adsorbierte Menge von ApoE auf den unterschiedlichen Partikeln. Plantacare 2000 UP (0,1%) Rutin-Nanopartikeln und Plantacare 2000 UP (1,1%) Rutin-Nanopartikel adsorbierten ähnliche Mengen von ApoE durch ihre identische Zusammensetzung auf ihren Oberflächen. Die Tween 80-Rutin Nanopartikel haben den höchsten Anteil an ApoE, was die besondere Bedeutung von Tween 80 Beschichtung auf die ApoE Adsorption zeigt. Die Poloxamer 188 Rutin-Nanopartikel adsorbierten kein ApoE aufgrund von sterischen Effekten und der Hydrophilie der PEO-Ketten auf der Oberfläche der Nanopartikel. ApoE ist in der Lage, Arzneistoffe ins Gehirn zu bringen. Daher haben die Tween 80 Rutin-Nanopartikel das Potenzial für ein Gehirn-Targeting, aber ihr *in vivo* Verhalten muss in nächsten Schritten in Tieren nachgewiesen werden. Somit wird die Perspektive eröffnet mit Rutin-Nanokristallen Alzheimer zu behandeln.

Letztendlich hat diese Arbeit die Proteinadsorptionmuster und die Proteinadsorptionskinetik auf verschiedenen Nanocarriern (SLN beschichtet mit verschiedenen Surfactants, Nanoemulsionen, unterschiedliche Hämoglobinpartikel und verschiedene Rutin-Nanokristalle) untersucht. Die Ergebnisse zeigen, dass die Eigenschaften der Partikeloberflächen die Proteinadsorption stark beeinflussen können (aufgrund von sterischen Effekten, hydrophoben Effekten, elektrostatischen Effekten usw.). Schließlich können die Arzneistoffträger mit dem höchsten Potential auf Grundlage ihrer Proteinadsorptionsmuster ausgewählt werden. Aber ihr *in vivo* Verhalten muss im nächsten Schritt in Tieren verifiziert werden. Somit stellt diese Arbeit einen Leitfaden dar, um das gewünschte Arzneimittel herstellen zu können.

Viele Herausforderungen bleiben dennoch bis heute im Bereich des „Drug Targetings“: z. B. das Verständnis, wie Plasmaproteine an Partikel *in vivo* adsorbieren oder die Partikel besser in das Zielgewebe zu transportieren. Eingehende Studien in diesem Bereich sind in der Zukunft erforderlich. Alle diese Studien zielen auf die Entwicklung und die Verbesserung der Arzneistoffträger, damit diese Arzneistoffe

besser ins Zielgewebe transportieren, um somit in der Nanomedizin angewendet werden zu können.

# 10. References

Aggarwal P., Hall J.B., McLeland C.B., Dobrovolskaia M.A. and McNeil S.E. (2009). "Nanoparticle interaction with plasma proteins as it relates to particle biodistribution, biocompatibility and therapeutic efficacy." Advanced Drug Delivery Reviews 61(6): 428-437.

Alyautdin R., Gothier D., Petrov V., Kharkevich D. and Kreuter J. (1995). "Analgesic activity of the hexapeptide dalargin adsorbed on the surface of polysorbate 80-coated poly(butyl cyanoacrylate) nanoparticles." European Journal of Pharmaceutics and Biopharmaceutics 41(1): 44-48.

Alyautdin R.N., Tezikov E.B., Ramge P., Kharkevich D.A., Begley D.J. and Kreuter J. (1998). "Significant entry of tubocurarine into the brain of rats by adsorption to polysorbate 80-coated polybutylcyanoacrylate nanoparticles: An in situ brain perfusion study." Journal of Microencapsulation 15(1): 67-74.

Anderson N.L. and Anderson N.G. (1991). "A two-dimensional gel database of human plasma proteins." Electrophoresis 12(11): 883-884.

Baszkin A. and Lyman D.J. (1980). "The interaction of plasma proteins with polymers. I. Relationship between polymer surface energy and protein adsorption/desorption." Journal of Biomedical Matericals Research 14(4): 393-403.

Bäumler H. and Georgieva R. (2010). "Coupled Enzyme Reactions in Multicompartment Microparticles." Biomacromolecules 11(6): 1480-1487.

Bisgaier C.L., Siebenkaas M.V. and Williams K.J. (1989). "Effects of apolipoproteins A-IV and A-I on the uptake of phospholipid liposomes by hepatocytes." The Journal

of Biological Chemistry 264: 862-866.

Bjellqvist B., Pasquali C., Ravier F., Sanchez J.C. and Hochstrasser D.F. (1993). "A nonlinear wide-range immobilized pH gradient for two-dimensional electrophoresis and its definition in a relevant pH scale." Electrophoresis 14(1): 1357-1365.

Blunk T. (1994). "PhD Thesis: Plasmaproteinadsorption auf kolloidalen Arzneistoffträgern." Christian-Albrechts-Universität Kiel, Germany.

Blunk T., Hochstrasser D.F., Sanchez J.C., Müller B.W. and Müller R.H. (1993). "Colloidal carriers for intravenous drug targeting: plasma protein adsorption patterns on surface-modified latex particles evaluated by two-dimensional polyacrylamide gel electrophoresis." Electrophoresis 14(1): 1382-1387.

Blunk T., Lück M., Calvor A., Hochstrasser D.F., Sanchez J.C., Müller B.W. and Müller R.H. (1996). "Kinetics of plasma protein adsorption on model particles for controlled drug delivery and drug targeting." Eueopean Journal of Pharmaceutics and Biopharmaceutics 42(4): 262-268.

Caglio S. and Righetti P.G. (1993). "On the pH dependence of polymerization efficiency, as investigated by capillary zone electrophoresis." Electrophoresis 14(1): 554-558.

Camner P., Lundborg M., Lastbom L., Gerde P., Gross N. and Jarstrand C. (2002). "Experimental and calculated parameters on particle phagocytosis by alveolar macrophages." Journal of Applied Physiology 92(6): 2608-2616.

Carignano M.A. and Szleifer I.I. (2000). "Prevention of protein adsorption by flexible and rigid chain molecules." Colloids and Surfaces B: Biointerfaces 18(3-4): 169-182.

Cattel L., Ceruti M. and Dosio F. (2003). "From conventional to stealth liposomes: a new frontier in cancer chemotherapy." Tumori 89: 237-249.

Cedervall T., Lynch I., Foy M., Berggard T., Donnelly S.C., Cagney G., Linse S. and Dawson K.A. (2007). "Detailed identification of plasma proteins adsorbed on copolymer nanoparticles." Angewandte Chemie International Edition 46(30): 5754-5756.

Chen R. (2013). "PhD Thesis: Tailor-made antioxidative nanocrystals: production and in vivo efficacy." Freien Universität Berlin, Germany

Davis S.S. (1981). "Colloids as drug-delivery systems." Pharmaceutical Technology 5: 71-78.

Dehouck B., Fenart L., Dehouck M.P., Pierce A., Torpier G. and Cecchelli R. (1997). "A new function for the LDL receptor: Transcytosis of LDL across the blood-brain barrier." The Journal of Cell Biology 138(4): 877-889.

Diederichs J.E. (1996). "Plasma protein adsorption patterns on liposomes: establishment of analytical procedure." Electrophoresis 17(3): 607-611.

Diels A.M.J. and Michiels C.W. (2006). "High-Pressure Homogenization as a Non-Thermal Technique for the Inactivation of Microorganisms." Critical Reviews in Microbiology 32: 201-216.

Douglas S.J., Davis S.S. and Illum L. (1986). "Biodistribution of poly(butyl 2-cyanoacrylate) nanoparticles in rabbits." International Journal of Pharmaceutics 34(1-2): 145-152.

Dzandu J.K., Johnson J.F. and Wise G.F. (1988). "Sodium dodecyl sulfate-gel

electrophoresis: Staining of polypeptides using heavy metal salts." Analytical Biochemistry 174(1): 157-167.

Ehrlich P. (1906). "Collected studies on immunity." John Wiley, New York: pp. 404-443.

Fawcett J.S. and Morris C.J.O.R. (1966). "Molecular-Sieve Chromatography of Proteins on Granulated Polyacrylamide Gels." Separation Science 1(1): 9-26.

Gelfi C. and Righetti P.G. (1981). "Polymerization kinetics of polyacrylamide gels I. Effect of different cross-linkers." Electrophoresis 2(4): 213-219.

Gessner A., Lieske A., Paulke B.R. and Müller R.H. (2002). "Influence of surface charge density on protein adsorption on polymeric nanoparticles: analysis by two-dimensional electrophoresis." European Journal of Pharmaceutics and Biopharmaceutics 54(2): 165-170.

Gessner A., Lieske A., Paulke B.R. and Müller R.H. (2003). "Functional groups on polystyrene model particles: influence on protein adsorption." Journal of Biomedical Materials Research Part A 65A(3): 319-326.

Gessner A., Olbrich C., Schroder W., Kayser O. and Müller R.H. (2001). "The role of plasma proteins in brain targeting: species dependent protein adsorption patterns on brain-specific lipid drug conjugate (LDC) nanoparticles." International Journal of Pharmaceutics 214(1-2): 87-91.

Gessner A., Paulke B.R. and Müller R.H. (2000). "Analysis of plasma protein adsorption onto polystyrene particles by two-dimensional electrophoresis: comparison of sample application and isoelectric focusing techniques." Electrophoresis 21(12): 2438-2442.

Göppert T.M. (2005). "PhD Thesis: Plasma protein adsorption on parenterally administered colloidal drug carriers for crossing the blood brain barrier." Freie Universität Berlin, Germany.

Göppert T.M. and Müller R.H. (2003). "Plasma protein adsorption of Tween 80- and Poloxamer 188-stabilized solid lipid nanoparticles." Journal of Drug Targeting 11(4): 225-231.

Göppert T.M. and Müller R.H. (2004). "Alternative sample preparation prior to two-dimensional electrophoresis protein analysis on solid lipid nanoparticles." Electrophoresis 25(1): 134-140.

Göppert T.M. and Müller R.H. (2005a). "Protein adsorption patterns on poloxamer- and poloxamine-stabilized solid lipid nanoparticles (SLN)." European Journal of Pharmaceutics and Biopharmaceutics 60(3): 361-372.

Göppert T.M. and Müller R.H. (2005b). "Polysorbate-stabilized solid lipid nanoparticles as colloidal carriers for intravenous targeting of drugs to the brain: Comparison of plasma protein adsorption patterns." Journal of Drug Targeting 13(3): 179-187.

Göppert T.M. and Müller R.H. (2005c). "Adsorption kinetics of plasma proteins on solid lipid nanoparticles for drug targeting." International Journal of Pharmaceutics 302(1-2): 172-186.

Görg A., Boguth G., Obermaier C., Scheibe B. and Weiss W. (1995). "Booklet of the "Hands-on Course. ICES" 95 Meeting." Paris.

Görg A., Postel W., Weser J., Günther S., Strahler J.R., Hanash S.M. and Somerlot L.

(1987). "Elimination of point streaking on silver-stained two-dimensional gels of addition of iodoacetamide to the equilibration buffer." Electrophoresis 8(2): 122-124.

Gref R., Lück M., Quellec P., Marchand M., Dellacherie E., Harnisch S., Blunk T. and Müller R.H. (2000). "'Stealth' corona-core nanoparticles surface modified by polyethylene glycol (PEG): influences of the corona (PEG chain length and surface density) and of the core composition on phagocytic uptake and plasma protein adsorption." Colloids Surf B Biointerfaces 18(3-4): 301-313.

Gregoriadis G. (1993). "Liposomes Technology." CRC Press.

Gulyaev A.E., Gelperina S.E., Skidan I.N., Antropov A.S., Kivman G.Y. and Kreuter J. (1999). "Significant transport of doxorubicin into the brain with polysorbate 80-coated nanoparticles." Pharmaceutical Research 16(10): 1564-1569.

Hames B.D. (1998). "Gel electrophoresis of proteins: A practical approach." Oxford Univeristy Press.

Harnisch S. and Müller R.H. (1998). "Plasma protein adsorption patterns on emulsions for parenteral administration: establishment of a protocol for two-dimensional polyacrylamide electrophoresis." Electrophoresis 19(2): 349-354.

Harnisch S. and Müller R.H. (2000). "Adsorption kinetics of plasma proteins on oil-in-water emulsions for parenteral nutrition." Eueopean Journal of Pharmaceutics and Biopharmaceutics 49(1): 41-46.

Higgins R.C. and Dahmus M.E. (1979). "Rapid visualization of protein bands in preparative SDS-polyacrylamide gels." Analytical Biochemistry 93: 257-260.

Hochstrasser D.F., Harrington M.G., Hochstrasser A.C., Miller M.J. and Merril C.R.

(1988). "Methods for increasing the resolution of two-dimensional protein electrophoresis." Analytical Biochemistry 173(2): 424-435.

Hoogland C, Sanchez J.C., Tonella L., Binz P.A., Bairoch A., Hochstrasser D.F. and Appel R.D. (2000). "The 1999 SWISS-2DPAGE database update." Nucleic Acids Research 28(1): 286-288.

Illum L. and Davis S.S. (1987). "Targeting of colloidal particles to the bone marrow." Life Sciences 40(16): 1553-1560.

Illum L., Davis S.S., Müller R.H., Mak E. and West P. (1987). "The organ distribution and circulation time of intravenously injected colloidal carriers sterically stabilized with a blockcopolymer-poloxamine 908." Life Sciences 40(4): 367-374.

Illum L., Hunneyball I.M. and Davis S.S. (1986). "The effect of hydrophilic coatings on the uptake of colloidal particles by the liver and by peritoneal macrophages." International Journal of Pharmaceutics 29(1): 53-65.

Juliano R.L. (1988). "Factors affecting the clearance kinetics and tissue distribution of liposomes, microspheres and emulsions." Advanced Drug Delivery Reviews 2(1): 31-54.

Kreuter J. (2001). "Nanoparticulate systems for brain delivery of drugs." Advanced Drug Delivery Reviews 47(1): 65-81.

Kreuter J., Petrov V.E., Kharkevich D.A. and Alyautdin R.N. (1997). "Influence of the type of surfactant on the analgesic effects induced by the peptide dalargin after its delivery across the blood-brain barrier using surfactant-coated nanoparticles." Journal of Controlled Release 49(1): 81-87.

Kreuter J., Shamenkov D., Petrov V., Ramge P., Cychutek K., Koch-Brandt C. and Alyautdin R.N. (2002). "Apolipoprotein-mediated transport of nanoparticle-bound drugs across the blood-brain barrier." Journal of Drug Targeting 10(4): 317-325.

Lee C., Levin A. and Branton D. (1987). "Copper staining: A five-minute protein stain for sodium dodecyl sulfate-polyacrylamide gels " Analytical Biochemistry 166(2): 308-312.

Leroux J.C., Alleman E., De Jaeghere F., Doelker E. and Gurny R. (1996). "Biodegradable nanoparticles: From sustained release formulations to improved site specific drug delivery." Journal of Controlled Release 39(2-3): 339-350.

Leroux J.C., Gravel P., Balant L., Volet B., Anner B.M., Allemann E., Doelker E. and Gurny R. (1994). "Internalization of poly(D,L-lactic acid) nanoparticles by isolated human leukocytes and analysis of plasma proteins adsorbed onto the particles." Journal of Biomedical Materials Research 28(4): 471-481.

Leroux J.C., Jaeghere F.D., Anner B., Doelker E. and Gurny R. (1995). "An investigation on the role of plasma and serum opsonins on the internalization of biodegradable poly(DL-lactic acid) nanoparticles by human monocytes." Life Sciences 57: 695-703.

Liliemark E., Sjostrom B., Liliemark J., Peterson C., Kallberg N. and Larsson B.S. (1995). "Targeting of teniposide to the mononuclear phagocytic system (MPS) by incorporation in liposomes and submicron lipid particles; an autoradiographic study in mice." Leukemia & Lymphoma 18(1-2): 113-118.

Lind K., Kresse M. and Müller R.H. (2001). "Comparison of protein adsorption patterns onto differently charged hydrophilic superparamagnetic iron oxide particles obtained in vitro and ex vivo." Electrophoresis 22(16): 3514-3521.

Lück M. (1997). "PhD Thesis: Plasmaproteinadsorption als möglicher Schlüsselfaktor für eine kontrollierte Arzneistoffapplikation mit partikulären Trägern." Freie Universität Berlin, Germany.

Lück M., Pistel K.F., Li Y.X., Blunk T., Müller R.H. and Kissel T. (1998). "Plasma protein adsorption on biodegradable microspheres consisting of poly(d,l-lactide-co-glycolide), poly(l-lactide) or ABA triblock copolymers containing poly(oxyethylene Influence of production method and polymer composition." Journal of Controlled Release 55(2-3): 107-120.

Lück M., Schröder W., Harnisch S., Thode K., Blunk T., Paulke B.R., Kresse M. and Müller R.H. (1997). "Identification of plasma proteins facilitated by enrichment on particulate surfaces: analysis by two-dimensional electrophoresis and N-terminal microsequencing." Electrophoresis 18(15): 2961-2967.

Lück M., Schroder W., Paulke B.R., Blunk T. and Müller R.H. (1999). "Complement activation by model drug carriers for intravenous application: determination by two-dimensional electrophoresis." Biomaterials 20(21): 2063-2068.

Lynch I. and Dawson K.A. (2008). "Protein-nanoparticle interactions." Nanotoday 3(1-2): 40-47.

Maassen S., Fattal E., Müller R.H. and Couvreur P. (1993). "Cell cultures for the assessment of toxicitiy and uptake of polymeric particulate drug carriers." STP pharma sciences 3(1): 11-22.

Mehnert W. and Mader K. (2001). "Solid lipid nanoparticles: Production, characterization and applications." Advanced Drug Delivery Reviews 47(2-3): 165-196.

Merril C.R. and Goldman D. (1984). "In two-dimensional gel electrophoresis of proteins." Academic Press, New York.

Merril C.R., Switzer R.C. and Van Keuren M.L. (1979). "Trace polypeptides in cellular extracts and human body fluids detected by two-dimensional electrophoresis and a highly sensitive silver stain." Proceedings of the National Academy of Sciences of the United States of America 76(9): 4335-4339.

Moghimi S.M., Muir I.S., Illum L., Davis S.S. and Kolb-Bachofen V. (1993). "Coating particles with a block co-polymer (poloxamine-908) suppresses opsonization but permits the activity of dysopsonins in the serum." Biochimica et Biophysica Acta (BBA)-Molecular Cell Research 1179(2): 157-165.

Müller R.H. (1991). "Colloidal carriers for controlled drug delivery and targeting." Wissenschaftliche Verlagsgesellschaft.

Müller R.H. (1996). "Zetapotential und Partikelladung in der Laborpraxis-Einführung in die Theorie, praktische Meßdurchführung, Dateninterpretation." Wissenschaftliche Verlagsgesellschaft Stuttgart, 254 S.

Müller R.H., Dingler A., Runge S.A., Schneppe T. and Gohla S. (2000a). "Large scale production of solid lipid nanoparticles (SLNTM) and nanosuspensions (DissoCubesTM), ." in: Wise D (ed.) Handbook of Pharmaceutical Controlled Release Technology: 359-376.

Müller R.H. and Heinemann S. (1989). "Surface Modelling of Microparticles as Parenteral Systems with High Tissue Affinity. In: Gurny, R., Junginger, H.E. (Eds.), Bioadhesion Possibilities and Future Trends." Wissenschaftliche Verlagsgesellschaft: 202-214.

Müller R.H., Lippacher A. and Gohla S. (2000b). "Solid Lipid Nanoparticles (SLN ) as Carrier System for the Controlled Release of Drugs." in: Wise D (ed.) Handbook of Pharmaceutical Controlled Release Technology: 377-391.

Müller R.H., Lück M., Harnisch S. and Thode K. (1997). "Intravenously injected particles: surface properties and interaction with blood proteins-The key determining the organ distribution." Plenum Press, New York.

Müller R.H., Lück M. and Kreuter J. (2001). "Medicament excipient particles for tissue specific application of a medicament." PCTapplication: PCT/EP98/064299 (P053601).

Müller R.H. and Lücks J.S. (1996). "Arzneistoffträger aus festen Lipidteilchen, Feste Lipidnanosphären (SLN), Medication vehicles made of solid lipid particles (solid lipid nanospheres-SLN)." European Patent No. 0605497.

Müller R.H., Maassen S., Weyhers H. and Mehnert W. (1996). "Phagocytic uptake and cytotoxicity of solid lipid nanoparticles (SLN) sterically stabilized with poloxamine 908 and poloxamer 407." Journal of Drug Targeting 4(3): 161-170.

Müller R.H., Mäder K. and Gohla S. (2000). "Solid lipid nanoparticles (SLN) for controlled drug delivery- a review of the state of the art." European Journal of Pharmaceutics and Biopharmaceutics 50(1): 161-177.

Müller R.H., Mehnert W., Lücks J.S., Schwarz C., zur Muhlen A., Weyhers H., Freitas C. and Ruhl D. (1995). "Solid lipid nanoparticles (SLN)-An alternative colloidal carrier system for controlled drug delivery." European Journal of Pharmaceutics and Biopharmaceutics 41(1): 62-69.

Müller R.H. and Schmidt S. (2002). "PathFinder technology for the delivery of drugs to the brain." New Drugs 2: 38-42.

Müller R.H. and Souto E.B. (2005). "Lipid nanoparticles (SLN and NLC) for drug delivery." in: Kumar R, Tabata Y, Domb A: Nanoparticles for Pharmaceutical Applications.

O' Mullane J.E., Artursson P. and Tomlinson E. (1987). "Biopharmaceutics of microparticulate drug carriers." Annals of the New York Academy of Sciences 507: 120-140.

O'Farrell P.H. (1975). "High resolution two-dimensional electrophoresis of proteins." The Journal of Biological Chemistry 250: 4007-4021.

Ogawara K., Furumoto K., Nagayam S., Minato K., Higaki K. and K. T. Kai T. (2004). "Pre-coating with serum albumin reduces receptor-mediated hepatic disposition of polystyrene nanosphere: implications for rational design of nanoparticles." Journal of Controlled Release 100(3): 451-455.

Olbrich C., Kayser O., Lamprecht A., Kneuer C., Lehr C.M. and Müller R.H. (2000). "Interactions of fluorescent solid lipid nanoparticles (SLN) with macrophage-like cells visualized by CLSM." 3rd World Meeting APGI/APV, Berlin: 331-332.

Patel H.M. (1992). "Serum opsonins and liposomes: Their interaction and opsonophagocytosis." Critical Reviews in Therapeutics Drug Carrier Systems 9(1): 39-90.

Pecora R. (2000). "Dynamic light scattering measurement of nanometer particles in liquids." Journal of Nanoparticle Research 2: 123-131.

Price M.E., Cornelius R.M. and Brash J.L. (2001). "Protein adsorption to polyethylene glycol modified liposomes from fibrinogen solution and from plasma." Biochimica et Biophysica Acta (BBA)-Biomembranes 1512(2): 191-205.

Ragland W.L., Benton T.L., Pace J.L., Beach F.G. and Wade A.E. (1978). "Analysis of proteins in polyacrylamide gels by scanning for fluorescence." Electrophoresis 78: 217-230.

RIghetti P.G., Bossi A., Giglio M., Vailati A., Lyubimova T. and Briskman A.V. (1994). "Is gravity on our way? The case of polyacrylamide gel polymerization." Electrophoresis 15(1): 1005-1013.

Righetti P.G. and Caglio S. (1993). "On the kinetics of monomer incorporation into polyacrylamide gels, as investigated by capillary zone electrophoresis." Electrophoresis 14(1): 573-582.

Scherphof G., Roerdink F., Hoekstra D., Zborowski J., Wisse E., Gregoriadis G. and Allison A.C. (1980). "Liposomes in Biological Systems." John Wiley, Chichester: 179-210.

Schmidt S. (2002). "PhD Thesis: Parenterale O/W-Emulsionen Plasmaproteininteraktion und Inkorporation von Arzneistoffen." Freien Universität Berlin, Germany

Schwarz C., Mehnert W., Lücks J.S. and Müller R.H. (1994). "Solid lipid nanoparticles (SLN) for controlled drug delivery. I. Production, characterization and sterilization." Journal of Controlled Release 30(1): 83-96.

Senior J., Crawley J.C. and Gregoriadis G. (1985). "Tissue distribution of liposomes exhibiting long half-lives in the circulation after intravenous injection." Biochimica et

Biophysica Acta (BBA) - General Subjects 839(1): 1-8.

Senior J.H. (1987). "Fate and behavior of liposomes in vivo: A review of controlling factors." Critical Reviews in Therapeutic Drug Carrier Systems 3(2): 123-193.

Switzer R.C., Merril C.R. and Shifrin S. (1979). "A highly sensitive silver stain for detecting proteins and peptides in polyacrylamide gels." Analytical Biochemistry 98(1): 231-237.

Thiele L., Diederichs J.E., Reszka R., Merkle H.P. and Walter E. (2003). "Competitive adsorption of serum proteins at microparticles affects phagocytosis by dendritic cells." Biomaterials 24(8): 1409-1418.

Thode K. (1996). "PhD Thesis: Specific contrast agents for magnetic resonance tomography: Physico-chemical characterisation and studies on plasma protein adsorption." Freie Universität Berlin, Germany.

Thode K., Lück M., Semmler W., Müller R.H. and Kresse M. (1997). "Determination of plasma protein adsorption on magnetic iron oxides: sample preparation." Pharmaceutical Research 14(7): 905-910.

Vroman L. and Adams A.L. (1986). "Adsorption of proteins out of plasma and solutions in narrow spaces." Journal of Colloid and Interface Science 111(2): 391-402.

Vroman L., Adams A.L., Fischer G.C. and Munoz P.C. (1980). "Interaction of high molecular weight kininogen, factor XII, and fibrinogen in plasma at interfaces." Blood 55(1): 156-159.

Weisgraber K.H., Mahley R.W., Kowal R.C., Herz J., Goldstein J.L. and Brown M.S. (1990). "Apolipoprotein C-I modulates the interaction of apolipoprotein E with

beta-migrating very low density lipoproteins (beta-VLDL) and inhibits binding of beta-VLDL to low density lipoprotein receptor-related protein." The Journal of Biological Chemistry 265(22453-22459).

Weyhers H., Lück M., Mehnert W., Souto E.B. and Müller R.H. (2005). "Surface Modified Solid Lipid Nanoparticles (SLN) Analysis of Plasma Protein Adsorption Patterns by two-dimensional Polyacrylamide Gel Electrophoresis (2-D PAGE)." International Journal of Molecular Medicine and Advance Sciences 1(2): 196-201.

Xiong Y. (2012). "PhD Thesis: Herstellung von Mikropartikeln zum Sauerstofftransport auf Hämoglobinbasis." Freie Universität Berlin, Germany.

# Publications

## Abstracts

Yujuan Zhang and Rainer H. Müller; Separation methods of oil-in-water emulsions from plasma for 2D-PAGE, P36, “Tag Der Pharmazie”, DPhG Landesgruppe Berlin-Brandenburg, Berlin, 6 Juli, 2012.

Yujuan Zhang, Yu Xiong, Hans Bäumler, Rainer H. Müller; Blood substitutes: Adsorption protein patterns on different i.v. hemoglobin particles, W5235, Annual Meeting of the American Association of Pharmaceutical Scientists (AAPS), Chicago, 14-18 October, 2012.

Yujuan Zhang and Rainer H. Müller; Time-dependent protein adsorption patterns on i.v. oil-in-water nanoemulsions,W5236, Annual Meeting of the American Association of Pharmaceutical Scientists (AAPS), Chicago, 14-18 October, 2012.

## Proceeding

Yujuan Zhang, Run Chen, Cornelia M. Keck, Rainer H. Müller; Intravenous Rutin Nanocrystals with Potential Use for Alzheimer Treatment, Abstract ID: 100143, the 40th Annual Meeting & Exposition of the Controlled Release Society, July 21-24, 2013, in Honolulu, Hawaii, U.S.A.

## Papers

Yujuan Zhang; Comparing the interparticle coupling effect on sensitivities of silver and gold nanoparticles, Journal of Quantitative Spectroscopy and Radiative Transfer, 2012, 113(8): 578-581.

Yujuan Zhang; Investigation of gold and silver nanoparticles on absorption heating and scattering imaging, Plasmonics, 2011, 6(2): 393-397.

Yujuan Zhang, Rao Huang, Xianfang Zhu, Lianzhou Wang, and Chenxu Wu; Synthesis, properties, and optical applications of noble metal nanoparticle-biomolecule conjugates (review), Chinese Science Bulletin, 2012, 57(2-3): 238-246.

Yujuan Zhang and Xianfang Zhu; Synthesis of quasi-square silver nanoparticles for LSPR sensor, Chinese Journal of Spectroscopy Laboratory, 2010, 27(4): 1579-1582.

## Patents

Rao Huang, Gaoqing Lu, Lianzhou Wang, Chenxu Wu, Yujuan Zhang, and Xianfang Zhu; Preparation method of dead square nanoparticle array structure with two-dimensional square lattice arrangement, Publication Number: CN 101774535 A.

Gaoqing Lu, Yinyan Luo, Lianzhou Wang, Yujuan Zhang, and Xianfang Zhu; Preparation method of honeycomb nanoparticle array structure with two-dimensional hexagonal lattice arrangement, Publication Number: CN 101774536 A.

# Curriculum Vitae

The curriculum vitae is not included in the online version for reasons of data protection.